DISSERTATION

GRASSLAND SENSITIVITY TO EXTREME DROUGHT:

ASSESSING THE ROLE OF COMMUNITY FUNCTIONAL COMPOSITION

Submitted by

Robert James Griffin-Nolan

Graduate Degree Program in Ecology

In partial fulfillment of the requirements

For the Degree of Doctor of Philosophy

Colorado State University

Fort Collins, Colorado

Summer 2019

Doctoral Committee:

    Advisor: Alan K. Knapp

    Troy W. Ocheltree
    Melinda D. Smith
    David T. Tissue

ABSTRACT

GRASSLAND SENSITIVITY TO EXTREME DROUGHT:

ASSESSING THE ROLE OF COMMUNITY FUNCTIONAL COMPOSITION

Climate change is expected to cause droughts that are reminiscent of the dust bowl. While all ecosystems are negatively affected by drought to some degree, grasslands are among those most sensitive. Accurate forecasting of which grasslands are most sensitive to drought is imperative to conserving the many economically and aesthetically valuable services these ecosystems provide. This dissertation utilizes both observational and experimental data, coupled with a systematic literature review, to assess the mechanisms of differential grassland sensitivity to drought.

Long-term records of precipitation and aboveground net primary production (ANPP), a key metric of ecosystem function, suggest that xeric grasslands are more sensitive to drought than mesic grasslands. I provide further support for this trend using recent observations of the response and recovery of ANPP following a short-term natural drought in six grassland sites. Predicting the ecological consequences of long-term extreme drought, however, requires a mechanistic understanding of drought sensitivity beyond its climatic determinants, especially considering two sites with similar climatic means can differ dramatically in their sensitivity to climate extremes. Plant traits, which act as proxies for more complex physiological functions, can be scaled through the community (i.e. weighted by species relative abundance) to explain and forecast ecosystem responses to environmental change. Few studies, however, measure community-weighted traits in the context of altered water availability. Following a systematic review of >500 manuscripts, I identify clear knowledge gaps in the field of plant traits research and provide guidelines for using

plant traits to understand ecosystem sensitivity to PPT. Specifically, plant trait surveys could be improved by a selection of traits that reflect physiological functions directly related to plant water use with traits weighted by species relative abundance. Informed by these guidelines, I test and validate a high throughput method for assessing leaf turgor loss point, a key metric of drought tolerance, using an osmometer. The osmometer method paves the way for rapid community-scale surveys of drought tolerance across functional types.

Finally, I employ a coordinated, long-term rainfall exclusion experiment to assess the drought sensitivity of ANPP and community functional composition (i.e. community-weighted trait means and trait diversity) across six grassland sites. Four years of experimental drought (i.e. 66% removal of growing season rainfall) led to reduced ANPP across all six grasslands, with the sensitivity of ANPP being highly correlated with community functional composition. Specifically, functionally diverse plant communities, as well as those with a high abundance of species with conservative resource use strategies, experienced smaller relative reductions in ANPP following drought. Additionally, drought treatments led to increased functional diversity and decreased community scale drought tolerance, largely due to species re-ordering following dominant species mortality. Increased functional diversity may stabilize ecosystem functioning in response to future drought. However, the shifts in community-scale drought strategies may increase ecosystem drought sensitivity, depending on the nature and timing of recurrent drought. The role these two mechanisms will play in determining ecosystem recovery from and response to future drought will be fascinating to assess. Overall, my research demonstrates the importance of plant traits in understanding differential ecosystem sensitivity to extreme drought, especially when the appropriate traits are measured and weighted by species relative abundance.

ACKNOWELDGEMENTS

While I am the sole author of this dissertation, none of the work described here would have been possible without the help and support of countless others. For this reason, the pronoun "we" is used throughout many of the following chapters.

I would first like to thank those who introduced me to the field of global change ecology and have been a guiding hand from the beginning of my graduate studies. To my advisor, Dr. Alan Knapp, who has read and revised innumerable drafts of my work, thank you for being an exceptional and enthusiastic mentor and for providing me with the freedom to explore my own research interests. To my stellar committee members, thank you for providing guidance throughout my PhD. As a first-year graduate student, I had never seen or used a pressure chamber, and leaf water potential was a mysterious concept to me. Thus, I'd like to thank Dr. Troy Ocheltree for introducing me to the field of leaf hydraulics and for always encouraging me to try out new methods. To Dr. Melinda Smith, thank you for leading me into the field of community ecology and always considering me for collaborative and professional development opportunities. And to Dr. David Tissue, thank you for being a mentor away from home. While much of my international research is not discussed in this dissertation, Dr. Tissue has always been willing to provide detailed and constructive advice on a variety of projects and was integral to chapter 3.

I have had the good fortune of being surrounded by so many talented fellow ecologists during my time at Colorado State University. Specifically, I'd like to thank past and current members of the Knapp and Smith labs for their valuable feedback and generous support in the field: Ingrid Slette, Jeff Carroll, Alison Post, Kevin Wilcox, Melissa Johnston, Elsie Denton, Maddie Shields, Andrew Felton, Ava Hoffman, Nate Lemoine, Lauren Baur, Francis Chaves, John

Lastly, I'd like to thank my friends and family. To my parents and siblings, thank you for your endless support and encouragement. To the wonderful GDPE community here in Fort Collins, you have made my time in graduate school some of the best years of my life – Thank You!

DEDICATION

To my parents,
who have always encouraged me to write.

TABLE OF CONTENTS

CHAPTER 1: INTRODUCTION

1.1 Background

Ecologists strive to understand the interactions between organisms and their environment. Data collected from experiments and observational studies conducted on a variety of spatial/temporal scales and levels of ecological organization are used to develop theoretical models describing these interactions (Levin, 1992). In the next century, however, organisms will be living in novel environments both in terms of climate and biotic interactions (Vitousek et al., 1997). Climate change offers a unique opportunity for ecologists to both test and modify these established ecological relationships and incorporate new observations from novel experimental frameworks. For instance, the temporal relationship between observed annual precipitation (PPT) and aboveground net primary production (ANPP), a key metric of ecosystem function, is traditionally described with a linear model (Huxman et al., 2004); however, the addition of data from experiments that add or remove water beyond the historical range of PPT, thereby creating a novel and extreme environment, changes the ANPP-PPT relationship from linear to non-linear and saturating (Knapp et al., 2017; 2018). The emergence of coordinated, long-term and multi-site experiments, along with observations of naturally occurring climate extremes, will further parameterize these relationships to allow for accurate forecasting of the ecological consequences of climate change.

Earth's global temperature has been steadily rising for the past century, largely due to anthropogenic emissions of greenhouse gases (IPCC, 2013). Assuming 'business as usual' practices of fossil fuel burning and land degradation (i.e., RCP-8.5 projections), globally averaged temperatures could rise 2.6 °C to 4.8 °C by the end of the 21st century (IPCC, 2013). These

projected changes in temperature will lead to further intensification of Earth's water cycle. Specifically, with every 1 °C increase in temperature, the water holding capacity of the atmosphere increases by 7%, effectively increasing total PPT amount (Trenberth, 2011). The spatial and temporal distribution of PPT will be highly variable, however, with many regions of the world, including the American Southwest and Great Plains, expected to experience unprecedented drought as rates of evapotranspiration increase (Dai, 2011; 2013; Cook et al., 2015). The impacts of drought on human populations are well known (e.g. water scarcity, declining crop yields, increased conflict); however, many of these socio-economic implications are inherently linked to the ecological and biophysical consequences of drought (O'Brien and Leichenko, 2000). It is therefore critical to understand the underlying mechanisms of ecosystem sensitivity to drought, especially in water-limited regions that are expected to become drier with climate change (Cook et al., 2015).

Grasslands cover 30% of North America and are highly sensitive to changes in PPT given that most are water-limited ecosystems (Knapp and Smith, 2001; Hsu et al., 2012; Pendall et al., 2018). Additionally, grasslands provide a variety of ecosystem services such as forage production for livestock, soil stabilization, wildlife habitat, and hydrologic buffering (Noy-Meir, 1973; Field et al., 1998; Pendall et al., 2018). Grasslands of the United States also act as a carbon sink, with net ecosystem carbon uptake rates of ~55 Tg per year (Pendall et al., 2018), much of which is stored belowground (Silver et al., 2010). These ecosystems are therefore important resources for mitigating anthropogenic climate change. Increased drought frequency and duration will likely influence the future carbon storage potential of grasslands, especially in C_4 grasslands where PPT is the primary climatic determinant of plant growth and ANPP (Churkina and Running, 1998). Across North America, ANPP increases from west to east with increasing mean annual

precipitation (MAP) (Webb et al., 1983; Sala et al., 1988; Knapp and Smith, 2001). Xeric ecosystems tend to be more sensitive to interannual variation in precipitation than mesic ecosystems, as evidenced by a steeper slope in the temporal relationship between ANPP and PPT (Huxman et al., 2004). Low precipitation sensitivity of ANPP in mesic sites has been attributed to co-limitation of resources (e.g. nutrients and light) and/or differences in vegetation structure (Paruelo et al. 1999; Veron et al. 2002). While extreme drought negatively affects both xeric and mesic ecosystems (Huxman et al., 2004), these temporal models suggest xeric ecosystems should be more drought sensitive than mesic ecosystems. Long-term records of ANPP and PPT provide little evidence of this, however, as extreme climate events are rare by definition (Smith, 2011). To study climate extremes, ecologists must either take advantage of naturally occurring 1/100-year type droughts, or experimentally manipulate precipitation.

Drought is often defined simply as a 'prolonged absence or marked deficiency of precipitation' (IPCC, 2013). There are several secondary characteristics of drought (e.g. increased solar radiation, higher temperatures, and insect outbreaks; McDowell et al., 2008) that are difficult to manipulate in experimental settings. Observational studies of natural drought are thus very important for understanding baseline ecosystem responses to drought. In 2012, grasslands of the central US experienced an extreme natural drought which led to an equivalent 40% reduction in PPT, relative to MAP, across the region. The equivalent magnitude and duration of this drought provided an opportunity to assess differential drought sensitivity of ANPP across several perennial grasslands, ranging from desert to tallgrass prairie (Knapp et al., 2015). As predicted by Huxman et al. (2004), xeric grasslands experienced greater relative reductions in ANPP compared to mesic sites following this natural drought (Knapp et al., 2015). While short-term observational studies are invaluable for testing ecological theory, the extreme droughts of the 21st century are expected

to last multiple years (Dai, 2013), with the recent drought in California suggesting this is already occurring (Griffin and Anchukaitis, 2014). Forecasting how ecosystems will respond to such long-term extreme drought requires coordinated multi-site experiments.

The 'Extreme Drought in Grasslands Experiment' (EDGE) was established following the natural drought of 2012 in the same six central US grasslands surveyed by Knapp et al. (2015). The EDGE project utilizes large rainfall exclusion shelters that block 66% of incoming growing season rainfall for four years, effectively imposing the most extreme drought on record for this region. The six sites span a large precipitation gradient (MAP range: 244 – 864 mm) and are representative of the major grassland types of North America: desert grassland, shortgrass prairie, C_3-dominated mixed grass prairie, C_4-dominated mixed grass prairie, and tallgrass prairie. Key response variables measured include above- and belowground net primary productivity, plant community composition, and soil respiration. As theory would suggest (Huxman et al., 2004), and observational evidence supports (Knapp et al., 2015), a four-year extreme drought should lead to decreased ANPP across all sites, with higher drought sensitivity at the driest sites. Establishing the climatic drivers of drought sensitivity sets a baseline for forecasting ecosystem sensitivity to drought on broad spatial scales. Within semi-arid regions, however, two sites may differ dramatically in their sensitivity to drought even though they share a similar climate (Knapp et al., 2015). The goal of my dissertation, therefore, is to develop a more mechanistic framework for understanding ecosystem sensitivity to drought.

Our understanding of ecosystem properties is limited by our ability to mechanistically link plant physiological processes to the pools and/or fluxes of energy and materials within ecosystems (Enquist et al., 2003). Plant traits, which act as proxies for more complex physiological functions, can be scaled through the community (i.e. weighted by species relative abundance) to explain and

forecast ecosystem responses to environmental change (Suding et al., 2008). In the context of ecosystem drought sensitivity, appropriate traits must be identified which represent physiological strategies related to water use efficiency (Brodribb, 2017). Leaf-level gas exchange is an extremely inefficient process at the molecular level, with up to 400 molecules of H_2O lost per molecule of CO_2 gained through stomata (Nobel, 1999). Regulation of plant water-use efficiency is thus central to plant strategies for coping with drought. In water-limited grasslands, plant species differ in both temporal and spatial patterns of water-use (Weaver, 1958; Nippert and Knapp, 2007; Kooyers, 2015). Many C_3 species take advantage of springtime soil moisture, low temperature, and minimal competition from neighboring C_4 grasses to accumulate biomass early in the growing season (Ode et al. 1980). Such 'drought avoidance' strategies make these species less sensitive to summer drought as much of their vegetative life cycle is completed before mid-summer when competitively superior C_4 species dominate (Knapp et al., 1998). CAM plants (i.e., Cacti and succulents) are infamous temporal 'drought avoiders' as their stomata are open only during nighttime hours when evapotranspiration is minimized. Deep-rooted forbs/shrubs can avoid drought by tapping into deeper soil water pools that are isolated from both competitive and evaporative pressures (Nippert and Knapp, 2007). Interestingly, many deep-rooted species often bring water from deeper soil pools and re-distribute it in shallower soil layers (i.e. hydraulic lift), thereby allowing shallow-rooted species to avoid drought (Yu and D'Odorico, 2015). Rare ephemeral species exhibit 'drought escape' strategies whereby the entire plant life cycle, from germination to flowering, is completed during brief periods of high soil moisture (Kooyers, 2015). Thus, while many 'drought escaping' species live in arid or semi-arid regions of the world, they never experience physiological drought stress. The term, 'drought tolerance', applies only to those species that experience tissue dehydration and still attempt to maintain gas exchange and physiological

function as soil moisture declines (Kooyers, 2015). Drought tolerant species are at constant risk of physiological stress either due to carbon starvation or hydraulic failure (McDowell et al. 2008). To maintain high photosynthetic rates, plants must maintain high stomatal aperture and transpiration; however, as soil moisture declines and the atmospheric vapor pressure deficit increases, maintained transpiration can cause physical stress to xylem conduits (Zimmermann, 1983). Decreased leaf water potential can induce xylem cavitation and hydraulic failure as air bubbles are sucked into xylem conduits and spread rapidly under extreme negative pressures (Pockman et al., 1995). Thus, plants are faced with a tradeoff between potentially irreversible damage to their hydraulic network or reduced carbon assimilation (Meinzer et al. 2010). The degree of stomatal control over leaf water status is described as either isohydric (i.e. conservative strategy of closing stomata early to maintain high water potential) or anisohydric (i.e. risky strategy of maintained stomatal conductance with declining leaf water potential), with most plants falling somewhere in between (Skelton et al. 2015; Ocheltree et al. 2016; Fu et al. 2019).

Direct quantification of plant drought strategies (i.e., drought avoidance, escape, or tolerance) requires lengthy procedures which are often impractical to implement across multiple species on broad spatial/temporal scales (Sack et al. 2002; Brodribb et al. 2003; Skelton et al. 2015; Meinzer et al. 2016). Plant trait ecology has been recognized as an efficient means of linking plant physiology with community ecology to predict ecosystem responses to climate change (Reich, 2014). Plant traits are defined here as easily measured characteristics that are representative of physiological function. For example, leaf traits such as specific leaf area (SLA; the ratio of leaf area to leaf dry mass) and leaf nitrogen content (LNC) are well correlated with maximum photosynthetic rate (Reich et al., 1998; Evans and Poorter, 2001), and have previously been used to sort species according to drought tolerance vs. avoidance strategies (Frenette-Dussault et al.,

6

2012; Kooyers, 2015). When weighted by species relative abundance, community SLA and LNC are descriptive of spatial and temporal dynamics of ANPP (Garnier et al., 2004; Reich, 2012) and thus may be linked to ecosystem drought sensitivity. Using plant traits to understand grassland responses to drought may be especially informative given that ANPP in these ecosystems is generally controlled by 1-3 species (Smith and Knapp, 2003).

In the following chapters, I utilize both experimental and observational data, coupled with a systematic literature review, to investigate the mechanisms of differential ecosystem sensitivity to extreme drought. First, I describe an observational study that demonstrates differential ecosystem sensitivity to and recovery from a natural drought (chapter 2). Using a systematic literature review (chapter 3), I identify clear knowledge gaps in the field of plant traits research and provide guidelines for using plant traits to understand ecosystem sensitivity to PPT. In chapter 4, I describe a method for rapidly assessing leaf level drought tolerance and validate this method for use in herbaceous plants. Finally, in chapter 5, I employ a plant trait-based framework within a coordinated, long-term, and multi-site drought experiment (i.e., EDGE – *described above*) to assess the impacts of long-term drought on community functional composition and identify mechanisms of ANPP drought sensitivity.

1.2 Summary of Chapters

In 2013, annual PPT returned to near average amounts at each of the six EDGE sites, providing an opportunity to assess potential legacy effects of the 2012 drought on ANPP recovery. Legacy effects are defined as alterations in resources or ecosystem properties that continue to affect an ecosystem post-drought (Yahdjian and Sala, 2006). In chapter 2, I describe the legacy effects of the 2012 drought at each of the six EDGE sites and test two main hypotheses. First, I test whether legacy effects of drought are negative across all six EDGE sites. Long-term records of ANPP and

PPT suggest that dry years lead to negative legacy effects (i.e., lower ANPP following the return of average PPT than would be expected; Sala et al., 2012) due to plant mortality and/or a sustained deficit in soil moisture after drought subsides (Reichmann et al., 2013). While positive legacy effects are less common, they are not unheard of (Whitford et al. 1995). During dry years, nitrogen (N) mineralization continues while plant N-uptake is diminished (Hofer et al., 2017). Thus, positive legacy effects of drought can occur due to a pulse in available nutrients with replenished soil moisture. Second, I test the hypothesis that drought sensitivity is correlated with the magnitude of legacy effects (Smith, 2011). In other words, if ANPP is highly responsive to precipitation, then greater sensitivity during dry years should correspond to greater sensitivity to wet (or average) years, regardless of legacy directionality (i.e. positive/negative). In addition to testing current ecological theories, I introduce the six focal grassland sites within which EDGE is implemented.

Chapter 3 describes the results of a systematic review of >500 manuscripts that all assess plant traits within the context of altered water availability. Plant traits can be used to predict ecosystem responses to environmental change using a response–effect trait framework (Suding et al., 2008). To do this, appropriate traits must be identified that explain a species' influence on ecosystem function ("effect traits") and the response of those species to environmental change ("response traits"). Response traits are often identified and measured along gradients in plant resources, such as water availability; however, PPT explains very little variation in most plant traits globally. Given the strong relationship between plant traits and ecosystem functions, such as ANPP, and between ANPP and PPT, the lack of correlation between PPT and plant traits is surprising. This literature review categorizes this broad field of research and provides a framework for future surveys of plant traits within the context of altered water-availability. The overarching goal of this review is to identify potential causes for the weak relationship between commonly

measured plant traits and water availability so that we may identify more appropriate response traits.

Hydraulic traits linked to drought tolerance (e.g., leaf vulnerability to cavitation) often require tedious and lengthy measurement protocols. Plant trait ecologists require high throughput methods for measuring plant traits on a variety of species/genotypes and on large spatial and temporal scales. In chapter 4, I describe a method for rapidly assessing a key metric of leaf-level drought tolerance in herbaceous plants. Leaf turgor loss point (π_{TLP}; the leaf water potential at which cells lose turgor causing the plant to wilt) is traditionally estimated from pressure-volume curves. The osmometer method for assessing π_{TLP} from leaf osmotic potential at full turgor (π_o) increases the measurement speed of this trait by 50-fold compared to the traditional method; however, it has only been tested in woody species (Bartlett et al., 2012a). In this chapter, I extend the use of the osmometer method to herbaceous plant species, particularly graminoids, and assess the mechanistic value of π_o as a drought tolerance trait in grasslands.

Finally, I describe the impact of four years of experimental drought on ANPP and functional composition of six North American grasslands. Functional composition is defined by both functional diversity and community-weighted trait means (CWMs). Functional composition can affect the stability of aboveground net primary production (ANPP) in response to climate extremes. Further complexity arises, however, when functional composition itself responds to environmental change. In chapter 5, I describe both the response of functional composition to long-term drought as well as the corresponding effect that has on ecosystem function at broad spatial and temporal scales.

CHAPTER 2: LEGACY EFFECTS OF A REGIONAL DROUGHT ON ABOVEGROUND
NET PRIMARY PRODUCTION IN SIX CENTRAL US GRASSLANDS[1]

2.1 Summary

Global climate models predict increases in the frequency and severity of drought worldwide, directly affecting most ecosystem types. Consequently, drought legacy effects (drought-induced alterations in ecosystem function post-drought) are expected to become more common in ecosystems varying from deserts to grasslands to forests. Drought legacies in grasslands are usually negative and reduce ecosystem function, particularly after extended drought. Moreover, ecosystems that respond strongly to drought (high sensitivity) might be expected to exhibit the largest legacy effects the next year, but this relationship has not been established. We quantified legacy effects of a severe regional drought in 2012 on post-drought (2013) aboveground net primary productivity (ANPP) in six central US grasslands. We predicted that (1) the magnitude of drought legacy effects measured in 2013 would be positively related to the sensitivity of ANPP to the 2012 drought, and (2) drought legacy effects would be negative (reducing 2013 ANPP relative to that expected given normal precipitation amounts). The magnitude of legacy effects measured in 2013 was strongly related ($r^2 = 0.88$) to the sensitivity of ANPP to the 2012 drought across these six grasslands. However, contrary to expectations, positive legacy effects (greater than expected ANPP) were more commonly observed than negative legacy effects. Thus, while the sensitivity of ANPP to drought may be a useful predictor of the magnitude of legacy effects, short term (1-year) severe droughts may cause legacy effects that are more variable than those observed after multi-year droughts.

---

[1] Griffin-Nolan RJ, Denton EM, Johnston M, Carroll CJW, Collins SL, Smith MD, Knapp AK. (2018). Legacy effects of a regional drought on aboveground net primary production in six central US grasslands. *Plant Ecology*, 219(5), 505-515

2.2 Introduction

Drought, defined meteorologically as a "prolonged absence or marked deficiency of precipitation" (IPCC 2013), has shaped the structure and functioning of grasslands globally, particularly those in central North America (Woodhouse and Overpeck 1998; Clark et al. 2002). Severe droughts, and climate extremes more broadly (Smith 2011), are expected to increase in frequency and intensity with climate change, and there is evidence that drought severity has already increased (Dai 2011; 2013; Ponce-Campos et al 2013; Trenberth et al. 2014; Griffin and Anchukaitis 2014; Cook et al 2015). In general, drought results in a decline in ecosystem functions such as aboveground net primary production (ANPP) and soil CO_2 flux (Hoover et al. 2014; Shi et al. 2014). Drought also alters structural attributes, such as tiller and rooting density (Plaut et al 2013; Reichmann et al. 2013), which can have prolonged post-drought effects on ecosystem function.

Drought legacies, defined as alterations in resources or ecosystem properties that continue to affect an ecosystem post-drought (*sensu* Yadjidan & Sala 2006), can be negative or positive (Sala et al. 2012), and thus can either exacerbate or offset (partially) the negative effects of drought on ecosystem function. Negative drought legacies, characterized by reduced ANPP after a drought relative to that expected, may occur when there is a soil moisture deficit that persists after the drought (despite increased precipitation inputs), or if there is drought-induced mortality of plants or senescence that constrains ANPP responses after drought has subsided (Yahdjian and Sala 2006; Sala et al. 2012; Reichmann et al. 2013). Positive drought legacies, when ANPP is higher than expected after a drought (Seastedt and Knapp 1993), have been linked to increased light availability (Slik 2004) or elevated soil nitrogen (N) availability after drought (Whitford et al. 1995; Reynolds et al. 1999; Hofer et al. 2017). From an analysis of long-term records of

precipitation and ANPP in 16 grasslands, Sala et al. (2012) concluded that drought legacies are predominantly negative in grasslands worldwide. A recent analysis of forest tree growth after drought led to a similar conclusion (Anderegg et al. 2015). The impact of drought legacies is predicted to be positively related to drought severity and the magnitude of ecosystem responses to drought (Yahdjian and Sala 2006; Smith 2011); thus, negative drought legacies are expected to become more pronounced in the future as drought severity intensifies.

Grassland ecosystems, which cover >30% of Earth's terrestrial surface, are ideal study systems for assessing the impacts of drought and subsequent drought legacies on ANPP because most are water-limited ecosystems (Noy-Meir 1973; Webb et al. 1978; Sala et al. 1988) and are highly responsive to changes in precipitation (Knapp and Smith 2001; Hsu et al. 2012). In 2012, grasslands in the central US experienced a severe and extensive drought (the fourth largest drought since 1895) characterized by a ~40% reduction in growing season precipitation across the region (Knapp et al. 2015). Taking advantage of the regional uniformity of these precipitation reductions, Knapp et al. (2015) assessed ecosystem sensitivity to the 2012 drought of six native grassland ecosystems ranging from a desert grassland in New Mexico to a mesic tallgrass prairie in Kansas. The sensitivity of ANPP to drought varied two-fold among these six grasslands and was negatively correlated with mean annual precipitation (MAP), a pattern that is consistent with previous models predicting the high sensitivity and responsiveness of xeric ecosystems to drought (Huxman et al. 2004; Diffenbaugh et al. 2008).

The differential drought sensitivity observed across the major grasslands of the central US, combined with a return to average precipitation in 2013 (Table 2.1), provided an opportunity to assess the legacy effects of the 2012 drought on ecosystem function (ANPP) in 2013. We tested two hypotheses: (1) that legacy effects of drought in these grasslands would be negative (Sala et

al. 2012) given the severity of the 2012 drought (rated as severe to extreme, http://www.droughtmonitor.unl.edu/), and (2) that differences in drought sensitivity among these grasslands would be positively related to the *magnitude* of the legacy effects observed, regardless of whether legacies were positive or negative (Yahdjian and Sala 2006; Smith 2011) (Fig. 2.1).

2.3 Materials and Methods

2.3.1 Study sites

Potential legacy effects of the 2012 drought were measured in 2013 in the same six grassland ecosystems used by Knapp et al. (2015) to determine drought sensitivity. These six sites encompass the major grassland types in the central US spanning a west-east MAP gradient of 244 to 863 mm (>3-fold difference) as well as a north-south mean annual temperature (MAT) gradient of 6.8 ºC (Table 2.1). Soil textures across these sites vary from sandy to clay loams (Burke et al. 1989, 1991; Keift et al. 1998). ANPP was quantified in un-grazed pastures in 2012 and 2013. Apart from the two mixed-grass prairie sites (HYS and HPG; Table 2.1), which were lightly grazed two years prior to this study, these sites had not been grazed by domestic herbivores for >10 years prior to the 2012 drought. The tallgrass prairie site (KNZ) is subjected to frequent (annual) prescribed fire, a common management practice in the region that has replaced the frequent wildfires that historically maintained the structure and function of this grassland (Knapp et al. 1998).

2.3.2 ANPP and climate data

From each grassland site, historical ANPP data were compiled from the literature or from online data sources and combined with ANPP measured at each site in 2012 and 2013. ANPP was also measured in 2014 and 2015 to provide a more robust measure of long-term mean ANPP and ensure that ANPP pre- and post-drought (after the single legacy year) were similar. This resulted in 8 to 32 years of data for each site (see Knapp et al. (2015) for additional details on data sources).

Corresponding data on annual precipitation amounts were taken from on-site rain gauges when available or retrieved from the nearest NOAA weather station (http://www.ncdc.noaa.gov/). Both long-term mean ANPP and MAP were calculated excluding data from the 2012 drought year and 2013 legacy year.

Estimates of ANPP were based on end-of-season or peak biomass harvests for the SGS, HPG, HYS, and KNZ sites. In contrast, biomass was estimated allometrically twice during the growing season for the two Sevilleta sites (SBK and SBL) using species-specific equations with changes over time used to estimate ANPP (Muldavin et al. 2008). Succulent plant ANPP was not included in productivity estimates and was a relatively minor component of the vegetation in most plots. Sample sizes and specific plot dimensions varied slightly depending on the study prior to 2012. In 2013, all aboveground biomass was harvested at the end of the growing season from three 0.1-m^2 quadrats randomly located within thirty 4-m^2 plots for SGS, HPG, HYS, and KNZ (n=90 quadrats/site). Similarly, ANPP was estimated using species-specific allometric equations from four 1-m^2 quadrats within ten 4-m^2 plots for SBK and SBL (n=40 quadrats/site) (Muldavin et al. 2008). In all cases, biomass produced in previous years (easily identified by grey coloration) was excluded from estimates of current year ANPP.

2.3.3 Data analysis

Long-term datasets were used to calculate mean ANPP and precipitation, with 95% confidence intervals (CI), for each site. The relative ANPP responses in 2012 (drought sensitivity) and 2013 (drought legacy effects) were calculated as anomalies from mean ANPP:

$$\text{Drought Sensitivity} = \left| \frac{2012 \text{ ANPP} - \text{Mean ANPP}}{\text{Mean ANPP}} \right|$$

$$\text{Drought legacy effects} = \frac{2013 \text{ ANPP} - \text{Mean ANPP}}{\text{Mean ANPP}}$$

14

This measure of legacy effects was justified as 2013 precipitation amounts fell within the 95% CI of MAP at five of six sites (a significant 9% reduction from MAP was observed at KNZ in 2013), thus average ANPP would be expected in the absence of legacy effects (Table 2.1). Legacy effects were considered statistically significant if 2013 ANPP was above (positive legacy) or below (negative legacy) the 95% CI for the site-specific long-term mean of ANPP. Drought sensitivity is shown as the absolute value of 2012 ANPP anomalies; thus, higher values indicate higher sensitivity. A general linear model was used to determine whether the drought sensitivity magnitude (i.e. absolute value) was related to the drought legacy effects (including directionality); however, a second regression analysis was included using the magnitude (absolute value of drought legacy effects) to observe potential relationships between relative ANPP responses that may be hidden due to legacy directionality (Fig. 2.1).

The magnitude of drought legacy effects was also regressed against variables that have been shown to be predictive of lagged ANPP responses to precipitation. These included the difference in precipitation between the drought and recovery year relative to MAP for each site ([2013 Precipitation - 2012 Precipitation]/MAP) as well as the Standardized Precipitation Evapotranspiration Index (SPEI) (Yahdjian and Sala 2006). SPEI, a common measure of drought severity, was calculated for the 2012 growing season defined separately for each site (April-Sept for SGS, HPG, HYS, and KNZ and April-Oct for SBK and SBL; Knapp et al. 2015). All regression analyses and confidence intervals were calculated in R version 3.4.0.

2.4 Results

The drought in 2012 reduced ANPP in all six grasslands relative to the long-term mean, ranging from a 35% reduction in the southern mixed grass prairie (HYS), the least drought sensitive site, to >65% reductions in both Sevilleta sites, SBL and SBK, the most drought sensitive

15

sites (Fig. 2.2). Despite near average precipitation in 2013, ANPP deviated significantly from the long-term mean at most sites, ranging from a 49% relative *reduction* in the C3-dominated northern mixed grass prairie (HPG) to a >145% relative *increase* at both SBL and SBK (Fig. 2.2).

Contrary to our predictions, we observed positive drought legacy effects on ANPP more frequently than negative legacy effects across these six grasslands (Fig. 2.2). Legacy effects (i.e. significant deviations from the expected mean ANPP, given average precipitation levels) were evident in four of the six grasslands (SBK, SBL, HPG, and KNZ; Fig. 2.2). Three of these legacy effects were positive (SBK, SBL, and KNZ), with a negative legacy effect observed at HPG. There was no observable drought legacy effect on ANPP in the southern mixed grass prairie (HYS) or shortgrass prairie (SGS). It is worth noting that 2013 was the most productive year on record for the Sevilleta sites (14 and 16 years of LTER data for SBL and SBK, respectively), despite receiving an average amount of annual rainfall.

Drought legacy effects were significantly correlated with drought sensitivity across these six grassland sites (Fig. 2.3A). This positive relationship was much stronger when drought sensitivity was regressed against the magnitude of legacy effects, irrespective of legacy directionality (R^2=0.88; Fig. 2.3B). The variability in the magnitude of legacy effects across sites was much higher than the variability in drought sensitivity (ANPP anomaly range of 0.36 and 1.85 for 2012 and 2013, respectively; Fig. 2.3). The magnitude of drought legacy effects was not correlated with either SPEI or the difference in precipitation between the drought and post-drought years, two variables commonly used to explain drought legacy effects on ANPP (Table A1.1; Yahdjian and Sala 2006). Finally, we saw no evidence of any lagged effects of the 2012 drought on ANPP in 2014 or 2015, although precipitation during these years was less comparable across sites than in 2012 and 2013.

2.5 Discussion

Drought legacies can extend the influence of drought well beyond its meteorological occurrence. Legacy effects of drought, and more broadly the lagged effects of antecedent precipitation on current year ecological processes (Ogle et al. 2015), have been widely reported to be negative (Yahdjian and Sala 2006; Sala et al. 2012; Reichmann et al. 2013; Anderegg et al. 2015); however, positive, as well as a complete lack of drought effects on post-drought function, have also been reported (Seastedt and Knapp 1993; Slik 2004; Hermance et al. 2015; Wagg et al. 2017). For example, an experimentally induced 2-yr extreme drought elicited extreme ANPP responses (significantly rare compared to historical responses; Smith 2011) in the Konza tallgrass prairie, yet there was no post-drought legacy effect on ecosystem function (ANPP) the next year (Hoover et al. 2014). Thus, greater understanding of the potential relationship between the sensitivity of ecosystems to drought and legacy effects of drought is needed, particularly given the forecasted increase in drought severity and frequency (Dai 2011; 2013).

In this study, we observed legacy effects of the severe 2012 regional drought on ecosystem function (ANPP) in 2013 and, as predicted by Smith (2011), we found a strong correlation between the ecosystem drought sensitivity and the magnitude of the legacy effect observed post-drought (Fig. 2.3B). Although Sala et al. (2012) concluded that drought legacies are predominately negative in grasslands, positive legacies were observed in half of the grasslands studied here (Fig. 2.2). A significant negative legacy effect was observed in only one grassland, HPG, the site with the highest C_3 grass cover. It is worth noting that HPG experienced the most severe drought in 2012, as indicated by SPEI (Table 2.1), which may have contributed to the negative legacy effect. As expected, no legacy effect was detected in the grassland that was least responsive to the 2012 drought (HYS). While considerable plot-level variability in ANPP suggests a lack of legacy effects

at SGS (Fig. 2.2 – SGS), the mean for 2013 ANPP was well above the long-term mean. Additionally, Hermance et al. (2015) observed a positive legacy effect of the 2012 drought in the shortgrass steppe of Colorado (SGS) based on NDVI estimates of plant production in 2013. ANPP at the two Sevilleta sites (SBK and SBL) was historically high in 2013 (Fig. A1.3), which we attribute to drought legacy effects; however, rainfall patterns in 2013 likely played a role in this system, where ANPP is highly responsive to the timing and size of rain events in the late summer monsoon season (Muldavin et al. 2008).

Although negative drought legacies have several potential mechanisms, results from field experiments suggest that plant mortality or loss of meristematic tissues (stems, buds, tillers, etc.) during extreme or prolonged drought can be particularly important for constraining plant growth post-drought, even when abundant precipitation is available (Yahdjian and Sala 2006; Reichmann et al. 2013). Indeed, meristem limitation has been proposed as a mechanism limiting production responses to increased precipitation in many chronically water limited ecosystems (Knapp and Smith 2001; Dahgleish and Hartnett 2006). Although we did not attempt to quantify plant mortality or meristem density after the 2012 drought, observations made at each site during end of season sampling did not reveal any obvious increases in plant mortality. It is likely that drought of extended duration or greater severity would be required for such plant mortality and increased meristem limitation to occur.

Positive drought legacies are most commonly attributed to higher soil N availability post-drought, a result of continued N-mineralization but reduced N-uptake during drought (Seastedt and Knapp 1993; Whitford et al. 1995; Reynolds et al. 1999; Yahdjian et al., 2006; Sala et al. 2012; Hofer et al. 2017). Indeed, N dynamics are highly correlated with variation in NPP among grasslands globally (Stevens et al. 2015). Although Reichmann et al. (2013) showed that N-

addition could not offset the negative effects of drought-induced meristem reductions, the effects of N-fertilization may become apparent if plant mortality is minimal, such as during a 1-year drought.

It is tempting to conclude that relatively short-term (1-year) severe droughts are more likely to lead to positive legacy effects whereas long-term, or more extreme droughts that cause mortality, will result in negative legacy effects; however, there is abundant evidence that negative drought legacy effects can result from single-year droughts (Oesterheld et al. 2001; Sala et al. 2012; Fig. 2.2 – HPG). This variability in legacy effects of short-term drought may be particularly pronounced in more water-limited ecosystems where rainfall timing and event size are strong determinants of the variability in ANPP, soil N availability and drought sensitivity (Heisler-White et al. 2008; Raz-Yaseef et al. 2010; 2012; Cherwin and Knapp 2012; Petrie et al. 2015).

Precipitation is expected to become more variable in the near future, with the frequency of both short-term (1-yr) and long-term droughts increasing (Dai 2011; 2013; Ponce-Campos et al 2013; Trenberth et al. 2014; Griffin and Anchukaitis 2014; Cook et al 2015). A clear understanding of how the magnitude and directionality of legacy effects on ecosystem function differ between short vs. long-term droughts is crucial given the implications for carbon storage and nutrient cycling. This is especially true within arid and semi-arid ecosystems, such as grasslands, which often experience both short- and long-term droughts (Ahlström et al. 2015). The strong correlation between the sensitivity of ANPP to drought and the magnitude of drought legacy effects the following year suggests that greater understanding of the determinants of differential ecosystem sensitivity to drought will also provide insight into ecosystem function post-drought.

2.6 Tables

Table 2.1. Site characteristics for six central US grasslands affected by the 2012 regional drought. Mean annual precipitation (MAP; ±95% confidence intervals [CI]), mean annual temperature (MAT), and mean aboveground net primary production (ANPP; g m-2 ±95% CI). Mean ANPP and MAP were calculated excluding 2012 and 2013 values. ANPP (±SE for plot variability) and precipitation (PPT) amounts are shown for 2012 and 2013. Standardized Precipitation Evapotranspiration Index (SPEI) was calculated for the site-specific 2012 growing season. Climatic data were taken from the nearest NOAA sites or from LTER rain gauges. See Fig. A1.1 and A2.2 for distributions of long-term ANPP and precipitation data. Sites include a desert grassland [Sevilleta National Wildlife Refuge, dominated by black grama, *Bouteloua eriopoda* (C_4) – SBK] and a southern shortgrass steppe [Sevilleta National Wildlife Refuge, dominated by blue grama (*Bouteloua gracilis* (C_4)) – SBL] in New Mexico; a northern shortgrass steppe [Central Plains Experimental Range, dominated by *B. gracilis* – SGS] in Colorado; a northern mixed-grass prairie [High Plains Grassland Research Center, co-dominated by *Pascopyron smithii* (C_3) and *B. gracilis* – HPG] in Wyoming; as well as a southern mixed-grass prairie [Hays Agricultural Research Center, co-dominated by *P. smithii*, *Bouteloua curtipendula* (C_4), and *Sporobolus asper* (C_4) – HYS] and a tallgrass prairie [Konza Prairie Biological Station, dominated by *Andropogon gerardii* (C_4) and *Sorghastrum nutans* (C_4) – KNZ] in Kansas.

	Site[a]	MAP (mm)	MAT (ºC)	Mean ANPP (g m^{-2})	2012 PPT (mm)	2013 PPT (mm)	2012 ANPP (g m^{-2})	2013 ANPP (g m^{-2})	2012 SPEI
SBK	Sevilleta Black grama	244±39	13.4	98±39	187	251	34±6	243±17	-1.49
SBL	Sevilleta Blue grama	257±52	13.4	66±26	195	299	19±3	189±20	-1.49
SGS	Shortgrass Steppe	366±30	9.5	94±16	189	362	42±2	126±20	-2.16
HPG	High Plains Grassland	415±44	7.9	137±30	232	447	69±3	69±3	-2.4
HYS	Hays Agricultural Research Center	581±96	12.3	246±57	362	547	159±9	245±12	-1.82
KNZ	Konza Prairie	864±74	13	413±42	569	787	250±8	492±16	-1.57

2.7 Figures
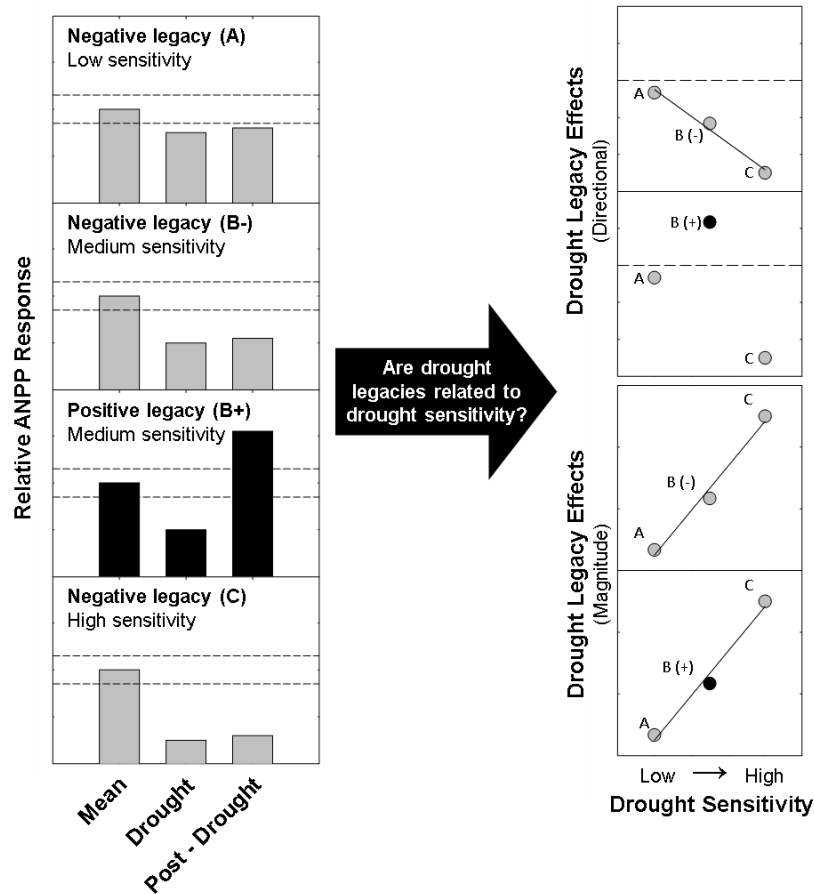
Figure 2.1. Hypothetical ANPP responses of three grasslands varying in drought sensitivity (from least to most sensitive: A, B, C) and potential legacy effects. Depicted on the left are differential responses of aboveground net primary productivity (ANPP) for each site during a drought year and a post-drought year. Long-term mean ANPP with 95% CI (dashed lines) is also shown for reference. Assuming the drought was of equal magnitude across all sites and precipitation in the post-drought year was near average, drought sensitivity and legacy effects can be calculated as anomalies from the long-term mean ANPP (i.e. % deviation) in the drought year and post-drought year, respectively. Legacy directionality is indicated as anomalies above (+) or below (-) the 95% CI for mean ANPP. As predicted by Sala et al. (2012), negative legacy effects are shown across all sites; however, an alternative positive legacy effect of similar magnitude is shown for the site with medium drought sensitivity (B+). Potential cross-site relationships between drought sensitivity and legacy effects (depicted on the right) can incorporate negative (●) and positive (●) legacy effects or simply focus on the magnitude of the legacy effect by plotting the absolute value of the post-drought ANPP response. (The dashed line in the "directional" relationship represents zero legacy effect with positive legacies being above the line and negative legacies below it). The relationship between the responsiveness of ecosystems during and post drought is more accurately visualized using the drought legacy magnitude.

21
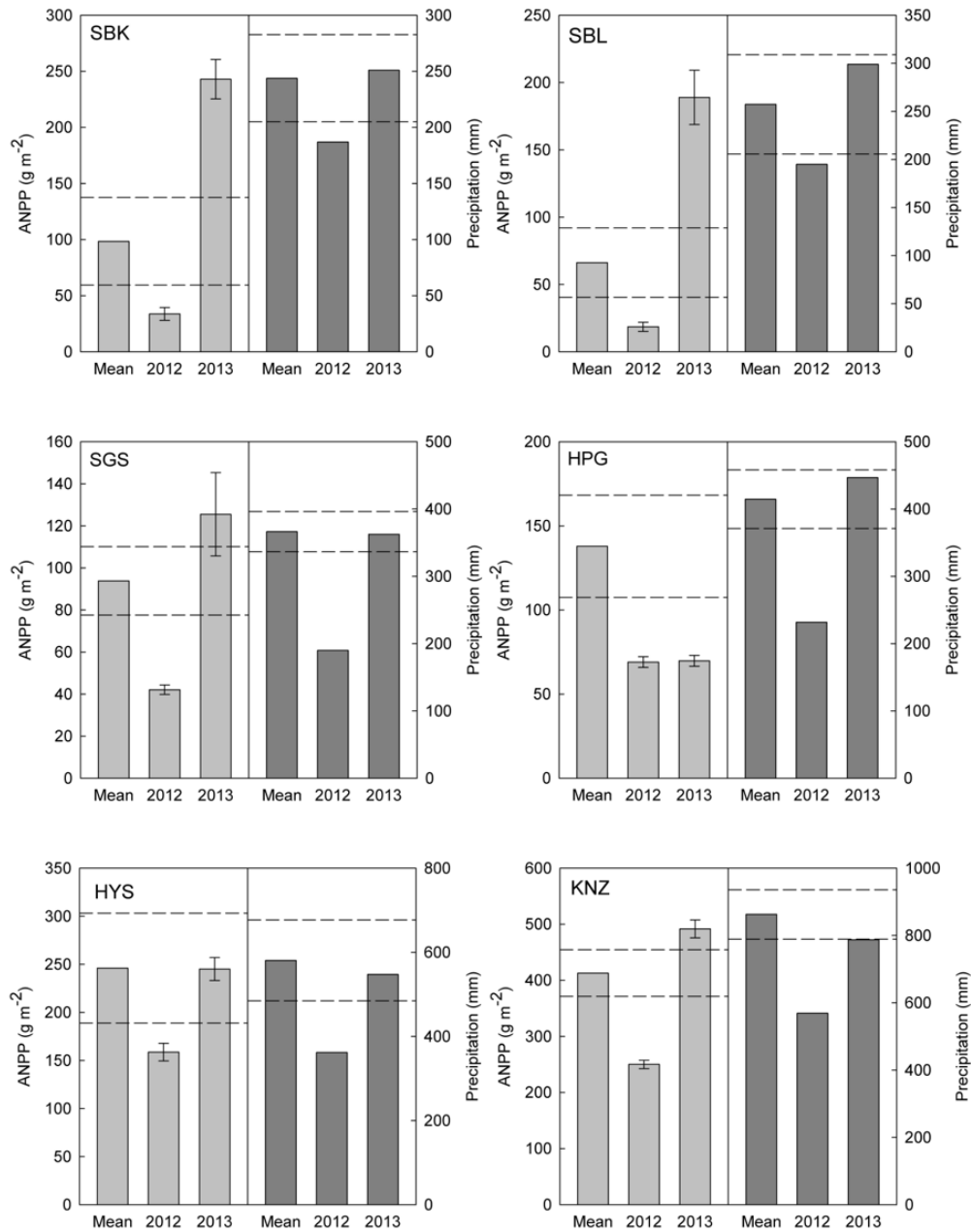
Figure 2.2. Aboveground net primary production (ANPP, ▨) and annual precipitation (■) for six central US grasslands: Sevilleta – black grama (SBK), Sevilleta – blue grama (SBL), Shortgrass Steppe (SGS), High Plains Grassland (HPG), Hays (HYS), and Konza prairie (KNZ). For each site, the long-term means (excluding 2012 and 2013) for ANPP and Precipitation are shown with 95% confidence intervals (dashed lines) as well as 2012 and 2013 mean ANPP (±SE of plot variability) and annual precipitation. Given the near average precipitation in 2013, ANPP responses outside of the 95% CI are considered statistically significant legacy effects (α=0.05). Years of long-term data per site: SBK=16, SBL=14, SGS=28, HPG=11, HYS=8, KNZ=32.
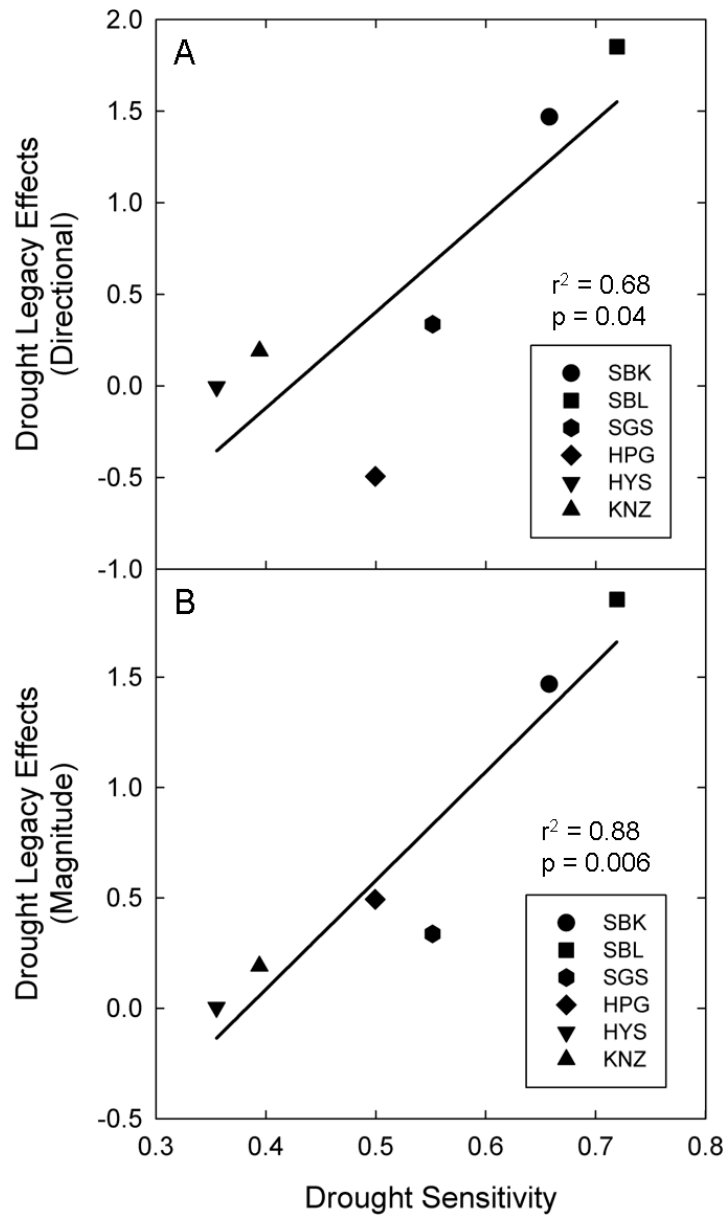
Figure 2.3. The relationship between drought sensitivity and legacy effects across six central US grasslands (**A**). Both positive and negative ANPP anomalies are included in this "directional" relationship. The relationship between drought sensitivity and legacy effects more accurately presented and strengthened when the magnitude of the legacy effects is shown (**B**). See Table A1.1 for linear model results. By calculating the magnitude, or absolute value, of ANPP anomalies, the responsiveness of ANPP in the drought year can be compared to responsiveness in the recovery year, irrespective of directionality. This relationship suggests that a large ANPP response to a 1-year severe drought may lead to a large ANPP response in the recovery year, regardless of whether the response is positive or negative. See Table 2.1 for site abbreviations and Fig. A.1.3 for the distribution of ANPP anomalies over time for each site. *Drought sensitivity* = |2012 ANPP – Mean ANPP / Mean ANPP|. *Drought legacy effects* = 2013 ANPP – Mean ANPP / Mean ANPP.

CHAPTER 3: TRAIT SELECTION AND COMMUNITY WEIGHTING ARE KEY TO UNDERSTANDING ECOSYSTEM RESPONSES TO CHANGING PRECIPITATION REGIMES[2]

3.1 Summary

Plant traits can be used to predict ecosystem responses to environmental change using a response-effect trait framework. To do this, appropriate traits must be identified that explain a species influence on ecosystem function ('effect traits') and the response of those species to environmental change ('response traits'). Response traits are often identified and measured along gradients in plant resources, such as water-availability; however, precipitation explains very little variation in most plant traits globally. Given the strong relationship between plant traits and ecosystem functions, such as net primary productivity (NPP), and between NPP and precipitation, the lack of correlation between precipitation and plant traits is surprising.

We address this issue through a systematic review of >500 published studies that describe plant trait responses to altered water-availability. The overarching goal of this review was to identify potential causes for the weak relationship between commonly measured plant traits and water-availability so that we may identify more appropriate 'response traits'.

We attribute weak trait-precipitation relationships to an improper selection of traits (e.g. non-hydraulic traits) and a lack of trait-based approaches that adjust for trait variation within communities (only 4% of studies measure community-weighted traits). We then highlight the mechanistic value of hydraulic traits as more appropriate 'response traits' with regard to precipitation, which should be included in future community-scale trait surveys.

---

[2] Griffin-Nolan RJ, Bushey J, Carroll CJW, Challis A, Chieppa J, Garbowski M, Hoffman A, Post AK Slette, IJ, Spitzer D, Zambonini D, Ocheltree TW, Tissue D, Knapp AK. (2018). Trait selection and community weighting are key to understanding ecosystem responses to changing precipitation. *Functional Ecology*, 32, 1746–1756.

Trait-based ecology has the potential to improve predictions of ecosystem responses to predicted changes in precipitation; however, this predictive power depends heavily on the identification of reliable response and effect traits. To this end, trait surveys could be improved by a selection of traits that reflect physiological functions directly related to water-availability with traits weighted by relative abundance.

3.2 Introduction

Global climate change models predict a future with more frequent climate extremes (e.g. drought) and increased inter- and intra-annual variability in precipitation, which will fundamentally alter the spatial and temporal patterns of water-availability in terrestrial ecosystems worldwide (Trenberth, 2011; Dai, 2011; 2013; Ciais et al., 2013; IPCC; 2013). These predicted changes in precipitation will alter terrestrial ecosystem properties such as net primary production (NPP), carbon (C) cycling, and biodiversity, along with other important ecosystem services. The sensitivity of these ecosystem functions to changes in precipitation can vary among ecosystems, although a mechanistic understanding of this variability remains unresolved (Smith, Knapp, and Collins 2009; Luo et al. 2011, Knapp et al. 2015).

One approach to advance our understanding of ecosystem responses to environmental change is to use a response-effect trait framework (Suding et al. 2008). This framework categorizes species in a community based on 'effect traits' representing their relative influence (strong or weak) on specific ecosystem functions, such as NPP. For example, plant functional traits such as specific leaf area (SLA), leaf nitrogen content, and leaf area index have been used to explain plot level variability in NPP from grasslands to forests (Garnier et al. 2004; Reich, 2012; Forrestel et al. 2017). 'Response traits' are used to describe the change in relative abundance or size of a species in response to environmental change. In the context of water-availability, traits related to

25

hydraulic function (e.g. plant hydraulic conductance) are most likely to respond to precipitation (Reich, 2014), yet the extent to which these traits are used in the response-effect framework has yet to be surveyed (Rosado et al. 2014). Appropriate response and effect traits, once identified, can be used to understand shifts in community composition due to environmental filtering (Suding et al. 2008).

Experimental tests of the response-effect trait framework have generally been conducted over short time scales (i.e. 1-2 years; Klumpp and Soussana, 2009); however, climate change is expected to cause long-term chronic alterations in plant available water (Smith et al. 2009). Thus, the response-effect trait framework may be most useful for predicting ecosystem responses to altered precipitation if merged with the hierarchical response framework (Smith et al. 2009), which describes temporal dynamics of ecosystem responses to chronic changes in resource availability (Fig. 3.1). The response of an ecosystem to chronic resource alteration can be predicted over time depending on the relative importance of (1) dominant species physiology, (2) species reordering within communities, and (3) species migration (Smith et al. 2009). A wealth of literature describes the physiological responses of dominant species to extreme climate events (reviewed by Felton and Smith, 2017); however, a community-wide survey of plant response and effect traits is required to predict community shifts in response to long-term chronic alterations in water-availability. The predictive power of 'effect traits' is dependent on relevant 'response traits' of the dominant species as well as the response/effect traits of subordinate and transient species that may change in abundance with climate change (Grime, 1998; Suding et al. 2008). Thus, incorporating the response-effect trait framework into the hierarchical response framework requires the identification of appropriate response and effect traits (Fig. 3.1).

Plant ecologists have long observed and measured traits along climatic gradients to determine environmental filters of community assembly (Diaz, Cabido, & Casanoves, 1998). These trait-climate relationships can be used to identify plant 'response traits', a key research objective in community ecology (Suding et al. 2008); however, precipitation explains very little global variation in commonly measured plant traits (Wright et al., 2004; Moles et al., 2014; Forrestel et al., 2017). This is surprising given the utility of traits for understanding ecosystem function (Diaz and Cabido, 1997; Garnier et al., 2004; Reich, 2012; van der Sande et al., 2017) and the strong relationship between precipitation and NPP, which is widely considered a key metric of ecosystem function (Sala et al., 1988; Knapp & Smith, 2001; Huxman et al., 2004; Fahey and Knapp 2007; Knapp et al. 2017). To address this issue and better understand how traits might be used to forecast responses to alterations in precipitation regimes, we conducted a systematic review of plant traits literature in the context of altered water-availability. We aim to categorize how plant traits are measured across biomes to (1) identify potential reasons for weak trait-climate relationships and (2) reveal relevant knowledge gaps that can be addressed with future research. More specifically, we aim to highlight the value of hydraulic traits for providing a mechanistic understanding of plant responses to water-availability, especially when assessed at the community level. Lastly, we discuss the ecological significance of identifying response and effect traits for predicting differential ecosystem responses to precipitation.

3.3 Systematic Review

We reviewed the literature on plant trait research within the context of water-availability to categorize the most commonly measured traits and their method of measurement. In total, 1,341 manuscripts (published in 215 peer-reviewed journals from the years 1991- mid 2017) were identified using key words broadly related to plant traits and water-availability (See A2.1 in

Appendix 2). Each manuscript was screened and included in our review if it met the following criteria: (1) one or more plant trait(s) were measured on vascular plants from non-agricultural terrestrial ecosystems; (2) plant traits were measured across contrasting levels of water-availability; and (3) inclusion of a statistical test relating trait values to water-availability. A list of plant traits (defined as: "Any morphological, physiological or phenological feature measurable at the individual level, from the cell to the whole-organism level, without reference to the environment or any other level of organization" – Violle et al., 2007) was compiled from the TRY database (www.try-db.org) and the standardized plant traits handbook (Pérez-Harguindeguy et al., 2013) to help define criteria #1. Modeled or simulated traits were not included in this review. Plants in pots or common garden experiments were included only if plant available water was manipulated. Criteria #2 was met by precipitation gradients and/or experimental manipulations of soil moisture. Criteria #3 was included in our screening protocol to exclude studies that measured plant traits at varying levels of water-availability but did not explicitly analyze plant responses to water (e.g. traits were measured at different soil moisture levels, but statistical significance of trait-water relationships was not assessed).

The plant functional type (PFT) surveyed in each manuscript was recorded as either (1) graminoid, (2) forb (non-graminoid herbaceous), (3) shrub, (4) broad-leaf tree, (5) needle-leaf tree, or (6) other (e.g. ferns). If multiple plant PFTs were studied in one manuscript and the traits measured were specific to each PFT, then the manuscript was counted as two separate studies, one for each PFT. For each manuscript, the source of variation in water-availability was recorded as either a (1) spatial precipitation gradient, (2) temporal (seasonal) precipitation gradient, (3) temporal (inter-annual) precipitation gradient, (4) local microclimate/edaphic differences (i.e., shallow vs. deep soils), (5) water addition/removal (field setting), or (6) water additional/removal

(greenhouse setting). Traits were categorized according to the organ measured (leaf, stem, root/belowground organ, reproductive organ, or whole-plant trait) and by trait category (morphological, anatomical, biochemical, photosynthetic, hydraulic, phenological, and/or other; Table 3.1). Lastly, the ecological scale at which traits were measured was recorded as: (1) single population of a single species, (2) multiple populations of a single species, (3) single populations of multiple species, (4) multiple populations of multiple species, or (5) community-weighted trait (CWT; trait values presented as the mean of a plot/community with each species' trait value weighted by relative abundance, such as percent cover/basal area).

3.4 Plant traits and water-availability: progress to date

A total of 568 manuscripts (42% of those initially identified) were included based on our screening protocol. Within these papers, a clear division was observed whereby publications have focused on plant traits of either woody (W) or herbaceous (H) growth forms with relatively few studies comparing the two forms (W = 334 manuscripts; H = 183 manuscripts; Both = 51 manuscripts; Fig. A2.1). Thus, at present, woody species (primarily tall-statured trees) dominate this field of plant traits research. The striking divide within plant trait ecology between W- and H-focused manuscripts was unexpected given that many traits, such as those of the leaf economic spectrum, can easily be measured in both growth forms (Weiher et al., 1999; Wright et al., 2004). Increased data sharing and the prevalence of large trait databases (e.g. TRY database; Kattge et al., 2011) should facilitate trait comparisons across functional groups. Additionally, we observed very few differences between W- and H- focused manuscripts in the methods used to alter water-availability (Fig. A2.2-A) or the ecological scale of trait measurements (Fig. A2.2-B), which should make data synthesis across growth forms more feasible.

The dichotomy between W- and H- focused manuscripts revealed clear growth form differences in types of traits measured (See Appendix A2.2 and Fig. A2.2). Hydraulic traits were more often measured on W species than H species (W: 47%; H: 26%; percentages based on number of manuscripts relative to the total number per growth form), and photosynthetic traits were more commonly measured on H species (W: 13%; H: 36%). This trend could be due to increased interest in the hydraulic mechanisms of tree mortality within the last decade (McDowell et al., 2008; Allen et al., 2010; Adams et al., 2017). It may also reflect the historical importance of measuring water uptake, storage, and transport in long-lived trees compared to herbaceous plants with small water storage capacity and, consequently, more challenging techniques for assessing hydraulic properties. Given that the water transport system and carbon economy in plants are intrinsically linked, dual measurements of these physiological traits would likely reveal more informative 'response traits'. One promising linkage between these two trait categories is the quantification of isohydricity, based on stomatal and hydraulic sensitivity to drought, a technique that has been used successfully in both woody (Skelton, West, & Dawson, 2015) and herbaceous plants (Ocheltree, Nippert, & Prasad, 2016); however, isohydricity has yet to be incorporated into community scale response-effect trait surveys.

Combining W- and H- manuscripts revealed several trends across this subset of plant traits research. For example, leaf hydraulics (and stem hydraulics in the case of woody species) have been highly studied in response to water-availability, while the hydraulic traits of other organs have received minimal attention (Fig. 3.2). An understanding of leaf hydraulics is important given that leaves contribute the largest portion of hydraulic resistance in a plant (Sack & Holbrook, 2006); however, root hydraulics also provide critical understanding of whole plant recovery from extreme events such as drought (Lo Gullo et al., 1998) and merit increased attention. In general,

our survey identified a striking lack of research on root traits beyond simple morphological measurements (Fig. 3.2). Given the sensitivity of belowground processes to precipitation (Fay et al., 2003) and the importance of root traits as drivers of ecosystem function (Bardgett, Mommer, & De Vries, 2014), future response-effect trait surveys should consider measuring root traits. Indeed, a consideration of traits across all plant organs is necessary and currently lacking (Fig. 3.2). Recent evidence suggests that an economic trait spectrum describing plant strategies for acquiring light, nutrients, and water exists for both stems and roots, not just leaves (Reich, 2014; Prieto et al., 2015). Thus, surveys of traits along gradients in water-availability should include traits across all organs and trait categories (Table 3.1) to better identify appropriate response and effect traits.

Here, we have categorized trait measurements within the context of water-availability and identified several key research gaps needing attention (see Appendix A.2, Fig. 3.2, Fig. A2.1, and Fig. A2.2). A subset of these 568 manuscripts, however, was further analyzed to determine why traits do not align well with precipitation gradients and develop suggestions for how trait sampling methods can be altered to identify more appropriate 'response traits'.

3.5 Community-weighted response traits

Plant traits have been used to assess functional variation along climatic gradients (Diaz et al. 1998; Wright et al., 2004; ter Steege et al., 2006; Pepe et al., 2011) which assists model predictions of community assembly and species distributions with climate change (Thuiller et al., 2004; Suding et a. 2008). But as noted above, most commonly measured plant traits do not align well with precipitation gradients. For instance, mean annual precipitation (MAP) explained <1% of the global variance in specific leaf area (SLA; leaf area to dry mass ratio – correlated with maximum photosynthetic rate) across biomes (Wright et al., 2004) and was not significantly

related to SLA within grasslands (Forrestel et al., 2017). Furthermore, the combination of several climatic variables (mean annual temperature, MAP, vapor pressure deficit, and solar irradiance) explained <20% of the variance in five functional traits related to resource acquisition strategies (Reich, Wright & Lusk, 2007). These weak relationships have been attributed to MAP as a poor proxy for plant-available water. Indeed, other indices of aridity, and even temperature, may explain a larger portion of trait variation (Moles et al., 2014). However, the large precipitation gradient (MAP: 133 - 5,300 mm yr^{-1}) spanned in the Wright et al. (2004) analysis likely captured significant spatial variability in plant-available water. Additional complexity arises from well documented shifts in community composition due to chronic alterations in water-availability (Smith et al. 2009; Collins et al. 2012). Thus, 'response traits' that can explain community shifts likely exist and are masked along precipitation gradients due to high within-site trait variability (Freschet et al., 2010; Onada et al., 2011; Siefert et al., 2015).

Plants often display patterns of apparent niche differentiation which can be identified from observations of species abundance along hydrologically defined niche space (Silvertown et al., 1999), and more recently demonstrated within the context of water-availability using isotopic proxies for rooting depth (Nippert & Knapp, 2007). Niche differentiation can be manifest within a single site as high trait diversity, which must be accounted for in broad spatial surveys of plant traits. This can be accomplished by community-weighting traits, whereby community average trait values are presented for a single site with species traits weighted by their % cover or contribution to overall biomass. Assessing plant traits at the scale of the community inherently requires more time and effort. It is thus not surprising that only 23 of the 568 studies (4% of surveyed manuscripts) measured community-weighted traits (CWT; Fig. A2.1). While time-consuming, these community-scale trait measurements often improve trait-climate relationships, with 91% of

CWT-manuscripts presenting statistically significant relationships between CWT means and water-availability (see Table A2.1).

Community-scale trait measurements can account for a large portion of within-site trait variability, yet not all CWT-climate relationships are useful for predicting responses to changing water-availability (Fig. 3.3, Table A2.1). For example, the most commonly measured community-weighted trait, SLA, was not significantly related to water-availability in ~40% of studies. Moreover, those relationships that are significant often explain very little trait variability. A recent survey across >15,000 grassland locations in France revealed that community weighting commonly measured functional traits (e.g. SLA, leaf dry matter content (LDMC), and leaf N and P concentrations) yielded a statistically significant relationship between traits and precipitation, yet precipitation still explained <1% of trait variability (Borgy et al., 2017). Additionally, the most common CWTs (SLA, Height, and LDMC) do not show consistent directional relationships with water-availability (Fig. 3.3), which may suggest the utility of traits is site- or biome- specific.

To test this, we compared three similar studies that all measured seed mass (Sm) and SLA (two commonly measured CWTs related to reproductive and resource acquisition strategies, respectively) across precipitation gradients within grassland ecosystems. While these traits are expected to respond predictably to water-availability (Wright et al. 2004; Guittar et al. 2016; Rota et al. 2017; Butterfield et al. 2017), we observed variable CWT- precipitation relationships (positive, negative, and lack of relationship) across these studies even though the type of biome and water-availability gradient was consistent (Fig. 3.4). SLA is dependent on a variety of environmental variables and is constrained by leaf size (Milla et al. 2008), thus it is unsurprising that this trait does not consistently respond to altered water-availability; nonetheless, SLA is the most commonly measured CWT (Fig. 3.3). Community-weighting is necessary to account for trait

variability to identify likely 'response traits', however, it must be combined with an appropriate selection of traits (Rosado et al. 2014). Hydraulic traits are likely candidate 'response traits' given they are mechanistically linked to precipitation (Reich, 2014).

3.6 Hydraulic response traits

After reviewing the literature, we argue that traits of the leaf economic spectrum – the tradeoff between allocating resources to high photosynthetic rate and rapid growth vs. nutrient storage, herbivory defense, and longevity (Wright et al., 2004; Reich 2014) – are useful for assessing plant responses to nutrients (Niinemets & Sack, 2006) and light (Richardson et al., 2005), yet are unreliable within the context of water-availability (Wright et al., 2004; Reich et al. 2007), even when community-weighted (Fig. 3.3). A transition away from leaf economic traits and towards traits mechanistically linked to water transport is necessary to identify appropriate 'response traits' related to precipitation.

Recent work in diverse tropical rainforests suggests that anatomical traits related to hydraulic function, such as stomatal characteristics and vein density, are decoupled from common LES traits such that two trait spectrums exist: the economic spectrum (associated with light capture and carbon economics) and the hydraulic spectrum (associated with water transport; Li et al., 2015). Indeed, Reich (2014) has noted that LES traits should be measured in combination with traits related to the hydraulic safety vs. efficiency tradeoff (Zimmerman, 1983; Meinzer et al., 2010; Nardini, Pedà, & Rocca, 2012; Blackman et al., 2014; Ocheltree et al., 2016) to provide a more accurate description of water acquisition strategies. Water-availability in natural ecosystems is transient, depending on rainfall patterns and extreme events (i.e. drought), which are inherently rare and unpredictable (Smith, 2011). Thus, the inclusion of these traits related to water transport (leaf, stem, or root maximum hydraulic conductance - K_{max}) and drought tolerance (leaf turgor loss

point (Ψ_{TLP}) and vulnerability to xylem cavitation) allows for better understanding of plant responses to both high and low levels of water-availability (Reich, 2014). Additionally, these traits align well with precipitation gradients (Blackman, Brodribb, & Jordan, 2012) and are related to relative plant performance during drought (Kursar et al., 2009). Thus, we posit that the incorporation of hydraulic traits into community-scale surveys of plant response-effect traits should improve temporal predictions of ecosystem responses to chronic alterations in water-availability (Fig. 3.1).

Hydraulic traits were well surveyed in the manuscripts we reviewed (Fig. 3.2; n=232 or 41% of surveyed manuscripts), however, few hydraulic traits or even anatomical traits related to hydraulic function (e.g. xylem vessel area or stomatal density) were surveyed at the community scale (<10% of CWT-manuscripts; Table A2.1). Additionally, a large portion of hydraulic trait papers present trait values for a single species (n = 114 manuscripts) or make comparisons between species with no inclusion of relative abundance (n = 107 manuscripts). The lack of community-level hydraulic trait measurements likely reflects the lengthy lab procedures required to measure traits such as leaf hydraulic conductance and Ψ_{TLP} (Sack et al., 2002; Brodribb & Holbrook, 2003) versus the rapid field assessments of plant morphology (the most commonly measured trait category; Fig. 3.2).

Recent developments in high-throughput methods for assessing drought tolerance should encourage surveys of community-weighted hydraulic traits (Bartlett et al. 2012a). Bartlett et al. (2012a) describe a method for assessing Ψ_{TLP} with a vapor pressure osmometer which increases measurement speed fifty-fold and has since been used in broad-scale surveys of drought tolerance of tropical tree species (Maréchaux et al., 2015). Ψ_{TLP} has long been recognized as a valuable indicator of plant water stress and is correlated with plant-available water, as well as vulnerability

to xylem cavitation (Blackman, Brodribb, & Jordan, 2010). Rapid assessment of Ψ_{TLP} will facilitate surveys of community-weighted hydraulic traits across broad spatial scales; however, this technique still requires validation in herbaceous-dominated communities.

Anatomical traits related to hydraulic transport and water use efficiency, such as stomatal pore index (SPI; % of leaf area composed of stomata; Sack et al., 2003), can be easily measured at the community level as samples can be collected and preserved for later trait determination. Indeed, recent work suggests that community-weighted SPI is well correlated with MAP across both herbaceous and woody dominated ecosystems and is linked to spatial variation in NPP (Forrestel et al., 2017; Liu et al., 2017; Fig. 3.5). These findings suggest that SPI, and other anatomical traits linked to hydraulic function, are promising trait candidates for predicting NPP responses to chronic alterations in water-availability (Suding et al. 2008; Smith et al. 2009; Fig. 3.1).

3.7 Conclusions

Climate change will intensify Earth's hydrologic cycle leading to chronic alterations of plant available water (IPCC 2013), which will differentially affect terrestrial ecosystems. Commonly measured plant traits (e.g. SLA, plant height, leaf N, etc.) have been successfully used to predict plant growth and NPP dynamics (Diaz and Cabido, 1997; Garnier et al. 2004; Reich, 2012; Diaz et al. 2016; Forrestel et al., 2017; van der Sande et al., 2017), yet often do not align with gradients in water-availability (Wright et al. 2004). We attribute these weak Trait-precipitation relationships to an improper selection of traits. We argue that more useful 'response traits' can be identified along precipitation gradients if traits related to hydraulic function are measured at the community level. Once identified, 'response traits' can be regressed against well-known 'effect traits' to aid in predictions of ecosystem responses to global climate change (Suding

et al. 2008; Fig. 3.1). However, key to linking these traits to community and ecosystem responses is scaling them by their abundance (i.e. community-weighting). At present, trait-based approaches that adjust for trait variation within communities are uncommon (only 4% of studies measure community-weighted traits). Adopting this approach is critical, however, for incorporating shifts in community composition, or species re-ordering, that occur with chronic alterations in water-availability – as predicted by the hierarchical response framework (Smith et al. 2009).

3.8 Tables

Table 3.1. Definitions of categories used to classify traits, and examples for each category, used in a literature review of manuscripts with a focus on plant trait responses to altered water-availability. Definitions and examples were modified from those presented by Perez-Harguindeguy et al. (2013) and the TRY database.

Trait Category	Definition	Examples
Morphological	Traits dealing with (1) plant size, shape, mass, and form, or (2) organ ratios or (3) growth rate; generally measured at the organ scale and mostly associated with external parts of a plant.	Specific leaf area, seed mass, plant height, leaf thickness, specific root length, root:shoot ratios
Anatomical	Traits dealing with the presence, absence, density, or size of key plant characteristics at the tissue level (vascular, dermal, or ground tissue)	Trichome density, stomatal length, palisade mesophyll thickness
Biochemical	Traits involving concentrations, ratios, and use-efficiencies of plant nutrients, secondary compounds, or pH (not including biochemical compounds involved in photosynthesis)	Leaf N content, C:N ratio, lignin concentration, enzyme activity, leaf pH
Photosynthetic	Physiological/biochemical traits involved light capture, gas exchange, and carbon assimilation (including biochemical compounds such as chlorophyll and rubisco)	Net photosynthesis, stomatal conductance, chlorophyll fluorescence, chlorophyll a/b
Hydraulic	Physiological traits involved in plant water status, water transport, and water storage all in the liquid phase (including osmolytes concentrations)	Hydraulic conductivity, leaf turgor loss point, osmotic potential, minimum water potential
Phenological	Traits that deals with timing, seasonality, or lifespan	Flowering time, leaf lifespan
Other	Traits related to non-hydrological disturbances or biogeochemical cycles. Only used if trait does not fall within an above category	Frost resistance, flammability, decomposition rate, or palatability

3.9 Figures
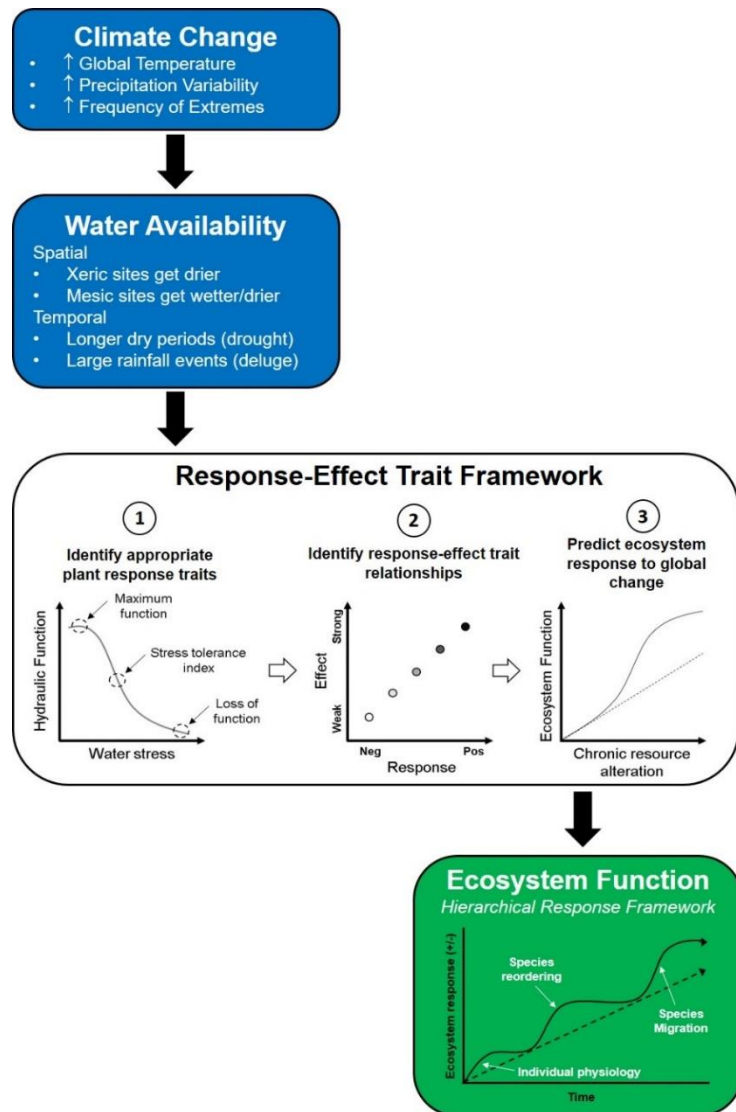
Figure 3.1. Climate change will impact ecosystem functioning in many ways, with changes in water-availability one of the primary mechanisms; however, ecosystems may differ dramatically in the magnitude and time scale of their responses to changes in water-availability. A response-effect trait framework can be used to predict ecosystem responses to altered water availability (the following is modified from Suding et al. 2008). First, reliable mechanistic traits must be identified. In the context of water-availability, hydraulic traits linked to maximum hydraulic function (e.g. leaf hydraulic conductance), loss of function (e.g. stomatal closure) and stress tolerance (e.g. vulnerability to xylem cavitation and turgor loss) are appropriate trait candidates given their physiological link to plant-available water (**#1**). Second, traits must be measured for multiple species within the community and regressed against traits linked to their effect on ecosystem function (**#2**; shades of grey represent different species in the community, each with a unique environmental response (positive/negative) and effect (strong/weak) on ecosystem function). An understanding of which species will respond to resource alterations along with the effect that those species have on ecosystem function can help improve predictions of ecosystem responses to chronic resource alteration (**#3**; shown are both linear and non-linear ecosystem responses to changes in resource availability driven by different combinations of response and effect traits). Once these goals are met, the predictions from the response-effect trait framework can be incorporated into long term predictions made by the hierarchical response framework. While physiological responses of species suffice for short-term predictions, response and effect traits can be incorporated into later stages of the hierarchical response framework to include community change via species re-ordering/migration (Smith et al. 2009).
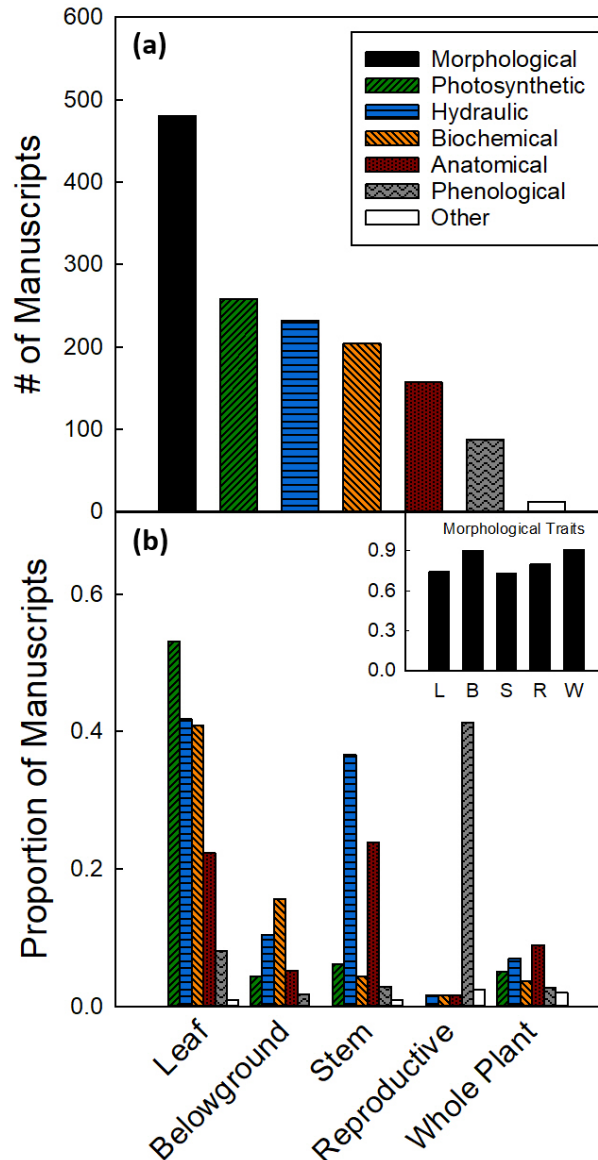
Figure 3.2. A comparison of the frequency with which traits are measured within each plant organ and trait category in response to altered water-availability. **(A)** The total number of manuscripts that measure each trait category across both herbaceous and woody species. **(B)** Data for trait category by organ comparisons are shown as the proportion of manuscripts that measure traits of each organ (e.g. proportion of "leaf manuscripts" that measure morphological traits). As manuscripts often present several traits (i.e. both leaf anatomical and morphological traits), the proportions presented here do not sum to 100. Morphological traits dominate the literature across all plant organs (~85% of manuscripts) and are thus shown separately as an inset (letters correspond to organ type). Leaf traits are well surveyed across all trait categories. Hydraulic traits are well studied in both leaves and stems (woody stems specifically), with very few manuscripts assessing either belowground or whole plant traits beyond morphology.
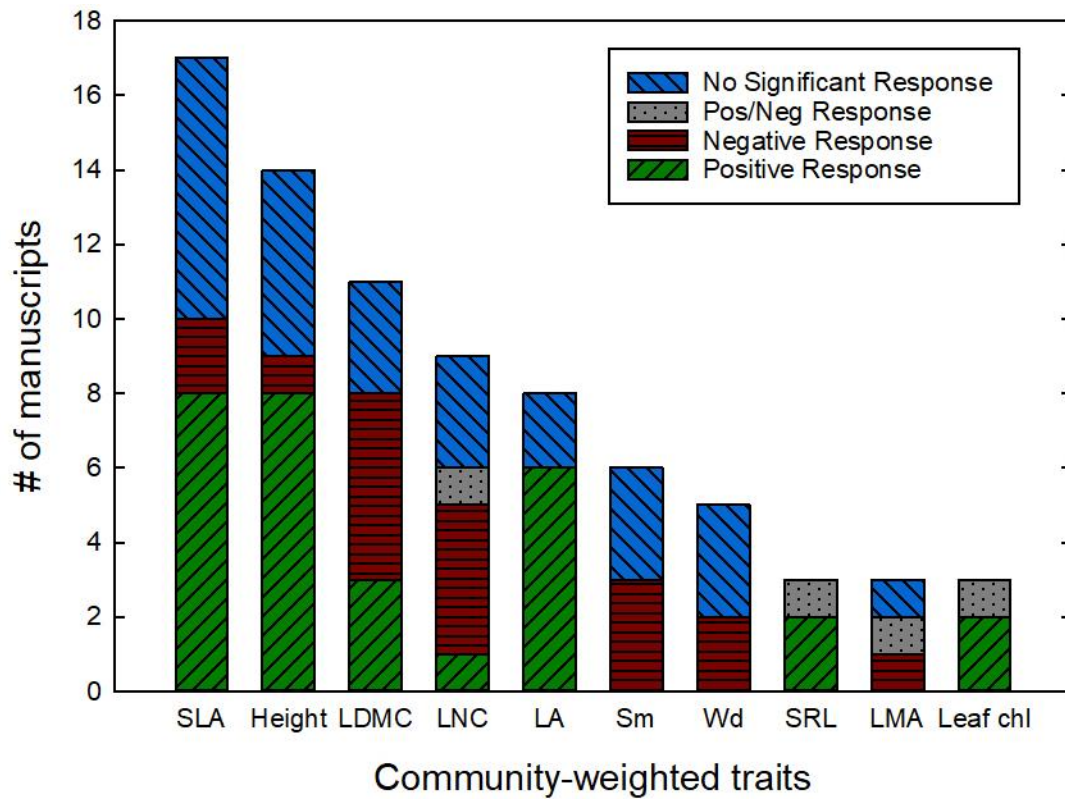
Figure 3.3. The specific plant traits that are most commonly measured as community-weighted traits (CWT) arranged in order of decreasing frequency (traits shown here were assessed in at least 3 of the manuscripts we surveyed). Also depicted is the proportion (stacked bars) of the manuscripts that show statistically significant ($p<0.05$) trait-by-water relationships as well as the directionality of those relationships. Note that the overwhelming majority of CWTs are morphological with very few physiological traits (hydraulic or photosynthetic). SLA = specific leaf area, Height = maximum plant height, LDMC = leaf dry matter content, LNC = leaf nitrogen content, LA = leaf area, Sm = seed mass, Wd = wood density, SRL = specific root length, LMA = leaf mass per area, Leaf chl = leaf chlorophyll content.
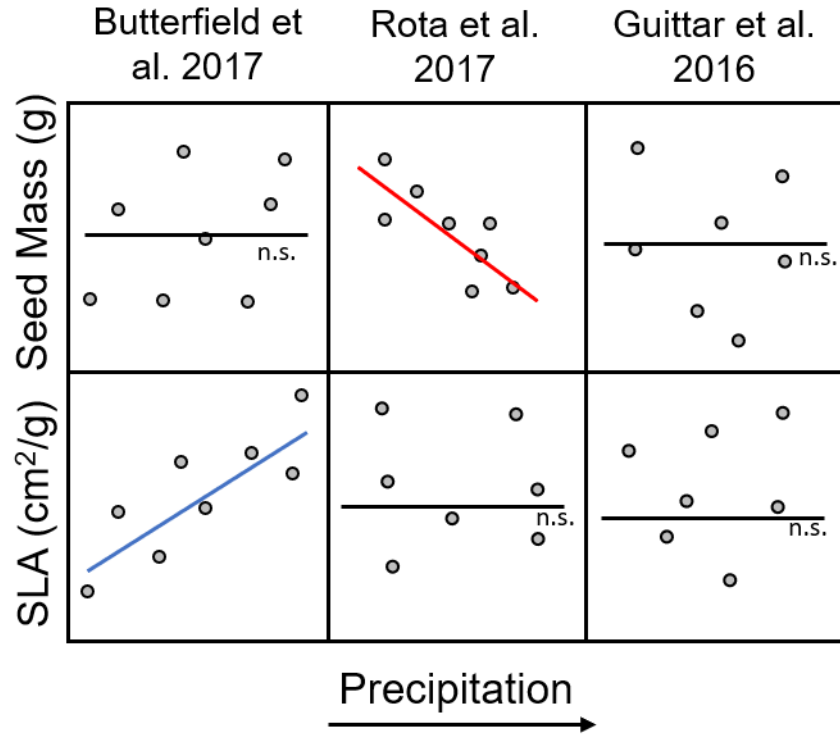
Figure 3.4. Specific leaf area (SLA) and seed mass (Sm) were identified as two of the most commonly measured community weighted traits. The expected individual and community-level responses of these traits to resource-availability are well described. In resource-limited environments, SLA is expected to decrease as individuals produce smaller leaves and/or more conservative species increase in abundance. Sm tends to decrease with resource availability due to increased success, and thus abundance, of smaller seeds with neutral effects on large seeds, which tend to be successful across resource gradients. The above examples describe results from three separate studies that assessed community-weighted SLA and Sm across spatial precipitation gradients within grasslands. Butterfield et al. (2017) show a significant SLA response (+) to increased water availability, but no significant Sm response. Rota et al. (2017) show a significant Sm response (-) to increased water availability, but no significant SLA response. Guittar et al. (2016) show no significant response for either trait. The inconsistent relationships seen across these studies conducted in the same vegetation type with similar methodologies suggest that these traits are not the appropriate 'response trait' candidates for assessing community responses to water-availability. While community-weighted traits are necessary to produce significant trait-climate relationships, it is also important to choose the correct trait candidates given the specific environmental and physiological context. Note: figures do not display actual data, but rather depict general relationships presented in these manuscripts.
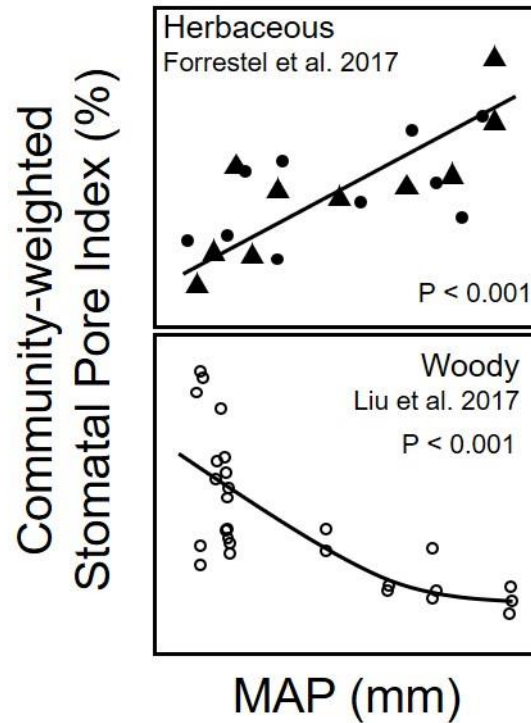
Figure 3.5. Relationships between mean annual precipitation (MAP) and community weighted stomatal pore index (SPI; % of leaf area composed of stomata) in herbaceous-dominated (South African [●] and North American [▲] grasslands; Forrestel et al. 2017) and woody-dominated communities [○] (temperate to tropic forests in China; Liu et al. 2017). SPI is an anatomical index of maximum stomatal conductance and plant water-use efficiency. Community weighted SPI is a likely candidate for determining broad-scale trait-precipitation relationships, although its interpretation may change depending on ecosystem type (woody- vs. herbaceous- dominated). Plotted data taken from Forrestel et al. 2017 and Liu et al. 2017 (note: axes for MAP and SPI are not to the same scale for each study).

CHAPTER 4: EXTENDING THE OSMOMETER METHOD FOR ASSESSING DROUGHT TOLERANCE TO HERBACEOUS SPECIES[3]

4.1 Summary

Community scale surveys of plant drought tolerance are essential for understanding semi-arid ecosystems and community responses to climate change. Thus, there is a need for an accurate and rapid methodology for assessing drought tolerance strategies across plant functional types. The osmometer method for predicting leaf osmotic potential at full turgor (π_o), a key metric of leaf-level drought tolerance, has resulted in a 50-fold increase in the measurement speed of this trait; however, the applicability of this method has only been tested in woody species and crops. Here, we assess the osmometer method for use in herbaceous grassland species and test whether π_o is an appropriate plant trait for understanding drought strategies of herbaceous species as well as species distributions along climate gradients. Our model for predicting leaf turgor loss point (π_{TLP}) from π_o ($\pi_{TLP} = 0.80\pi_o - 0.845$) is nearly identical to the model previously presented for woody species. Additionally, π_o was highly correlated with π_{TLP} for graminoid species ($\pi_{tlp} = 0.944\pi_o - 0.611$; $r^2 = 0.96$), a plant functional group previously flagged for having the potential to cause erroneous measurements when using an osmometer. We report that π_o, measured with an osmometer, is well correlated with other traits linked to drought tolerance (namely, leaf dry matter content and leaf vulnerability to hydraulic failure) as well as climate extremes linked to water-availability. The validation of the osmometer method in an herbaceous-dominated ecosystem paves the way for rapid community-scale surveys of drought tolerance across plant functional groups, which could improve trait-based predictions of ecosystem responses to climate change.

---

[3] Griffin-Nolan RJ, Ocheltree TW, Mueller KE, Blumenthal DM, Kray JA, and Knapp AK. (2019). Extending the osmometer method for assessing drought tolerance in herbaceous species. *Oecologia*, 189(2), 353-363.

4.2 Introduction

Accurate and efficient quantification of drought tolerance within plant communities is needed given that water is a primary limiting resource for plants across much of the world (Knapp et al. 2017) and extreme droughts are expected to become more common with climate change (Dai 2011; 2013; IPCC 2013). The response of ecosystem processes, such as aboveground net primary productivity, to drought has been shown to vary among ecosystems (Huxman et al. 2004), even within the same biome (Knapp et al. 2015); however, a mechanistic understanding of this variability is lacking. Hydraulic traits, such as leaf turgor loss point and xylem vulnerability to cavitation, can provide a mechanistic understanding of plant growth and survival as well as community assembly in response to water stress (*reviewed by* Reich 2014). When scaled up from measurements of individual plants and species, such traits may provide useful information regarding responses of communities and ecosystems to climate change (Suding et al. 2008). Unfortunately, hydraulic traits are infrequently measured in community-scale trait surveys (Griffin-Nolan et al. 2018a), likely due to the time-intensive measurement protocols they require (Sack et al. 2002; Brodribb and Holbrook 2003); thus, a key research need is the identification and validation of rapid, high-throughput methods for assessing drought tolerance that can be applied within and across plant functional types.

Leaf turgor loss point (π_{TLP}), the leaf water potential at which average cell turgor is lost and leaf wilting occurs, provides a wealth of physiological information pertaining to cell wall integrity, stomatal closure and, more generally, the extent to which plants can maintain metabolism as soil dries (Kramer and Boyer 1995; Bartlett et al. 2016; Meinzer et al. 2016). Given this and the strong correlation between π_{TLP} and water availability both within and between biomes, π_{TLP} is an ideal trait for assessing drought tolerance across broad spatial scales (Bartlett et al. 2012b). The

traditional protocol for quantifying π_{TLP}, pressure-volume (p-v) curves, requires a lengthy procedure (up to two days to produce curves for 4-6 leaves) which greatly limits the number of species or locations that can be viably surveyed. Fortunately, π_{TLP} can be estimated from leaf osmotic potential at full turgor, the component of water potential related to cellular solute concentration and a strong determinant of π_{TLP} (Bartlett et al. 2012a). Leaf osmotic potential at full turgor (π_o) is typically quantified from p-v curves as well; however, Bartlett et al. (2012b) recently described a method for rapidly measuring π_o using a vapor pressure osmometer. The method has resulted in a 30- to 50-fold increase in the measurement speed of π_{TLP} and has since been used to quantify community-scale drought tolerance in tropical rainforests (Maréchaux et al. 2015). Since its publication, the osmometer method, and the linear model for predicting π_{TLP} from π_o, has exclusively been used in ecosystems dominated by woody species (Maréchaux et al. 2015; Esperón-Rodríguez et al. 2018) or crops (Mart et al. 2016) and has yet to be validated in herbaceous plant communities, such as grasslands. Indeed, several studies have cautioned that osmometer estimates of π_o may prove inaccurate for leaves with dense large vein networks or thin leaves with large midrib veins (i.e. grass leaf blades) as the inclusion of such veins in tissue sampling may lead to apoplastic dilution (Kikuta and Richter 1992; Maréchaux et al. 2016); thus, testing of the osmometer method within grasslands including such species is needed.

The grassland biome covers more than 30% of Earth's terrestrial surface and provides valuable ecosystem services such as carbon storage, soil stabilization, forage production, and wildlife habitat (Noy-Meir, 1972; Field et al. 1998). Given that most grasslands are water-limited, they are an ideal study system for surveying drought tolerance and responses to future changes in Earth's hydrologic cycle (IPCC, 2013). Here, we focus on grasslands of the American Great Plains, a region characterized by highly variable precipitation and a high frequency of climate extremes

such as drought and flooding (Kunkel et al. 2013). Water-availability will likely become more variable in this region as some of these grasslands are expected to experience more frequent "dust-bowl"-like conditions by the end of the century (Karl, Melillo, and Peterson, 2009).

We conducted a survey of drought tolerance traits of common herbaceous plant species across three North American grasslands to address two main goals. First, we test the validity of the osmometer method (Bartlett et al. 2012a) for use on herbaceous plant species. Validation of this method will encourage community-scale surveys of drought tolerance across plant functional types, especially within a relatively drought sensitive region (i.e. grasslands; Huxman et al. 2004; Knapp et al. 2015), as well as address recent concerns of scientific reproducibility (Baker, 2016). Second, we assess the mechanistic value of π_o as a drought tolerance trait in grasslands. A central goal of trait-based ecology is to make generalized predictions of large-scale phenomenon (e.g. community assembly, nutrient cycling, dynamics of net primary production) using the composite traits of interacting organisms within a community (Shipley et al. 2016). Established links between species distributions, performance, and physiological traits are thus required, yet often difficult to identify (Paine et al. 2018). To this end, we test the hypothesis that π_o will be correlated with other mechanistic traits commonly used to describe leaf-level drought tolerance, namely leaf dry matter content (LDMC) and leaf vulnerability to hydraulic failure (Brodribb 2017). Additionally, we define the climatic extremes of species distributions and test the hypothesis that π_o is positively correlated with water-availability (i.e. species with more negative π_o will predominately inhabit arid regions) (Bartlett et al. 2012b). The degree to which this correlation is driven by the driest or wettest extreme of a species distribution will highlight the relative influence of abiotic stress tolerance (i.e. water-limitation) or biotic stress tolerance (i.e. competition with more resource acquisitive species), respectively, in controlling π_o of herbaceous species.

4.3 Materials and Methods

4.3.1 Plant material

We collected nine species of graminoids and ten species of forbs/subshrubs (non-woody) from three native grassland sites (predominately mixed-grass prairie) across Wyoming and Kansas during mid-summer 2015 (Table 4.1). Six plant samples, including soil and a portion of the root system, were unearthed at each site, placed in a reservoir of water, and covered with large plastic bags (n=6 pots/species/site). Plants were left in the dark for ~12 hours to allow leaves to fully rehydrate prior to p-v curve determination and osmometer measurements.

4.3.2 Osmometer method validation

Pressure-volume curves were measured on one leaf per plant sample (n=6 leaves/species) using the bench drying method (Schulte and Hinckley 1985). A recently expanded mature leaf was wrapped in parafilm wax and cut near the leaf base (parafilm was weighed and subtracted from subsequent leaf weight measurements). Immediately after cutting, the leaf was placed in a Scholander-style pressure chamber (PMS Instruments, Albany, OR, USA) to measure leaf xylem water potential (Ψ_{leaf}). Following water potential determination, the leaf and parafilm were weighed on a micro-balance ($\pm$ 0.1 mg, Ohaus Pioneer; Ohaus Corporation, Parsippany, NJ, USA). The leaf was then sealed in a plastic bag and placed in a dark drawer to allow slow dehydration. This process was repeated approximately 10 times for each leaf or until Ψ_{leaf} reached -4 MPa. The leaf was then rehydrated, scanned for leaf area at 300 dpi (Epson Perfection V600, Epson America Inc., Long Beach, Ca, USA), dried for 48h at 60°C and weighed. Leaf area was calculated using ImageJ software (https://imagej.nih.gov/ij/). Turgor loss point (π_{TLP}), osmotic potential at full turgor (π_{o*pv}) and leaf capacitance (C_{leaf}) were calculated for 5-6 leaves following standard

methods (Turner, 1988; Koide et al. 1989) and averaged for each species. Fresh weight of hydrated leaves and oven-dried weight were used to calculate LDMC (g dry mass g^{-1} fresh mass).

Within 24 hours of p-v curve determination, osmotic potential at full turgor was also estimated using a vapor pressure osmometer (π_{o*osm}) (VAPRO 5520 vapor pressure osmometer, Wescor, Logan, UT), following Bartlett et al. (2012b). Six leaves per species were clipped under water and fully hydrated overnight prior to measuring π_{o*osm}. A leaf disc was sampled from each hydrated leaf using a 5-mm biopsy punch (Miltex DP-5mm, Electrum Supply, Elkhart, IN), wrapped in tin foil, and submerged in liquid nitrogen for ~60 seconds to lyse the plant cell walls. The leaf disc was generally taken toward the apical portion of the leaf to avoid or minimize the sampling of large midrib veins, depending on leaf width. Bartlett et al. (2012b) warn of potential inaccuracies likely to arise when using the osmometer method on species with large midrib veins (e.g. grasses such as *Sorghastrum nutans*) as the symplastic solution may become diluted by xylem water. When possible, the leaf disc was taken from a portion of the lamina without any midrib present (e.g. species with broad leaves). For species with leaves that were narrower than our biopsy punch, several leaves were aligned next to each other and the sample was taken across multiple leaves to ensure comparable disc sizes were sampled across species. Each disc was then punctured ~15 times using forceps to facilitate rapid equilibration in the osmometer chamber. Leaf discs were quickly placed in the osmometer chamber following puncturing to minimize evaporation (<30 seconds between removal from liquid nitrogen and placement in osmometer chamber). Samples were left in the closed chamber for ~10 minutes to allow equilibration. Measurements were then made every two minutes until osmolarity reached equilibrium (<5 mmol kg^{-1} change in osmolarity between measurements). Osmolarity was then converted to osmotic potential at full turgor (π_{o*osm}) using the following equation: π_{o*osm} = osmolarity*-2.3958/1000.

Bartlett et al. (2012b) outline possible discrepancies in osmometer measurements that can arise due to the opposing effects of apoplastic dilution (which leads to overestimations of π_{o*osm}) and cell wall dissolution (which lead to underestimations of π_{o*osm}). To account for such discrepancies, we calculated 'predicted π_{o*osm}' following a model presented by Bartlett et al. (2012b) which includes estimates of these effects:

$$\pi_{o*predicted} = (a \times \pi_{o*pv*af}) + (b \times LDMC) + (c \times \pi_{o*pv*af} \times LDMC) + d \qquad \text{(eqn 2)}$$

where, LDMC is a proxy for cell wall investment and thus dissolution, while $\pi_{o*pv*af}$ is an estimate of osmotic potential at full turgor (from p-v curves) corrected for apoplastic dilution, using apoplastic fraction (a_f) is a proxy ($\pi_{o*pv*af} = \pi_{o*pv} * (1 - a_f)$). P-v curve estimates of a_f were set to zero for one species (ANGE) as estimates were not significantly different from zero. A slope of 1 for the relationship between measured and predicted π_{o*osm} would indicate that accounting for apoplastic dilution and cell wall dissolution corrects this bias in osmometer measurements (Bartlett et al. 2012a).

4.3.3 Leaf hydraulic conductance

Leaf hydraulic vulnerability curves were produced for 12 of the 19 focal species, including both graminoids and forbs/subshrubs, following the rehydration kinetics method (Brodribb and Holbrook 2003). The methodology described here is for graminoids, as vulnerability curves for forbs, subshrubs, and one sedge (*Carex duriuscula*) were taken from previously collected data (Ocheltree *in review*). Several tillers, each with at least two recently emerged leaves of comparable size, were clipped from the rehydrated samples and placed on a bench to dry slowly. Drying time varied from 30 seconds to three hours depending on the species and the desired level of dehydration. Prior to hydraulic conductance measurements, the tiller was sealed in a plastic bag and placed in a dark drawer for 2-3 minutes to allow any water potential gradients across a single

leaf to equilibrate. The more apical leaf was removed from the stem with a razor and placed in a pressure chamber to determine initial leaf water potential (Ψ_0). The second leaf was removed by cutting under filtered de-ionized water that had been de-gassed for 1hr and then rehydrated for a pre-determined amount of time (5-120 seconds depending on Ψ_0). The leaf was then re-cut slightly above the water line and placed in a pressure chamber to determine final rehydrated leaf water potential (Ψ_f). Leaf hydraulic conductance (K_{leaf}) was then calculated using initial and final leaf water potential as well as average capacitance (C_{leaf}; n=6) quantified from p-v curves:

$$K_{leaf} = \frac{C_{leaf} * \ln\left[\frac{\varphi_0}{\varphi_f}\right]}{t} \qquad\qquad \text{(eqn 1)}$$

where t is the rehydration time in seconds. K_{leaf} was calculated for 30-40 leaves varying in hydration status and regressed against Ψ_0. Maximum conductance (K_{max}) was estimated as the mean of the five highest values of K_{leaf} between Ψ_0 of -0.5 and -1 MPa. Leaf hydraulic vulnerability curves were produced by fitting logarithmic, linear, exponential, and sigmoidal models to data binned and averaged to 0.5 MPa intervals and selecting the model with the lowest Akaike Information Criteria (AIC; see Table A3.1 for AIC values). This model was used to calculate the leaf water potential at which K_{leaf} decreases to 50% of K_{max} (P50, in MPa). Vulnerability curves were made for a subset of graminoids in this study (Fig. A3.1), while P_{50} values for forbs/shrubs were taken from Ocheltree (*in review*).

4.3.4 Bioclimatic envelopes

Bioclimatic envelopes of temperature and precipitation were generated using the geographic range of each species. Spatial information on all reported occurrences of each species was downloaded from the Global Biodiversity Information Facility (GBIF; www.gbif.org). The number of reported occurrences ranged from 90 to 8,259 with an average of 1,193

occurrences/species. Climatic data from the nearest 0.5-km grid cell of each reported occurrence were collected from the WorldClim database (http://www.worldclim.org/bioclim). Because GBIF data is spatially biased and one region can be over-represented in a data set (Beck et al. 2014), we subsampled the climate data to remove this bias. If multiple occurrences fell within the same grid-cell of climate data from WorldClim, that grid cell was only used once in our analysis. Further, the occurrence data was filtered to remove any incorrect entries that reported occurrences in aquatic environments (ie. large bodies of water). We focused on variables including estimates of temperature and precipitation seasonality as well as annual summaries of temperature and precipitation (see Table A3.2 and the WorldClim database for a full list of climatic variables). The 5th and 95th quantiles of each variable were calculated from data compiled for all recorded occurrences to quantify bioclimatic envelopes that define the climatic extremes of a species' inhabited range. For example, the 5th quantile of 'precipitation during the wettest month' represents the precipitation during the wettest month in the driest locations of a species range. These bioclimatic envelope parameters have been shown to be more biologically relevant than regional annual climate statistics (Ocheltree et al. 2016).

4.3.5 Data Analyses

Univariate linear regression analyses were used to test for relationships among π_{TLP}, π_{o*pv}, and π_{o*osm}. The assumptions of linear regression (skewness, heteroscedasticity, etc.) were met for all models presented in this study. The slope and intercept of the models presented by Bartlett et al. (2012b) were compared to 95% confidence intervals (CI) of the slope and intercept of the models presented here. The PRESS and RMSE statistics for all method comparison models are available in Table A3.3. The most parsimonious model for estimating both π_{o*pv} and π_{TLP} was determined by calculating AICc values for linear mixed effects models including LDMC, a_f, π_{o*osm}

and all possible interactions as fixed effects (AICc values in Table A3.4). Leaf osmotic potential at full turgor (π_{o*osm}) was also regressed against P_{50} and LDMC to investigate correlations among these functional traits. Traits of different plant functional types (graminoids vs. forb/subshrub) were compared using t-tests. Additionally, hydraulic trait means from Bartlett et al. (2012b) were compared to the range of hydraulic trait values assessed in this study. Relationships between species-specific bioclimatic envelopes and π_{o*osm} were also assessed using a Pearson's correlation matrix ('cor' function in base R). R statistical software version 3.4.4 was used for all statistical analyses.

4.4 Results

4.4.1 Osmometer method validation

Leaf turgor loss point and osmotic potential at full turgor calculated from p-v curves were highly correlated among common herbaceous species within central US grasslands, with 96% of the variation in π_{TLP} explained by π_{o*pv} (Fig. 4.1). Additionally, π_{o*pv} was highly correlated with osmotic potential estimated from a vapor pressure osmometer (π_{o*osm}) (Fig. 4.2), with the slope and intercept not significantly different from that presented by Bartlett et al. (2012b); however, this model did diverge from a 1:1 relationship indicating some bias in osmometer measurements. Using Equation 2, we tested whether the divergence from a 1:1 line in this method comparison could be explained by the opposing effects of apoplastic dilution and cell wall dissolution. The relationship between $\pi_{o*predicted}$ and π_{o*osm} ($r^2=0.78$) did not differ significantly from a 1:1 relationship, indicating no bias after correcting for these factors (Fig. 4.3). Nonetheless, model selection for predicting π_{o*pv} from all combinations of fixed effects (π_{o*osm}, a_f, and LDMC, plus interactions) selected a model with just π_{o*osm} as the most parsimonious (AICc = 10.57; Table

A3.4) with the amount of variance explained only increasing by 13% with the inclusion of a_f and LDMC (plus interactions).

Leaf osmotic potential at full turgor measured with an osmometer was highly correlated with leaf turgor loss point across several common grassland species including graminoids, forbs and subshrubs (Fig. 4.4-A). This linear model for predicting π_{TLP} of predominantly herbaceous species is nearly identical to the woody species model presented by Bartlett et al. (2012b), with a minor offset for the y-intercept (-0.21 MPa). Additionally, the slope and intercept of their model fall within the 95% CI of the grassland model presented here. The strength of the grassland model was improved when forbs and subshrubs were excluded, with 96% of the variation in graminoid π_{TLP} explained by π_{o*osm} (Fig. 4.4-B) – this relationship also did not differ from that of Bartlett et al. (2012b). Among forbs/subshrubs, we did not observe a significant relationship between π_{TLP} and π_{o*osm}.

4.4.2 Mechanistic value of π_o

We found significant differences in trait values between plant functional types (PFT; graminoids vs. forbs/subshrubs). Graminoids had significantly lower pressure potential for all parameters (π_{TLP}, π_{o*pv}, and π_{o*osm}) than forbs/subshrubs (Fig. 4.5), with this PFT difference similar in magnitude to the regional differences observed by Bartlett et al. (2012b) between species sampled from a tropical forest site (annual rainfall = 1532 mm) and a common garden near UCLA (annual rainfall = 450 mm). These average differences between PFTs contributed substantially to the correlations between pressure potential parameters (e.g., π_{TLP} and π_o) among species (Figs. 4.1 – 4.3). Graminoid species also had significantly higher LDMC compared to forbs/subshrubs (mean = 0.39 and 0.25 g g^{-1}, respectively; t-test, p<0.001). No statistical comparisons of P_{50} across PFTs were tested due to the small sample size for forbs/subshrubs (n=3; Table 4.1).

Osmometer estimates of leaf osmotic potential at full turgor were highly correlated with other hydraulic and morphological traits that are indicative of drought tolerance. Specifically, π_{o*osm} was positively correlated with vulnerability to hydraulic failure (P_{50}; see Fig. A3.1 for vulnerability curves), and negatively correlated with leaf dry matter content (LDMC), suggesting there may be coordination among leaf drought tolerance characteristics of these species (Fig. 4.6). Additionally, LDMC was negatively correlated with P_{50} ($r^2 = 0.37$; p=0.02).

The bioclimatic envelopes assessed in this study represent climatic boundaries of a species distribution with high and low quantiles indicating the climate extremes that species experiences across their observed range. For graminoids, the bioclimatic envelope that explained the most variability in π_{o*osm} was mean annual precipitation (MAP) at the wettest extremes (95th quantile) of a species distribution (Fig. 4.7; MAP_{95th} was also significant correlated with π_{o*pv}; $r^2 = 0.60$). This significant positive relationship indicates that π_{o*osm} was less negative for graminoid species that occupy sites characterized by high annual rainfall. This relationship was driven by the wet extremes of a species distribution as there was only a moderately significant relationship between graminoid π_{o*osm} and the 5th quantile of MAP (p = 0.08). Temperature was not a significant predictor of graminoid π_{o*osm}. When PFTs were combined, however, the only significant predictor of π_{o*osm} was temperature; a weak positive relationship ($r^2 = 0.18$; p = 0.04) was observed between π_{o*osm} and the 5th quantile of temperature during the wettest quarter of the year. Given that most precipitation in grasslands falls within the spring/summer growing season (Rosenberg 1987), this bioclimatic envelope parameter represents the coldest growing season temperature extremes a species can tolerate. A positive relationship indicates that π_{o*osm} is more negative for species capable of growing in areas with low growing season temperatures. No significant trait×climate relationships were observed for forbs/subshrubs separately.

4.5 Discussion

4.5.1 Osmometer method validation

Leaf hydraulic traits of trees, such as π_o and π_{TLP}, are well correlated with spatial variability in annual moisture availability as well as tree distributions across moist and dry biomes (Bartlett et al. 2012b). The osmometer method for rapidly estimating these traits in woody species has facilitated community-scale surveys of leaf-level drought tolerance in several forest ecosystems (Bartlett et al. 2012a; Maréchaux et al. 2015); however, concerns about the utility of this method for estimating osmotic potential at full turgor of thin leaves with large midribs (e.g. graminoids) have prevented its application to a wide range of plant functional groups. Several of the graminoid species surveyed in this study have large leaf midribs, a characteristic that has the potential to diminish the proportion of extra-xylary water in the sample placed in the osmometer chamber. Considering that xylem typically contains lower sugar concentrations than other cells in the leaf (Peuke *et al.* 2001), the inclusion of the midrib in a sample could lead to an overestimation of π_o when using an osmometer compared to estimates from p-v curves (Bartlett et al. 2012a); however, we found no evidence of this potential bias among the species we sampled. We observed a significant relationship between osmotic potential at full turgor measured with an osmometer (π_{o*osm}) and p-v curves (π_{o*pv}) with all graminoid species falling along the 1:1 line (Fig. 4.2). A large midrib does not necessarily mean there is a larger proportion of xylem conduits relative to solute-rich mesophyll cells. For instance, large midribs typically have multiple vascular bundles that are similar in size and density to bundles outside of the midrib (Fig. A3.2; also see Evert and Eichhorn 2013). The midrib also has a large amount of parenchyma tissue which contributes to total leaf osmotic potential at full turgor. Thus, the inclusion of the midrib may not necessarily lower the proportion of extra-xylary water in a sample.

The slope and intercept of the relationship shown in Fig. 4.2 is not significantly different from the relationship presented by Bartlett et al. (2012b – *Fig. 2 within*). This relationship differs significantly from a 1:1 relationship indicating clear bias in osmometry. Such bias is expected in osmometer measurements of π_o due to the net effect apoplastic dilution and cell wall dissolution (Bartlett et al. 2012a). Rupturing of plant cell walls during sample processing causes water from the apoplast to dilute the sample leading to overestimations of π_o. Additionally, underestimation of π_o can occur as disturbed cell wall materials dissolve into the sample solution. We accounted for these opposing effects following equation 2 and found a 1:1 relationship between measured and predicted π_{o*osm} (Fig. 4.3), which is in line with measurements on leaves from woody species (Bartlett et al. 2012a). This highlights the robustness of this method as well as the importance of considering species-specific leaf vein networks and the net effect of apoplastic dilution and cell wall dissolution, which might change the fitted regression across leaf types.

We provide evidence that the osmometer method developed by Bartlett et al. (2012b) can be used to estimate leaf turgor loss point in herbaceous species commonly found in central US grasslands:

$$\pi_{tlp} = 0.80\pi_{o*osm} - 0.845 \qquad\qquad (eqn\ 3)$$

Not only was the relationship between π_{TLP} and π_{o*osm} statistically significant (Fig. 4.4-A), the model parameters were nearly identical to those presented by Bartlett et al. (2012b) for woody species, suggesting the same linear model can be applied across plant functional types. The striking similarity between the 'Grassland' and 'Bartlett' models is likely a result of: 1) the similar range in drought tolerance assessed in the two studies (Fig. 4.5); 2) the fact that this method samples similar proportions of mesophyll tissue despite anatomical differences between dicots and monocots; and 3) the dominant role of osmotic potential at full turgor in explaining turgor loss

point across all plants at a global scale (Bartlett et al. 2012b), and perhaps more so across plant functional types within communities (Fig. 4.1). Our results show that 72% of the variation in π_{TLP} across all species and 96% of the variation in π_{TLP} of graminoids was explained using the osmometer method, providing strong support for the validity of this technique both across functional groups and within graminoids. The lack of a correlation between π_{TLP} and π_{o*osm} for forbs/subshrubs may be due to the smaller range in π_{TLP} and π_{o*osm} values sampled. Given that forb species were all measured within the same site (HPG), we recommend additional measurements of π_{TLP} and π_{o*osm} of forb species across broad spatial aridity gradients. We suggest caution in interpreting π_{o*osm} of forb species until additional results on this growth form have been reported. We recommend using the following linear model for estimating leaf turgor loss point from π_{o*osm} of common C3 and C4 grass species:

$$\pi_{tlp} = 0.944\pi_{o*osm} - 0.611 \qquad\qquad (eqn\ 4)$$

4.5.2 Mechanistic value of π_o

This rapid measure of leaf drought tolerance for herbaceous species is especially useful if these traits can help us understand the ecological strategies of plants, which are often identified through analyses of trait covariation (Wright et al. 2004). We observed a negative relationship between π_{o*osm} and LDMC, a commonly measured leaf trait indicative of resource conservation strategies and leaf construction costs (Poorter and Garnier 1999) (Fig. 4.6). Large values of LDMC can result from either a large structural investment in leaf tissue and/or high concentrations of non-structural carbohydrates. Structural investments are generally considered to result from extensive cell wall investment, such as thick-walled xylem or a large proportion of small diameter vessels. The negative relationship we observed likely reflects both components of LDMC. We would expect plants with more negative π_{o*osm} to have a higher concentration of non-structural

carbohydrates or other osmolytes. In addition, especially in ecosystems with more severe or persistent water stress, plants that invest in more negative π_{o*osm} (i.e. lower turgor loss point) tend to further bolster their drought tolerance by investing in xylem that is resistant to hydraulic failure (Zhu et al. 2018), which is characterized by conduits with thick walls relative to their lumen diameter (Blackman *et al.*, 2010). Indeed, we did find a negative relationship between LDMC and resistance to hydraulic failure (P_{50}), which may reflect this investment in xylem. We also observed a significant relationship between π_{o*osm} and P_{50}, a valuable trait for defining hydraulic safety vs. efficiency tradeoffs and re-growth capabilities of grasses following drought (Ocheltree et al. 2016). Leaf resistance to hydraulic failure (i.e. P_{50}) is largely determined by leaf vein architecture (Scoffoni et al. 2011); thus, the osmometer method can provide both a valuable proxy for π_{TLP} as well as information about aspects of drought tolerance more closely associated with leaf structural investments (LDMC and P_{50}).

Trait-environment relationships are key for understanding species responses to climate change (Suding et al. 2008). In forested biomes, lower values π_o are associated with high aridity (Bartlett *et al.*, 2012b; Zhu *et al.*, 2018). For herbaceous plants, identifying climate variables that explain the distributions of species traits can be more difficult given the ability of these plants to occupy microsites within a landscape (Ricklefs and Latham 1992). Despite these potential limitations, we did find significant trait-environment relationships for π_{o*osm} of graminoids and PFTs combined. Graminoid species that more exclusively occupy xeric regions (low MAP) tend to have lower π_{o*osm} (Fig. 4.7) suggesting that π_{o*osm} helps plants to survive and reproduce where water is limiting, as observed for woody species (Bartlett *et al.*, 2012b); however, MAP at the driest extremes of graminoid species distributions (MAP_{5th}) was not significantly correlated with π_{o*osm}, while MAP of the wettest extremes was (Fig. 4.7). This indicates that the distribution of

drought tolerance traits for graminoids may be determined by competitive pressures that are maximized at the wetter end of their distribution where more acquisitive faster growing species dominate grassland communities. Allocating resources to lower π_{o*osm} is indeed advantageous in drier climates, however, it may prevent graminoid species from inhabiting mesic areas where the costs of such strategies (slower growth rates) outweigh the benefits.

Across functional types, temperature was the only significant climatic predictor of π_{o*osm}. Specifically, temperature of the wet season for the coldest regions of a species distribution explains only 18% of the variability in π_{o*osm} across PFTs. This significant, albeit weak, relationship may simply reflect functional type differences (graminoids vs. forbs/subshrubs; Fig. 4.5) and the temperature constraints on the geographic distribution of C4 vs. C3 plants (Sage and Monson 1999; Edwards and Still 2008) or adaptations for freezing tolerance (Liu and Osborne 2008). The lack of any significant trait×climate relationship for forbs/subshrubs highlights the potential lack of utility of this trait for understanding drought responses of these functional types, which tend to rely more on deep roots rather than drought tolerant leaves (Weaver 1958).

Until additional studies evaluate the relationship between π_{TLP} and π_{o*osm} *within* communities, including both herbaceous and woody-dominated ecosystems, it will remain unclear to what extent the tight coupling of π_{TLP} and π_{o*osm} across broad geographic scales and phylogenetic groups (*sensu* Bartlett et al. 2012a and this study) is representative of: 1) convergent, but partly independent responses of both π_{TLP} and π_{o*osm} to environmental gradients in space and time, or 2) stringent biophysical or ecological constraints on covariance between π_{TLP} and π_{o*osm} that operate independently of the spatial or phylogenetic scope of sampling. In other words, caution must be applied when interpreting the functional equivalence of π_{TLP} and π_{o*osm} among species within any given community. Additionally, although π_{TLP} and π_{o*osm} represent promising traits for

capturing differences in the ability of plants to maintain function and keep tissues alive at low water potentials, they do not capture drought *avoidance* strategies that enable plants to maintain high leaf water potential through water conservation or deep rooting profiles (Levitt 1980; Mitchell et al. 2016). Furthermore, π_{TLP} and π_{o*osm} are measured on fully rehydrated plants, which fails to capture the trait plasticity exhibited by some species when partially dehydrated. For example, π_{TLP} can change by >1.0 MPa in *Juniperus monosperma* within several hours, primarily due to osmotic adjustment (Meinzer *et al.*, 2014). On a global scale, however, osmotic adjustment typically accounts for up to a 0.5 MPa change in π_{TLP} (Bartlett *et al.*, 2014), and has little influence on species' ranks with respect to leaf-level drought tolerance, but there are clearly exceptions that should be considered when interpreting π_{TLP} and π_{o*osm} as indices of plant responses to drought.

4.6 Conclusions

In summary, leaf level drought tolerance of herbaceous species can be measured accurately and rapidly using the osmometer method. We provide evidence that π_{o*osm} predicts π_{TLP} of herbaceous species from a nearly identical linear model ($\pi_{tlp} = 0.80\pi_{o*osm} - 0.845$) and is well correlated with two other traits indicative of drought tolerance (LDMC and P_{50}) as well as species-specific distributions across gradients of precipitation. There is an urgent need for rapid techniques to assess plant community-scale drought tolerance (Griffin-Nolan et al. 2018a), as a hotter and drier climate will become the norm for many of Earth's ecosystems (IPCC 2013). To make predictions of how different plant functional types will respond to increased drought frequency and intensity, we need to identify baseline metrics of drought tolerance that are comparable across the plant kingdom. The osmometer method makes community-scale surveys of drought tolerance possible, which will improve trait-based predictions of ecosystem responses to climate change and

allow for a more integrative understanding of plant functional strategies for dealing with water stress.

4.7 Tables

Table 4.1. Herbaceous species surveyed in this study are shown along with collection sites, functional type, and trait means (SE). Traits include osmotic potential estimated from both an osmometer (π_{o*osm}) and p-v curves (π_{o*pv}), turgor loss apoint (π_{TLP}), vulnerability to cavitation (P_{50}), leaf dry matter content (LDMC), and apoplastic fraction (a_f). Collection sites include a northern mixed-grass prairie (High Plains Grassland Research Center, HPG; mean annual precipitation [MAP] = 415mm, mean annual temperature [MAT] = 7°C, coordinates = 41° 11' 52" N, 104° 53' 13" W) in Wyoming, a southern mixed-grass prairie (Hays Agricultural Research Center, HYS; MAP = 581mm, MAT = 12.3°C, coordinates = 39° 5' 9" N, 99° 9' 23" W) and a tallgrass prairie (Konza Prairie Biological Station, KNZ; MAP = 864mm, MAT = 13°C, coordinates 39° 05' N, 96° 35' W) in Kansas.

Species	Code	Collection Site	Functional Type	π_{o*osm} (MPa)	π_{o*pv} (MPa)	π_{TLP} (MPa)	P_{50} (MPa)	LDMC	a_f
Andropogon gerardii	ANGE	KNZ	Graminoid (C4 grass)	-1.2 (0.01)	-1.2 (0.04)	-1.7 (0.06)	-1.1	0.32	0
Bouteloua curtipendula	BOCU	HYS	Graminoid (C4 grass)	-1.8 (0.07)	-1.8 (0.11)	-2.5 (0.08)	-1.6	0.45	0.37
Bouteloua gracilis	BOGR	HPG	Graminoid (C4 grass)	-1.8 (0.02)	-1.7 (0.09)	-2.3 (0.12)	-1.1	0.46	0.16
Sorghastrum nutans	SONU	KNZ	Graminoid (C4 grass)	-0.9 (0.08)	-1.2 (0.06)	-1.6 (0.03)	-0.8	0.32	0.10
Sporobolus asper	SPAS	HYS	Graminoid (C4 grass)	-1.8 (0.12)	-1.6 (0.06)	-2.3 (0.12)	-2	0.41	0.11
Carex duriuscula	CADU	HPG	Graminoid (C3 sedge)	-2.7 (0.10)	-2.7 (0.16)	-3.2 (0.19)	-1.9	0.41	0.17
Hesperostipa comata	HECO	HPG	Graminoid (C3 grass)	-2.2 (0.06)	-2.2 (0.08)	-2.7 (0.13)	-2.3	0.44	0.39
Pascopyrum smithii	PASM	HPG	Graminoid (C3 grass)	-1.7 (0.02)	-1.6 (0.04)	-2.0 (0.07)	-1.8	0.38	0.20
Poa secunda	POSE	HPG	Graminoid (C3 grass)	-1.7 (0.11)	-1.5 (0.04)	-2.1 (0.12)	-	0.32	0.33
Leucocrinum montanum	LEMO	HPG	Monocot (forb)	-1.3 (0.06)	-0.8 (0.06)	-1.2 (0.11)	-	0.18	0.65
Astragalus drummondii	ASDR	HPG	Dicot (forb)	-0.7 (0.08)	-1.1 (0.12)	-1.5 (0.12)	-	0.24	0.58

Astragalus laximannii	ASLA	HPG	Dicot (forb)	-1.0 (0.13)	-1.7 (0.09)	-2.2 (0.10)	-	0.26	0.26
Astragalus shortianus	ASSH	HPG	Dicot (forb)	-0.7 (0.07)	-0.7 (0.11)	-1.0 (0.15)	-	0.17	0.76
Linaria dalmatica	LIDA	HPG	Dicot (forb)	-0.6 (0.16)	-1.0 (0.09)	-1.3 (0.10)	-0.9	0.19	0.36
Mertensia lanceolata	MELA	HPG	Dicot (forb)	-0.9 (0.06)	-1.2 (0.08)	-1.5 (0.09)	-0.5	0.21	0.19
Penstemon albidus	PEAL	HPG	Dicot (forb)	-0.6 (0.01)	-1.3 (0.14)	-1.6 (0.13)	-1.3	0.27	0.18
Sphaeralcea coccinea	SPCO	HPG	Dicot (forb)	-1.0 (0.04)	-1.4 (0.13)	-1.9 (0.15)	-1.8	0.3	0.41
Artemesia frigida	ARFR	HPG	Dicot (subshrub)	-1.4 (0.04)	-1.1 (0.04)	-1.5 (0.04)	-	0.35	0.50
Eriogonum effusum	EREF	HPG	Dicot (subshrub)	-0.6 (0.08)	-1.1 (0.07)	-1.5 (0.11)	-	0.32	0.48
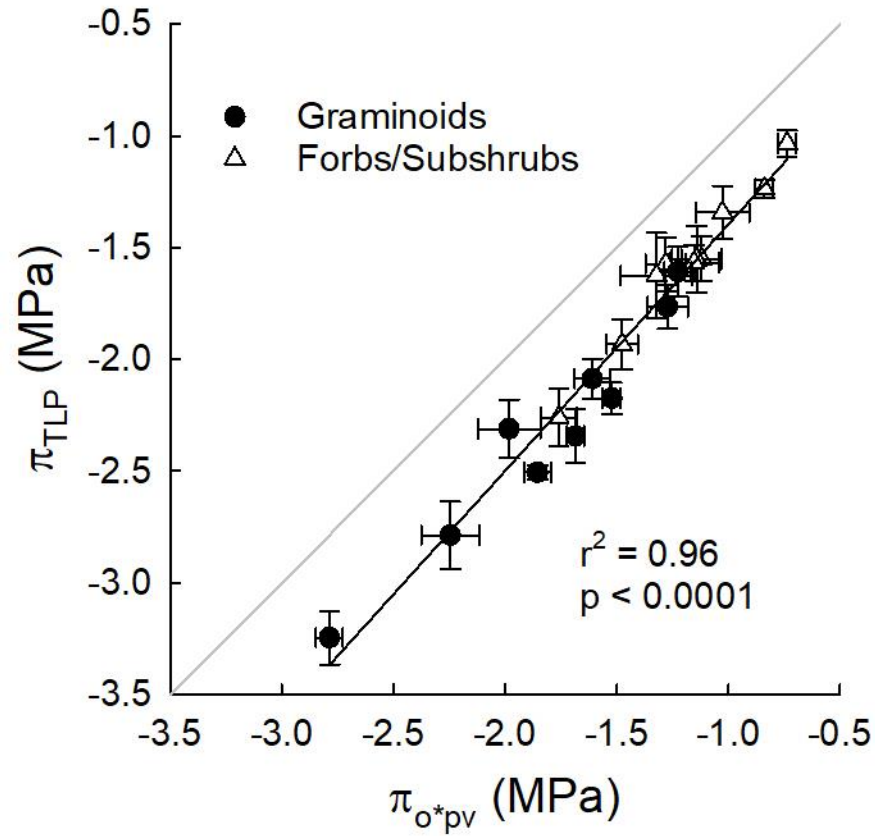
Figure 4.1. Leaf turgor loss point is largely controlled by leaf osmotic potential at full turgor, the component of leaf water potential determined by cellular solute concentrations. A strong linear relationship between osmotic potential at full turgor (π_{o*pv}) and osmotic potential at turgor loss point (π_{TLP}) estimated from pressure-volume curves is shown for largely herbaceous grassland species including graminoids, forbs, and subshrubs. The black line represents this model: $\pi_{TLP} = 1.103\pi_{o*pv} - 0.294$, while the grey line represents the 1:1 line and bi-directional error bars represent standard error.
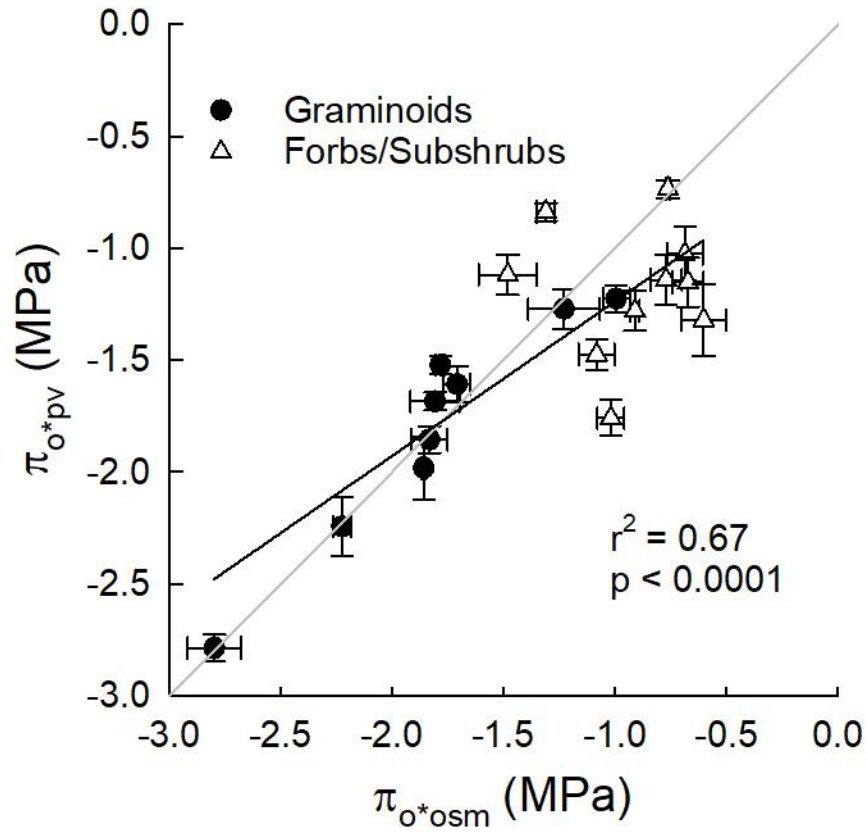
Figure 4.2. Osmotic potential at full turgor measured with a vapor pressure osmometer (π_{o*osm}) predicts that estimated from p-v curves (π_{o*pv}) with a slight deviation from the 1:1 line. The model shown here ($\pi_{o*pv} = 0.690\pi_{o*osm} - 0.5481$; black line) does not differ significantly from a similar model presented for woody species ($\pi_{o*pv} = 0.690\pi_{o*osm} - 0.5481$; Bartlett et al. 2012a) based on the 95% CI of the slope (0.45,0.92) and intercept (-0.8954093, -0.2007442). Graminoid species fall along the 1:1 line (grey line), while much of the scatter is due to variability in forb/subshrubs. Bi-directional error bars represent standard error.
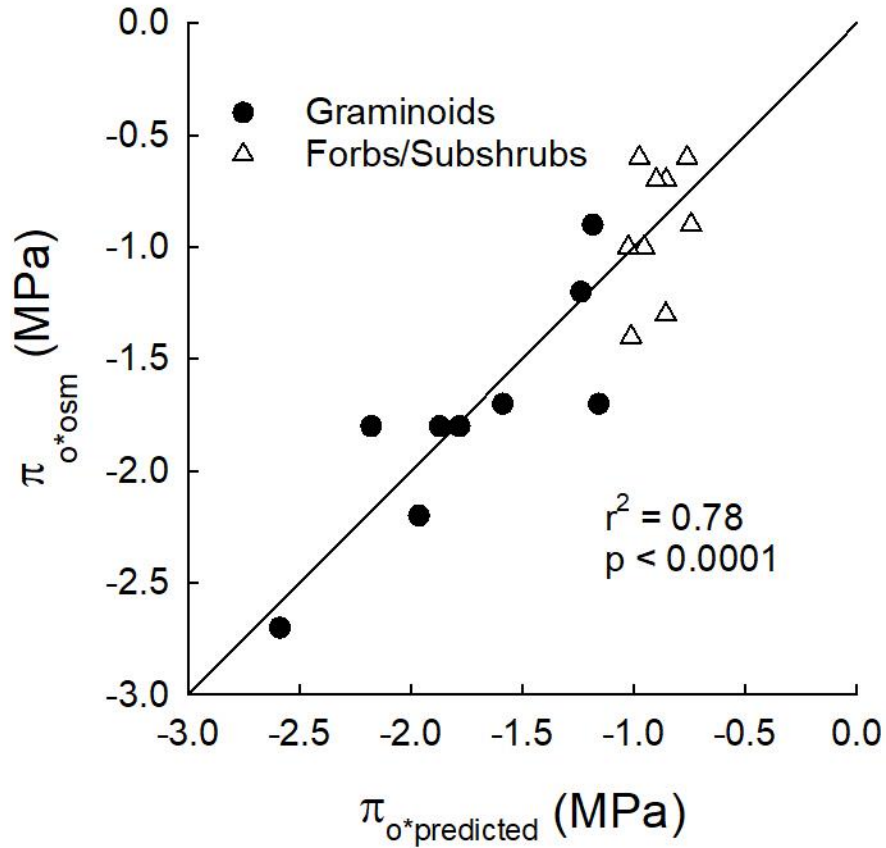
Figure 4.3. Correcting for discrepancies that arise from osmometry (see the departure from the 1:1 line in Figure 4.2), π_{o*osm} was recalculated using equation 2 (taken from Bartlett et al. 2012a). Osmometry can lead to over- and under estimations of π_o due to apoplastic dilution and cell wall dissolution, respectively. Here, predicted osmotic potential at full turgor ($\pi_{o*predicted}$) was calculated from a model that includes estimates of cell wall dissolution (leaf dry matter content as a proxy, LDMC), apoplastic fraction, and their interaction. The fitted regression between measured π_{o*osm} and $\pi_{o*predicted}$ has a slope of 1.0 ± 0.12 SE ($\pi_{o*osm} = 1.0\,\pi_{o*predicted} - 5.6e^{-6}$; plotted black line), as does the relationship including solely graminoids (slope = 0.9 ± 0.23 SE; see Table A3.2), indicating no bias after correcting for these factors. The counterbalancing effects of apoplastic dilution and cell wall dissolution suggest the osmometer method is robust for graminoid leaves (graminoids fall along the 1:1 line in Figure 4.2); however, the net effect of LDMC and a_f should be considered for other types of leaves. $\pi_{o*predicted} = -1.2684*\pi_{o*pv*af} + 1.4875*\text{LDMC} + 5.2601*\pi_{o*osm*af}*\text{LDMC} - 1.2147$.
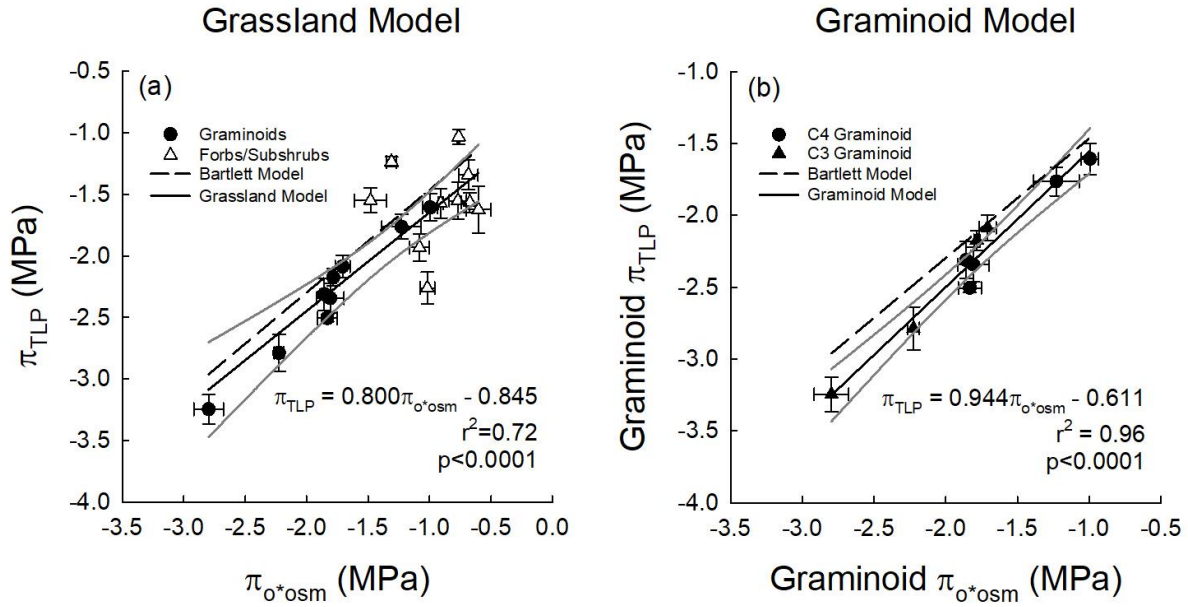
Figure 4.4. A linear model for predicting leaf turgor loss point (π_{TLP}) among grassland species using osmotic potential at full turgor estimated from a vapor pressure osmometer (π_{o*osm}). **(a)** The slope and intercept of the linear model developed by Bartlett et al. ($\pi_{tlp} = 0.832\pi_{osm} - 0.631$; dashed line) falls within the 95% CI of the slope (0.5552126, 1.0460131) and intercept (-1.2050772, -0.4852862) of the grassland model shown here (black line; grey line represents the 95% CI). The linear model equation depicted on the figure is for the grassland model, which includes graminoids, forbs and subshrubs. **(b)** The linear model including only graminoid species also does not differ significantly from the Bartlett model (dashed line) which falls within the 95% CI of the slope (0.7793554, 1.1086195) and intercept (-0.9190000, -0.3034649) of the graminoid model shown here (black line; grey line represents the 95% CI). No significant relationship was found for forbs/subshrubs alone. Symbols represent photosynthetic pathway (C4 vs. C3). Bi-directional error bars represent standard error.
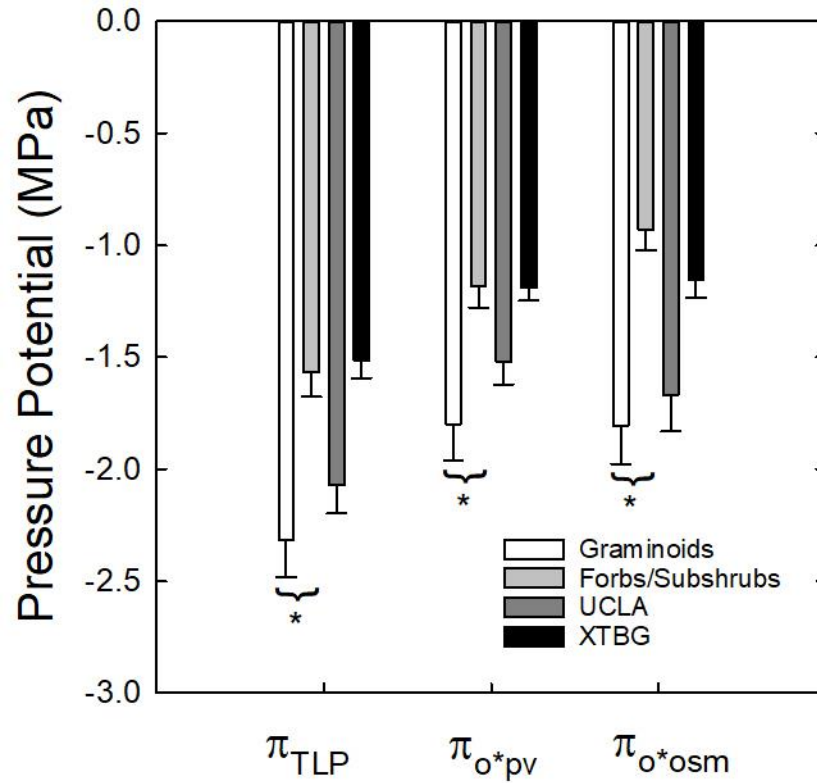
Figure 4.5. Turgor loss point (π_{TLP}) and osmotic potential at full turgor measured from pressure-volume curves (π_{o*pv}) and a vapor pressure osmometer (π_{o*osm}) are shown grouped by plant functional type (graminoids and forbs/subshrubs; mean ± SE). Forbs/subshrub species have significantly higher pressure potentials for each trait compared to graminoid species ($p<0.05$; denoted by *). Also shown are the pooled mean (± SE) for the species used in the Bartlett et al. (2012b) model sampled from two separate locations: a common garden near University of California Los Angeles (UCLA; annual rainfall = 450 mm) and a tropical forest plant community at Xishuangbanna Botanic Garden in China (XTBG; annual rainfall = 1532 mm).
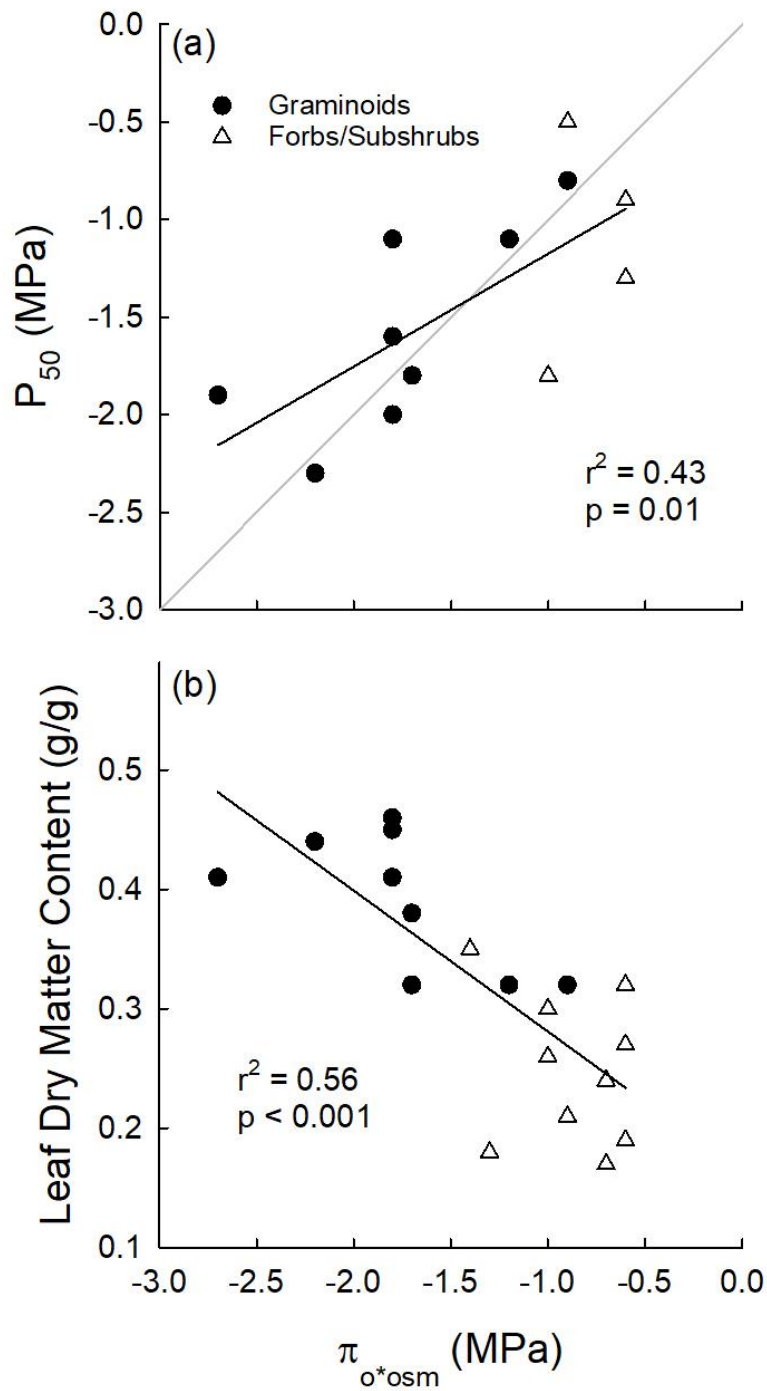
Figure 4.6. Osmotic potential at full turgor can be rapidly estimated from a vapor pressure osmometer (π_{o*osm}) and is correlated with other mechanistic plant traits such as **(a)** the leaf water potential at 50% loss of hydraulic conductance (P_{50}) and **(b)** leaf dry matter content (LDMC). The 1:1 line is shown as a grey line.
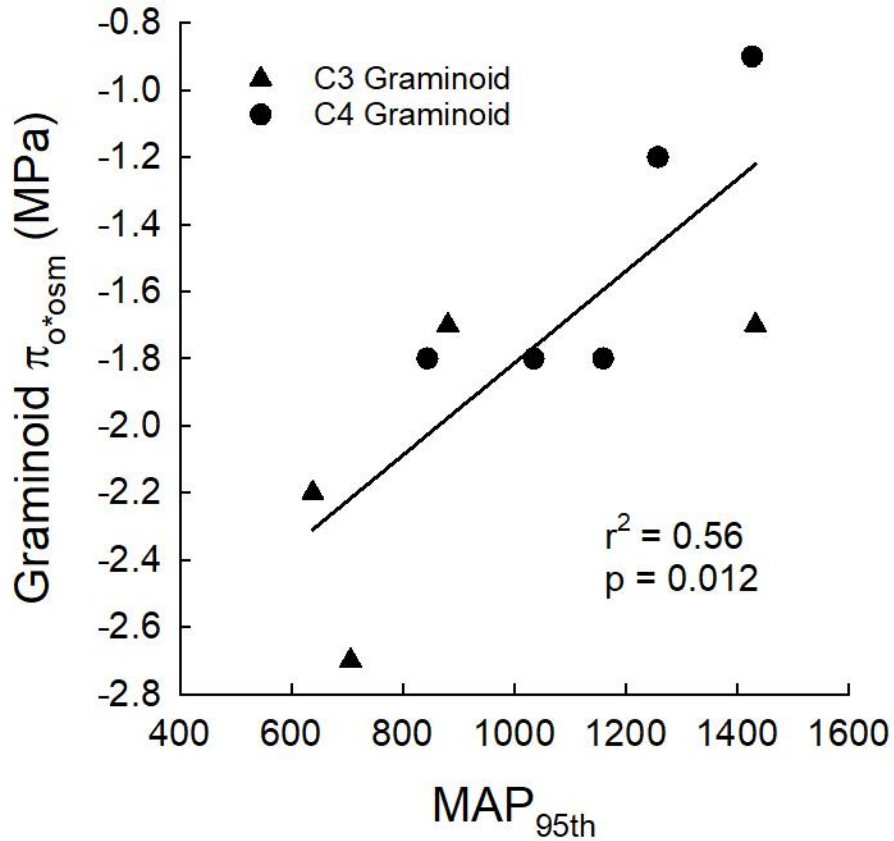
Figure 4.7. Mean annual precipitation at the wettest extremes of a species distribution (MAP_{95th}) explained a significant portion of interspecific variability (57%) in osmotic potential at full turgor measured with an osmometer (π_{o*osm}). A positive relationship indicates that species with lower π_{o*osm} (more negative) are found in drier regions of the central US. The wet extreme (i.e. 95th quantile) suggests that resource allocation to drought tolerance (i.e. low π_{o*osm}) is beneficial along an aridity gradient only until water becomes less limiting, at which point more mesic species with higher growth rates outcompete xeric species. At the dry extreme of species bioclimatic envelopes (5th quantile), π_{o*osm} was only moderately significantly correlated with precipitation during the wettest quarter of the year (p = 0.08).

CHAPTER 5: SHIFTS IN PLANT FUNCTIONAL COMPOSITION FOLLOWING LONG-TERM DROUGHT IN GRASSLANDS

5.1 Summary

Plant traits can provide unique insights into plant performance at the community scale. Functional composition, defined by both functional diversity and community-weighted trait means (CWMs), can affect the stability of aboveground net primary production (ANPP) in response to climate extremes. Further complexity arises, however, when functional composition itself responds to environmental change. The duration of climate extremes, such as drought, is expected to increase with rising global temperatures; thus, understanding the impacts of long-term drought on functional composition and the corresponding effect that has on ecosystem function could improve predictions of ecosystem sensitivity to climate change.

We experimentally reduced growing season precipitation by 66% across six temperate grasslands for four years and measured changes in three indices of functional diversity (functional dispersion, richness, and evenness), community-weighted trait means, and phylogenetic diversity (PD). Specific leaf area (SLA), leaf nitrogen content (LNC) and (at most sites) leaf turgor loss point (π_{TLP}) were measured for species cumulatively representing ~90% plant cover at each site.

Long-term drought led to increased community functional dispersion in three sites, with negligible effects on the remaining sites. Species re-ordering following the mortality/senescence of dominant species was the main driver of increased functional dispersion. The response of functional diversity was not consistently matched by changes in phylogenetic diversity. Community-level drought strategies (assessed as CWMs) largely shifted from drought tolerance to drought avoidance and/or escape strategies, as evidenced by higher community-weighted π_{TLP},

SLA, and LNC. Lastly, ecosystem drought sensitivity (i.e. relative reduction in ANPP) was positively correlated with SLA and negatively correlated with functional diversity.

Increased functional diversity following long-term drought may stabilize ecosystem functioning in response to future drought. However, shifts in community-scale drought strategies may increase ecosystem drought sensitivity, depending on the nature and timing of drought. Thus, our results highlight the importance of considering both functional diversity and abundance-weighted means traits of plant communities as their collective effect may either stabilize or enhance ecosystem sensitivity to drought.

5.2 Introduction

Ecosystem function is largely determined by the functional attributes of plant communities. Plant traits are useful for understanding how resources are acquired by plants (Reich, 2014; Wright et al., 2004) and consequently transferred to or stored in various ecosystem pools, such as plant biomass or soil organic matter (Lavorel & Garnier, 2002). Plant community functional composition, defined by community-weighted trait means (CWMs) and functional diversity (i.e., the distribution of traits within a community), can respond to environmental change and affect ecosystem processes, such as aboveground net primary production (ANPP), nutrient cycling, and decomposition (Díaz & Cabido, 2001). A trait-based response-and-effect framework has been proposed (Suding et al., 2008) whereby certain plant traits predict specific ecosystem functions (e.g., leaf nitrogen content is correlated with variability in ANPP; Garnier et al., 2004; Reich, 2012) while other traits indicate how species will shift in abundance in response to environmental change (e.g., conservative leaf water economic traits improve species tolerance to drought and warming; Anderegg et al., 2016; Soudzilovskaia et al., 2013). The importance of climate in governing functional composition is well supported by community scale surveys of plant traits on

73

broad spatial and temporal scales (Newbold et al., 2012; Reich & Oleksyn, 2004; Šímová et al., 2018; Wieczynski et al., 2019; Wright et al., 2005). Few studies, however, have assessed the response of both functional diversity and CWMs to climate extremes, which are rare by definition (Smith, 2011), and the corresponding effect on ecosystem functioning across space and time.

Rising global temperatures increase evapotranspiration and thus the intensity and duration of climate extremes, such as drought (Trenberth, 2011), with immediate and long-lasting negative impacts on Earth's vegetation (Breshears et al., 2005). The magnitude of vegetation responses to drought varies among ecosystems with xeric ecosystems generally being more sensitive than mesic ones (Huxman et al., 2004; Knapp et al., 2015). Ecosystem resistance and resilience to drought has been linked to species diversity, and functional diversity in particular (Díaz & Cabido, 2001; Isbell et al., 2015; Tilman & Downing, 1994; Tilman et al., 1997). Plant communities with high functional diversity are buffered against declines in ecosystem functions, such as ANPP, due to functional insurance (Anderegg et al., 2018; De La Riva et al., 2017; Grime, 1998; Pérez-Ramos et al., 2017). In other words, a greater diversity of species (and traits) increases the odds of one or more species surviving a drought and compensating for drought-induced senescence or mortality of other species. Beyond diversity, the mean composition of traits (as measured by CWMs) can confer ecosystem resistance and resilience to drought, especially if species with traits linked to drought survival (McDowell et al., 2008) and/or drought avoidance/escape strategies (Kooyers, 2015; Noy-Meir, 1973) are in high abundance.

Increasing complexity arises, however, when functional composition itself is altered by drought. An extreme climate event can act as an environmental filter allowing only certain species (and trait values) to persist, potentially leading to trait convergence and/or decreased functional and genetic diversity (Díaz et al., 1999; Grime, 2006; Whitney et al. 2019); however, an array of

biotic interactions influencing competition, coexistence, and niche differentiation can act simultaneously to structure communities in an opposite manner (Cadotte & Tucker, 2017; Kraft et al., 2015). Thus, given uncertain and counteracting roles of environmental filtering and niche differentiation, the net effects of drought on community functional composition are currently unpredictable. Indeed, the impact of drought, and aridity more broadly, on functional diversity is highly variable with positive (Cantarel et al., 2013), negative (Qi et al., 2015), and neutral (Copeland et al., 2016; Hallett et al., 2017) responses observed. These inconsistences are likely due to differences in the selection of traits and functional diversity indices, the duration and extremity of drought, and/or the spatial/temporal context in which aridity is being examined. Thus, coordinated, long-term, and multi-site experiments are needed to assess the impact of extreme drought on functional composition and ecosystem function.

The 'Extreme Drought in Grasslands Experiment' (EDGE) was established in 2012 to assess the drought-sensitivity of ANPP in six North American grasslands, ranging from desert to tallgrass prairie (Fig. 5.1; Table 5.1). Grasslands are ideal ecosystems for assessing drought sensitivity as ANPP in these systems is highly responsive to precipitation variability (Hsu et al., 2012; Knapp and Smith, 2001) and their short stature allows for easy installation of experimental drought infrastructure (Yahdjian & Sala, 2002). We surveyed plant traits of the most common species at each EDGE site (cumulatively representing ~90% plant cover) and tracked changes in three indices of functional diversity (e.g., functional dispersion, richness, and evenness) and abundance-weighted traits in response to a four-year experimental drought. Our trait survey included leaf turgor loss point (π_{TLP}), specific leaf area (SLA) and leaf nitrogen content (LNC). Leaf economic traits such as SLA and LNC have been associated with plant ecological strategies (e.g., fast vs. slow resource economies and drought tolerance vs. avoidance; Reich, 2014; Frenette-

Dussault et al., 2012) and are descriptive of ANPP dynamics (Garnier et al., 2004; Reich, 2012; Suding et al., 2008). Hydraulic traits such as π_{TLP} are informative of leaf-level drought tolerance and are expected to be predictive of plant responses to aridity (Bartlett, Scoffoni, & Sack, 2012; Griffin-Nolan et al., 2018a; Reich, 2014). Additionally, we measured plot-level phylogenetic diversity to assess whether functional and phylogenetic diversity are coupled in their response to drought (i.e., whether decreased functional diversity is driven by decreased genetic dissimilarity).

Drought resistance is multidimensional (i.e., a variety of traits can bestow or hinder drought resistance via a variety of mechanisms), thus, there are several plausible shifts in trait diversity and weighted-means in response to drought. Here, we test the hypothesis that high functional diversity and high abundance of conservative leaf economic traits confers greater resistance of ANPP to drought and ask how drought influences functional composition over time. A strong role of environmental filtering should be reflected in reduced functional diversity and altered community-weighted trait means, with the direction of the mean trait shift dependent on the role of various traits in shaping drought-resistance within and across ecosystems.

5.3 Methods

5.3.1 Site Descriptions

The impact of long-term drought on community functional diversity and abundance-weighted traits was assessed in six native grassland sites spanning a 620 mm gradient in mean annual precipitation (MAP) and a 5.5 °C gradient in mean annual temperature (Table 5.1; Knapp et al., 2015). These six sites encompass the four major grassland types of North America including desert grassland, shortgrass prairie, mixed grass prairie, and tallgrass prairie. Experimental plots were established in upland pastures that had not been grazed for over 10 years, apart from the two mixed grass prairie sites (HPG and HYS) which were last grazed 3 years prior to this study. The

76

tallgrass prairie site (KNZ) is burned annually following regional management regimes (Knapp et al., 1998), while other sites are unburned. Soil textures vary across sites from sandy to clay-loam (Burke et al. 1991; 1989; Kieft et al. 1998).

5.3.2 Experimental drought treatments

Drought was experimentally imposed at each site for four years using large rainfall exclusion shelters (Fig. 5.1A; Yahdjian & Sala, 2002). At each site, twenty 36-m^2 plots were established across a topographically uniform area and hydrologically isolated from the surrounding soil matrix using aluminum flashing and 6-mil plastic barriers installed to a depth of at least 20 cm. Plots were split into 4 subplots, each 2.5x2.5 m with a 0.5 m buffer on each side. Two of these subplots were designated for destructive measurements of plant biomass, one was designated for non-destructive surveys of species composition, and the final subplot was left for research on decomposition and microbial communities (Ochoa-Hueso et al., 2018; Fernandes et al. 2018).

Drought was imposed in ten plots per site by installing large shelters (10x10 m^2) which passively blocked 66% of incoming rainfall during each growing season – this is roughly equivalent to a 40% reduction in annual precipitation given that 60-75% of MAP falls during the growing season in these ecosystems (April-September for SGS, HPG, HYS, and KNZ; April-October for SBK and SBL). Rainfall exclusion shelters utilize transparent polyethylene panels arrayed at a density to reduce each rainfall event by 66%, thereby maintaining the natural precipitation pattern of each site (Knapp et al. 2017). The remaining ten plots per site were trenched and hydrologically isolated yet received ambient rainfall (i.e., no shelters were present). Treatment infrastructure was installed in the spring of 2012, yet drought treatments did not begin until April 2013 at the New Mexico sites (SBK and SBL) and 2014 at the northern sites (SGS, HPG, HYS, and KNZ).

Rain gauges were established in a subset of control and treatment plots. Rainfall exclusion shelters reduced annual precipitation by ~40% relative to ambient amounts across all six sites (Fig. 5.1B), a relative reduction comparable to the extreme drought that affected this region in 2012 (the 4th largest drought in the past century; Knapp et al., 2015). However, the experimental drought imposed here lasted four years rather than one.

5.3.3 Species composition

Species composition was assessed at each site during spring and fall of each year starting one year before treatments were imposed. Absolute aerial cover of each species was estimated visually within four quadrats (1 m^2) placed within the subplot designated for non-destructive measurements. For each plot and species, absolute cover was converted to average percent relative cover with the higher cover value in each year (spring or fall) used in the final analysis (Koerner & Collins, 2014). At the end of each growing season in the four northern sites, all aboveground biomass was harvested in three quadrats (0.1 m^2) which were placed randomly in one of two subplots designated for destructive measurements (altering between years). Biomass was sorted to remove the previous year's growth, dried for 48 hours at 60°C, and weighed to estimate total aboveground net primary production (ANPP). At the two Sevilleta sites (SBK and SBL), aboveground biomass was estimated in spring and fall using a non-destructive allometric approach (Muldavin et al. 2008) for each species occurring in each of the species composition subplots.

5.3.4 Plant traits

Traits of the most abundant plant species per site were measured in an area adjacent to experimental plots to avoid destructive measurements within plots. Thus, all traits were measured under ambient rainfall conditions. Plant traits were measured at different times of the growing season to capture peak growth and soil moisture conditions. For SBK and SBL, traits were

measured at the beginning of the 2017 monsoon season (early August) to ensure fully emerged green leaves were sampled. For SGS and HPG, all traits were measured in late May and early June of 2015 to capture the high abundance of C_3 species at these sites. For HYS and KNZ, traits were measured in mid-July 2015, during peak biomass.

Ten individuals were selected along a transect the length of the experimental infrastructure and two recently emerged, fully expanded leaves were clipped at the base of the petiole and placed in plastic bags containing a moist paper towel. Leaves (n=20 per species) were rehydrated in the lab, scanned, and leaf area was estimated using ImageJ software (https://imagej.nih.gov/ij/). Each leaf was then oven-dried for 48 hours at 60°C and weighed. Specific leaf area (SLA) was calculated as leaf area/leaf dry mass (m^2/kg). Dried leaf samples were then ground to a fine powder for tissue nutrient analyses. Leaf nitrogen content (LNC) was estimated on a mass basis using a LECO Tru-Spec CN analyzer (Leco Corp., St. Joseph, MI, USA).

Leaf turgor loss point (π_{TLP}) was estimated for each species using a vapor pressure osmometer (Bartlett et al. 2012a; Griffin-Nolan et al., 2019). Briefly, a single tiller (for graminoids) or whole individual (for forbs and shrubs) was unearthed to include root tissue and placed in a reservoir of water. Whole plant samples (n=6/species) were relocated to the lab and covered in a dark plastic bag for ~12 hours to allow for complete leaf rehydration. Leaf tissue was then sampled from 5-8 leaves/species using a biopsy punch. The leaf sample was wrapped in tin foil and submerged in liquid nitrogen for 60 seconds to rupture cell walls. Each disc was then punctured ~15 times using forceps to ensure cell lysis, and quickly placed in a vapor pressure osmometer chamber within 30 seconds of freezing (VAPRO 5520, Wescor, Logan, UT). Samples were left in the closed chamber for ~10 minutes to allow equilibration. Measurements were then made every two minutes until osmolarity reached equilibrium (< 5 mmol kg^{-1} change in osmolarity

between measurements). Osmolarity was then converted to leaf osmotic potential at full turgor (π_o) (π_o = osmolarity*-2.3958/1000) and further converted to π_{TLP} using a linear model developed specifically for herbaceous species (Griffin-Nolan et al. 2019): $\pi_{TLP} = 0.80\pi_o - 0.845$.

Estimates of functional diversity are highly sensitive to missing trait data (Pakeman, 2014). Our survey of plant traits failed to capture species that increased in abundance in other years or due to treatment effects. Thus, we filled in missing trait data using a variety of sources including published manuscripts or contributed datasets. Sampling year differed depending on data sources, but sampling methodologies followed the same or similar standardized protocols (Bartlett et al., 2012a; Perez-Harguindeguy et al., 2013; Griffin-Nolan et al. 2019) and traits were often measured during the same season and from plots adjacent to or nearby the EDGE plots (see A4.1 in Appendix 4). Data for π_{TLP} was lacking for desert species common in the Sevilleta grassland (SBK and SBL), thus our analyses at these sites was constrained to SLA and LNC. For the northern sites (SGS, HPG, HYS, and KNZ), sufficient π_{TLP} data were available and were included in all analyses.

The final trait dataset included trait values for species cumulatively representing an average of 90% plant cover in each plot. Observations with less than 75% relative cover represented by trait data were removed from all analyses (21 of 600 plot-year combinations were removed; final range: 75-100% plant cover/plot). For this core set of 579 observations, the number of species used to estimate indices of functional composition ranged from 11 to 37, with a mean of 28 species. Covariation between traits was tested across sites using log-transformed data ('cor' function in base R). A significant correlation was observed between LNC and π_{TLP} (r = 0.292), but not between SLA and π_{TLP} (r = 0.014) or SLA and LNC (r= -0.117).

5.3.5 Functional composition

Functional diversity is described by several indices, each of which describe different aspects of trait distributions within a community (Mason, De Bello, Mouillot, Pavoine, & Dray, 2013). Given uncertainty as to which index is most sensitive to drought and/or informative of ecosystem responses to drought (Botta-Dukát, 2005; Carmona et al. 2016; Laliberte and Legendre, 2010; Mason et al. 2013; 2003; Petchey and Gaston, 2002; Villéger et al., 2008), we calculated three separate indices of functional diversity using the *dbFD* function in the 'FD' R-package (Laliberte & Legendre, 2010; Laliberté & Maintainer, 2011). Using a flexible distance-based framework and principle components analyses, the *dbFD* function estimates functional richness (FRic; the total volume of *x*-dimensional functional space occupied by the community), functional evenness (FEve; the regularity of spacing between species within multivariate trait space), and functional dispersion (FDis; the multivariate equivalent of mean absolute deviation in trait space) (Villéger, Mason, & Mouillot 2008a; Laliberte & Legendre, 2010). FDis describes the spread of species within multivariate space and is calculated as the mean-weighted distance of a species to the community-weighted centroid of multivariate trait space. To control for any bias caused by the lack of π_{TLP} data for two sites (SBK and SBL), we also calculated FRic, FEve, and FDis using just two traits (SLA and LNC) across sites (i.e., two-dimensional diversity). Multivariate functional diversity indices can potentially mask community assembly processes occurring on a single trait axis (Spasojevic & Suding, 2012); thus, FRic, FEve, and FDis were also estimated separately for each of the three traits surveyed in this study.

Species richness is well correlated with both FRic and FDis and can have a strong effect on the estimations of these parameters, especially in communities with low species richness (Mason et al., 2013). To control for this effect, we compared our estimates of FRic and FDis to

those estimated from randomly generated null communities and calculated standardized effect sizes (SES) for each plot:

$$SES = \frac{observed\ FDis - mean\ of\ expected\ FDis}{standard\ deviation\ of\ expected\ FDis}$$

where the mean and standard deviation of expected FDis (or FRic) were calculated from 999 randomly generated null community matrices using a "name-swap" and "independent-swap" algorithm for FDis and FRic, respectively (R code modified from Swenson, 2014). These null model algorithms randomize the trait data matrix while maintaining species richness and occupancy within each plot. The "name-swap" method also maintains relative abundance within each plot, thus providing insight into processes structuring communities (Spasojevic & Suding, 2012). Observed FEve is independent of species richness and thus was not compared to null communities (Mason et al. 2013).

Finally, we calculated community-weighted means (CWMs) for each trait (weighted by species relative abundance), which further characterizes the functional composition of the community. Each index of functional diversity and CWMs was measured for each plot-year combination using the fixed trait dataset (i.e., traits collected in 2015/2017 plus contributed data) and % cover data from each year. Thus, the responses of CWMs and functional diversity to drought represent species turnover and interspecific trait differences. Intraspecific trait variability and trait plasticity were not assessed in this study, but these typically contribute substantially less to total trait variation than interspecific trait variability, even when sampling across broad spatial scales and strong environmental gradients (Siefert et al., 2015)

5.3.6 Phylogenetic diversity

We quantified phylogenetic distinctiveness at the plot level using Faith's phylogenetic diversity (PD) index (Faith, 1991). A mixture of nine protein coding and non-coding gene

sequences were acquired from NCBI GenBank for each species. Following sequence alignment and trimming, maximum likelihood trees were constructed using RAxML (1000 bootstrap iterations, with *Physcomitrella patens* as tree outgroup) (version 8.2.10) (Stamakis, 2014). Following tree construction, PD was calculated using the picante package in R (Kembel et al., 2010). To control for the effect of species richness, the standardized effect size (SES) of PD (PD_{ses}) was calculated using the "independent swap" null model in the picante package.

5.3.7 Data analysis

We tested for interactive effects of treatment, year, and site on functional/phylogenetic composition using repeated measures mixed effects models ('lme4' package; Bates, Mächler, Bolker, & Walker, 2014). Site, treatment, and year were included as fixed effects and plot was included as a random effect. Trait data were log-transformed when necessary to meet assumptions of normality. Separate models were run for multivariate and single trait functional richness and dispersion ($FDis_{ses}$ and $FRic_{ses}$), FEve, phylogenetic diversity (PD_{ses}), as well as each CWM (i.e., SLA, LNC, and π_{TLP}). Pairwise comparisons were made between drought and control plots within each year and for each site (Tukey-adjusted p-values). With the exception of xeric sites (e.g., Sevilleta), ambient temporal changes in species composition are often greater than treatment effects in global change experiments (Langley et al., 2018); therefore, functional and phylogenetic responses to drought are presented here as log response ratios (ln(drought/control)) for FEve and CWMs or treatment differences (i.e. drought – control) for PD_{ses}, $FDis_{ses}$, and $FRic_{ses}$. Calculating log response ratios of SES values was not appropriate as SES is often negative. Negative log response ratios are shown for community-weighed π_{TLP} as this trait is measured in negative pressure units (MPa). All analyses were repeated for two-dimensional diversity indices (i.e., those including just SLA and LNC).

The sensitivity of ANPP to drought was calculated as the % reduction in ANPP in drought plots for each site and for each year as follows:

$$Drought\ sensitivity = abs \left(100 \times \frac{ANPP_{drought} - ANPP_{control}}{ANPP_{control}} \right)$$

where ANPP is the mean value across all plots of that treatment in a given year. Drought sensitivity is presented as an absolute value (*abs*) such that large positive values indicate greater sensitivity (i.e. greater relative reduction in ANPP). Correlations between annual drought sensitivity (n=24; six sites and four years) and either current-year (cy) or previous-year (py) functional/phylogenetic composition indices (e.g., PD_{ses}, CWMs for each trait, as well as single trait and multivariate $FDis_{ses}$, $FRic_{ses}$, and FEve) were investigated using the *cor* function in base R, with p-values compared to a Benjamin-Hochberg corrected significance level of $\alpha=0.0047$ for 32 comparisons. Variables that were significantly correlated with drought sensitivity at this level were included as fixed effects in separate general linear mixed effects models with site included as a random effect. To avoid pseudo-replication, mixed effects models were then compared to null models (using AIC) where null models included only the random effect of site. Both marginal and conditional R^2 values (Nakagawa & Schielzeth, 2013) were calculated for each mixed effect model using the 'rsquared' function in the 'piecewiseSEM' package (Lefcheck, 2016). All analyses were run using R version 3.5.2 (R Core Team 2018).

5.4 Results

Drought treatments significantly altered community functional and phylogenetic composition with significant three-way interactions in mixed effects models for each diversity index, except $FRic_{ses}$, and each abundance-weighted trait (treatment*site*year; Table 5.2). The six grassland sites varied extensively in the magnitude and directionality of their response to drought, variation that was associated with diversity index, trait identity, and drought duration. The most

responsive functional diversity index across sites was functional dispersion ($FDis_{ses}$), with significant drought responses observed in all but two sites.

Four years of experimental drought led to significantly higher multivariate $FDis_{ses}$ in half of the sites (SBK, SGS, and HYS) with only a slight decline in $FDis_{ses}$ observed at SBL in year 3 of the drought (Fig. 5.2A). There were no observable treatment effects on $FDis_{ses}$ at the wettest site (KNZ) or at the coolest site (HPG). Single trait $FDis_{ses}$ did not consistently mirror multivariate $FDis_{ses}$, especially at the three driest sites (Fig. 5.2B-D). For instance, the increase in $FDis_{ses}$ at SBK was largely driven by increased functional dispersion of LNC (Fig. 5.2C), as $FDis_{ses}$ of SLA did not differ significantly between drought and control plots. For SBL, multivariate $FDis_{ses}$ masked the opposing responses of single trait $FDis_{ses}$. For example, in the first two years of drought, opposite responses of $FDis_{ses}$ of SLA and LNC canceled each other out, leading to no change in multivariate $FDis_{ses}$. It was not until year 3 that $FDis_{ses}$ of both SLA and LNC declined leading to a significant response in multivariate $FDis_{ses}$. For SGS, $FDis_{ses}$ of SLA increased in drought plots relative to control plots and remained significantly higher for the remainder of the experiment (Fig. 5.2B); however, this relative increase in $FDis_{ses}$ of SLA was not captured in multivariate measures of $FDis_{ses}$ due to a lack of response of $FDis_{ses}$ of LNC and π_{TLP} until the final years of drought (Fig. 5.2C-D). On the contrary, single trait $FDis_{ses}$ largely mirrored multivariate $FDis_{ses}$ for the three wettest sites with positive responses of $FDis_{ses}$ for each trait at HYS and no significant responses observed at HPG and KNZ (Fig. 5.2). Other indices of functional diversity (i.e., $FRic_{ses}$ and FEve) were moderately affected by drought treatments, depending on site, with treatment effects not consistent across years (see Appendix 4, Fig. A4.1, and Fig. A4.2). Estimates of functional diversity in 2-dimensional trait space (i.e., excluding π_{TLP} from estimates

of FDis$_{ses}$, FRic$_{ses}$, and FEve across sites) did not differ drastically from estimates in 3-dimensional trait space (Appendix 4 and Fig. A4.3).

Experimental drought led to a significant shift in community-weighted trait means across sites, largely away from conservative resource-use strategies (Fig. 5.3). Community-weighted specific leaf area (SLA$_{cw}$) initially decreased in response to drought for two sites (SBK and SBL); however, long-term drought eventually led to significant increases in SLA$_{cw}$ at all six sites relative to ambient plots (Fig. 5.3A). The positive effect of drought on SLA$_{cw}$ was not persistent in its significance or magnitude through the fourth year of the experiment for all the sites. Community-weighted LNC (LNC$_{cw}$) was unchanged until the final years of drought, at which point elevated LNC$_{cw}$ was observed for all sites but KNZ (Fig. 5.3B). Lastly, drought effects on community-weighted leaf turgor loss point (π_{TLP-cw}) were variable among sites with a significant decline in π_{TLP-cw} (i.e. more negative) at HPG, a significant increase in π_{TLP-cw} at SGS, a moderately significant increase at HYS (p=0.06), and no change observed at KNZ (Fig. 5.3C).

Phylogenetic diversity (PD$_{ses}$) was most sensitive to drought at the two driest sites, SBK and SBL, with variable effects observed at the wettest site, KNZ (Fig. 5.4). Drought led to increased PD$_{ses}$ at SBK in year 3 and decreased PD$_{ses}$ at SBL in year 4 (Fig. 5.4). At KNZ, PD$_{ses}$ alternated between drought-induced declines in PD$_{ses}$ and no difference between control and drought plots; however, PD$_{ses}$ of drought plots was significantly lower than control plots by the fourth year of drought. PD$_{ses}$ did not respond to drought treatments at SGS, HPG, or HYS.

Across all 32 tests, the only significant predictors of ANPP sensitivity (following a Benjamin-Hochberg correction for multiple comparisons) were (1) SLA$_{cw}$ of the previous year, (2) FEve of SLA of the current year, and (3) multivariate FEve of the current year (Table A4.2). These predictors were included as fixed effects in separate mixed effects models each with site as

a random effect. Following null model comparison (see methods), we observed a statistically significant positive relationship between drought sensitivity and previous year SLA_{cw} (Fig. 5.5A). In other words, grassland communities with low SLA_{cw} in a given year experienced less drought-induced declines in ANPP the following year. Significant negative correlations were observed between current year FEve (both multivariate and FEve of SLA) and drought sensitivity; however, null model comparisons rejected the model with multivariate FEve and accepted the model with FEve of SLA (Table A4.2).

5.5 Discussion

5.5.1 Functional diversity

We assessed the impact of long-term drought on functional diversity of six North American grassland communities (Table 5.1). Removal of ~40% of annual rainfall for four years negatively impacted ANPP (Fig. 5.1 & 5.5). In contrast, we observed positive effects of drought on functional dispersion (as compared to null communities; $FDis_{ses}$) in half of the grasslands surveyed here, with a negative response observed in only one site (Fig. 5.2). While several indices of functional diversity were measured in this study, $FDis_{ses}$ was the most responsive to drought (Fig. 5.2 and Table 5.2). Increased functional diversity following drought has previously been attributed to mechanisms of niche differentiation and species co-existence (Grime, 2006), while declines in diversity are attributed to drought acting as an environmental filter (Diaz, Cabido, & Casanoves, 1998; Díaz et al., 1999; Whitney et al. 2019). In grasslands, several indices of functional diversity respond strongly to interannual variability in precipitation (Gherardi & Sala, 2015). Dry years often lead to low functional diversity as the dominant drought tolerant grasses persist, while rare species exhibit drought avoidance (e.g., increased water-use efficiency and slower growth) or escape strategies (e.g., early flowering) (Gherardi & Sala, 2015; Kooyers, 2015). Wet years,

however, can lead to high diversity due to negative legacies of dry years acting on dominant grasses and the fast growth rate of rare species which take advantage of large rain events that penetrate deeper soil profiles (Gherardi &Sala, 2015). While traits linked to drought tolerance may allow a species to persist during transient dry periods, long-term intense droughts can lead to mortality of species exhibiting such strategies (McDowell et al., 2008). Here, the variable effects of drought on $FDis_{ses}$ can be explained by (1) mortality/senescence and reordering of dominant drought tolerant species (Smith, Knapp, & Collins, 2009), and (2) increases in the relative abundance of rare or subordinate drought escaping (or avoiding) species (Frenette-Dussault et al., 2012; Kooyers, 2015). Species are considered dominant if they have high abundance relative to other species in the community and have proportionate effects on ecosystem function (Avolio et al., 2019).

The increase in $FDis_{ses}$ in the final year of drought within the desert grassland site (SBK) corresponded with >95% mortality of the dominant grass species, *Bouteloua eriopoda*. This species generally contributes ~80% of total plant cover in ambient plots. The removal of the competitive influence of this dominant species allowed a suite of species characterized by a wider range of trait values to colonize this desert community. Indeed, overall trait space occupied by the community (i.e., $FRic_{ses}$) significantly increased in the final year of drought (Fig. A4.1). Mortality of *B. eriopoda* led to a community composed entirely of ephemeral species, deep-rooted shrubs, and fast-growing forbs (i.e. drought avoiders/escapers). It is worth noting that phylogenetic diversity (PD_{ses}) increased in the year prior to increased $FDis_{ses}$ and $FRic_{ses}$ (Fig. 5.4), which suggests phylogenetic and functional diversity are coupled at this site with perhaps a lagged effect of PD_{ses} on $FDis_{ses}$ and $FRic_{ses}$.

The southern shortgrass prairie site in New Mexico (SBL) was the only site to experience decreased FDis$_{ses}$ in response to drought (Fig. 5.2). This is surprising considering SBK and SBL are within several kilometers of one another (both within the Sevilleta National Wildlife Refuge) and experience a similar climate. This region is characterized by a sharp ecotone, however, resulting in divergent plant communities at SBK and SBL such that SBL is co-dominated by *B. eriopoda* and *Bouteloua gracilis*, a closely related C$_4$ grass. *B. gracilis* is characterized by greater leaf-level drought tolerance than *B. eriopoda* (π_{TLP} = -1.59 and -1.86 MPa for *B. eriopoda* and *B. gracilis*, respectively) which allows it to persist during drought. While *B. eriopoda* and *B. gracilis* both experienced drought-induced mortality (Baur et al. in prep), the greater persistence of *B. gracilis* led to stability in community structure with only moderate declines in FDis$_{ses}$ in the third year of drought. Transient declines in FDis$_{ses}$ may represent environmental filtering acting on subordinate species with traits much different from those of the dominant grasses. Indeed, decreased FDis$_{ses}$ at SBL was accompanied by increased functional evenness (FEve) (Fig. A4.2) and decreased PD$_{ses}$ (Fig. 5.4). Thus, the functional changes observed in this community were driven by both genetically and functionally similar species.

At the northern shortgrass prairie site (SGS), the response of FDis$_{ses}$ to drought was due to re-ordering of dominant species. The early season plant community at SGS is dominated by C$_3$ grasses and forbs, while *B. gracilis* represents ~90% of total plant cover in mid- to late summer (Oesterheld, Loreti, Semmartin, & Sala, 2001). The nature of our drought treatments (i.e. removal of summer rainfall) favored the subordinate C$_3$ plant community at this site. We observed a shift in species dominance from *B. gracilis* to *Vulpia octoflora,* an early season C$_3$ grass, beginning in year 2 of drought (Baur et al. in prep). The initial co-dominance of *B. gracilis* and *V. octoflora* increased FDis$_{ses}$ of SLA (Fig. 5.2B) as these two dominant species exhibit divergent leaf carbon

allocation strategies (SLA = 12.5 and 19.2 kg m^{-2} for *B. gracilis* and *V. octoflora*, respectively). This emphasizes the importance of investigating single trait diversity indices (Spasojevic & Suding, 2012) as this community functional change was masked by multi-variate measures of FDis$_{ses}$ (Fig. 5.2A). The eventual mortality of *B. gracilis* in the fourth year of drought led to significantly higher multivariate FDis$_{ses}$ (Fig. 5.2) as this late season niche was filled by species with a diversity of leaf carbon and nitrogen economies (LNC and SLA). Indeed, drought led to a 55% increase in Shannon's diversity index at SGS (Baur et al. in prep).

Functional diversity of the northern mixed grass prairie (HPG) was unresponsive to drought (Fig. 5.2). This site has the lowest mean annual temperature of the six sites (Table 5.1) and is largely dominated by C$_3$ species which exhibit springtime phenology and are highly dependent on the availability of snowmelt (Knapp et al., 2015). Thus, the nature of our drought treatment (i.e. removal of summer rainfall) had no effect on functional or phylogenetic diversity at this site (Fig. 5.2; Fig. 5.4). On the contrary, we observed increased FDis$_{ses}$ at the southern mixed grass prairie (HYS) in response to experimental drought (Fig. 5.2A). Again, drought treatments led to increased cover of dominant C$_3$ grasses and decreased cover of C$_4$ grasses (Baur et al. in prep). Here, increased multivariate FDis$_{ses}$ was largely mirrored by single trait FDis$_{ses}$ (Fig. 5.2, B-D). The three co-dominant grass species at this site (*Pascopyrum smithii* [C$_3$], *Bouteloua curtipendula* [C$_4$], and *Sporobolus asper* [C$_4$]*)* are characterized by remarkably similar π_{TLP} (ranging from -2.32 to -2.30 MPa). This similarity minimizes FDis$_{ses}$ of π_{TLP} as the weighted distance to the community-weighted trait centroid is minimized (see calculation of FDis in Laliberte & Legendre, 2010). Indeed, HYS has the lowest FDis of π_{TLP} relative to other sites (5-year ambient average: SGS = 0.67; HPG = 0.93; HYS = 0.36; KNZ = 0.37). In the final years of drought, plots previously inhabited by dominant C$_4$ grasses were invaded by perennial forbs and a

C_3 grass with higher π_{TLP} (*Bromus japonicus*; π_{TLP} = -1.6. Increased abundance of the dominant C_3 grass, *P. smithii*, maintained the community-weighted trait centroid near the original mean (-2.3 MPa), while the invasion of subordinate C_3 species led to increased dissimilarity in π_{TLP} (Laliberte & Legendre, 2010). Additionally, *P. smithii* is characterized by low SLA relative to other species at this site (SLA = 5.73 kg m^{-2} for *P. smithii* vs. the SLA$_{cw}$ = 12.3 kg m^{-2}). Thus, increased abundance of *P. smithii* contributed to the spike in FDis$_{ses}$ of SLA in year 3 of the drought (Fig. 5.2B).

No change in community composition was observed at the tallgrass prairie site (KNZ) and consequently we observed no change in FDis (Fig. 5.2). Drought did cause variable negative effects on PD$_{ses}$ at KNZ (Fig. 5.4); however, the response was not consistent and thus warrants further investigation. It is worth noting that the drought response of PD$_{ses}$ did not match FDis$_{ses}$ responses in either SGS, HYS, or KNZ (Fig. 5.4). It is therefore important to measure both functional and phylogenetic diversity as closely related species may differ in their functional attributes (Forrestel et al., 2017; Liu & Osborne, 2015).

5.5.2 Community-weighted traits

Functional composition of plant communities is described by both the diversity of traits as well as community-weighted trait means (CWMs), with the latter also having important consequences for ecosystem function (Garnier et al., 2004; Vile et al., 2006). We therefore assessed the impact of experimental drought on community-weighted means of several plant traits linked to leaf carbon, nitrogen and water economy. Leaf economic traits, such as SLA and LNC, describe a species strategy of resource allocation/use along a continuum of conservative to acquisitive (Reich, 2014). Empirically and theoretically, conservative species with low SLA and/or LNC are more likely to persist during times of resource-limitation, such as drought (Ackerly, 2004;

Wright, Reich, & Westoby, 2001; Reich 2014), and community-weighted SLA tends to decline in response to drought due to trait plasticity (Wellstein et al., 2017). Alternatively, high SLA and LNC have been linked to strategies of drought escape or avoidance (Frenette-Dussault et al., 2012; Kooyers, 2015). Here, we observed increased SLA_{cw} and LNC_{cw} with long-term drought in all six sites (Fig. 5.3A), suggesting a shift away from species with conservative resource-use strategies (i.e. drought tolerance) and towards a community with greater prevalence of drought avoidance and escape strategies. We likely overestimate these trait values given that we do not account for trait plasticity and the ability of species to adjust carbon and nutrient allocation during stressful conditions (Wellstein et al., 2017); however, our results do indicate species re-ordering towards a plant community with inherently higher SLA and LNC following long-term drought. This is likely due to the observed increase in relative abundance of early-season annual species (i.e., drought escapers) and shrubs (i.e., drought avoiders) across most sites (Baur et al., in prep), species that are characterized by high SLA and LNC. Forbs and shrubs tend to access deeper sources of soil water than grasses (Nippert & Knapp, 2007), a characteristic that has allowed them to persist during historical droughts (i.e. drought escape; Weaver, 1958) and may have allowed them to persist during our experimental drought. This further supports the conclusion of a community shift towards drought escape strategies and emphasizes the importance of measuring rooting depth, and root traits more broadly, which are infrequently measured in community-scale surveys of plant traits (Bardgett et al., 2014; Griffin-Nolan et al., 2018a).

While leaf economic traits, such as SLA and LNC, are useful for defining syndromes of plant form and function at both the individual (Díaz et al., 2016) and community-scale (Bruelheide et al., 2018), they are often unreliable indices of plant drought tolerance (e.g., leaf economic traits might not be correlated with drought tolerance within some communities, even if correlations

exists at larger scales) (Brodribb, 2017; Griffin-Nolan et al., 2018a; Rosado et al., 2013). We estimated community-weighted π_{TLP}, or the leaf water potential at which cell turgor is lost, which is considered a strong index of plant drought tolerance (Bartlett, Scoffoni, & Sack, 2012b). Theory and experimental evidence suggests that dry conditions favor species with lower π_{TLP} (Bartlett et al. 2012b; Zhu et al., 2018). While this may be true of individual species distributions ranging from grasslands to forests (Griffin-Nolan et al., 2019; Zhu et al., 2018), this has not been tested at the community scale or within a single community responding to long-term drought. Here, we show that community-scale π_{TLP} responds variably to drought with negative (HPG), positive (SGS and HYS), and neutral effects (KNZ) (Fig. 5.3C). While species can adjust π_{TLP} through osmotic adjustment and/or changes to membrane characteristics (Meinzer et al., 2014), this trait plasticity rarely affects how species rank in terms of leaf-level drought tolerance (Bartlett et al., 2014). Thus, these results suggest that community-scale, leaf-level drought tolerance decreased (i.e. higher π_{TLP}) in response to drought in half of the sites in which π_{TLP} was measured. The opposing effects of drought on community π_{TLP} for SGS and HPG is striking (Fig. 5.3C), especially considering these sites are ~50 km apart and have similar species composition. Increased grass dominance at HPG (Berger-Parker dominance index; Baur et al. in prep) resulted in decreased π_{TLP} (i.e., greater drought tolerance), while at SGS, the community shifted towards a greater abundance of drought avoiders/escapers. Forbs and shrubs in these grasslands tend to have higher π_{TLP} compared to both C_3 and C_4 grasses (Griffin-Nolan et al. 2019), which explains this increase in community-weighted π_{TLP}. Notably, the plant community at HPG is devoid of a true shrub species, which could further explain the unique effects of drought on the abundance-weighted π_{TLP} of this grassland.

5.5.3 Drought sensitivity of ANPP

Biodiversity, and functional diversity more specifically, is well recognized as an important driver of ecosystem resistance to extreme climate events (Anderegg et al., 2018; De La Riva et al., 2017; Pérez-Ramos et al., 2017). We tested this hypothesis across six grasslands by investigating relationships between several functional diversity indices and the sensitivity of ANPP to drought (i.e. drought sensitivity). We observed a significant negative correlation between functional evenness of SLA and drought sensitivity, providing some support for this hypothesis (Fig. 5.5B) while also emphasizing the importance of measuring single trait functional diversity indices (Spasojevic & Suding, 2012). The significant negative correlation between FEve of SLA_{cy} and drought sensitivity suggests that communities with evenly distributed leaf economic traits are less sensitive to drought. While other indices of functional diversity were weakly correlated with drought sensitivity (Table A4.2), all correlations were negative implying greater drought sensitivity in plots/sites with lower community functional diversity.

The strongest predictor of drought sensitivity was community-weighted SLA of the previous year (Table A4.2). The significant positive relationship observed in this study (Fig. 5.5A) suggests that plant communities with a greater abundance of species with high SLA (i.e. resource acquisitive strategies) are more likely to experience greater relative reductions in ANPP during drought in the following year. Furthermore, SLA_{cw} increased in response to long-term drought across sites (Fig. 5.3), which may result in greater sensitivity of these communities to future drought, depending on the timing and nature of drought. The lack of a relationship between π_{TLP} and drought sensitivity was surprising given that π_{TLP} is widely considered an important metric of leaf level drought tolerance (Bartlett, Scoffoni, & Sack, 2012). While π_{TLP} is descriptive of individual plant strategies for coping with drought, it may not scale up to ecosystem level processes

such as ANPP. We recognize that the lack of π_{TLP} data from the two most sensitive sites (SBK and SBL) limits our ability to accurately test the relationship between community-weighted π_{TLP} and drought sensitivity of ANPP. Our results clearly demonstrate, however, that leaf economic traits such as SLA are informative of ANPP dynamics during drought (Garnier et al., 2004; Reich, 2012).

It is important to note that this analysis equates space for time with regards to functional composition and drought sensitivity. The drivers of the temporal patterns in functional composition observed here (i.e., species re-ordering) are likely not the same drivers of spatial patterns in functional composition and may have separate consequences for ecosystem drought sensitivity. Nonetheless, these alterations to functional composition will likely impact drought legacy effects (i.e. lagged effects of drought on ecosystem function following the return of average precipitation conditions). This is especially likely for these six grasslands given that they exhibit strong legacy effects even after short-term drought (Griffin-Nolan et al., 2018b).

5.6 Conclusions

Grasslands provide a wealth of ecosystem services, such as carbon storage, forage production, and soil stabilization (Knapp et al. 1998; Schlesinger and Bernhardt, 2013). The sensitivity of these services to extreme climate events is driven in part by the functional composition of plant communities (De La Riva et al., 2017; Naeem & Wright, 2003; Pérez-Ramos et al., 2017; Tilman, Wedin, & Knops, 1996). Functional composition responds variably to drought (Cantarel et al., 2013; Copeland et al., 2016; Qi et al., 2015), with long-term droughts largely understudied at broad spatial scales.

We imposed a four-year experimental drought which significantly altered community functional composition of six North American grasslands, with potential consequences for ecosystem function. Long-term drought led to increased community functional dispersion in three

sites and a shift in community-level drought strategies (assessed as abundance-weighted traits) from drought tolerance to drought avoidance and escape strategies. Species re-ordering following dominant species mortality/senescence was the main driver of these shifts in functional composition. Drought sensitivity of ANPP (i.e. relative reduction in ANPP) was linked to both functional diversity and community-weighted trait means. Specifically, drought sensitivity was negatively correlated with community evenness of SLA and positively correlated with community-weighted SLA of the previous year.

These findings highlight the value of long-term climate change experiments as many of the changes in functional composition were not noticeable until the final years of drought. Additionally, our results emphasize the importance of measuring both functional diversity and community-weighted plant traits. Increased functional diversity following long-term drought may stabilize ecosystem functioning in response to future drought. However, a shift from community-level drought tolerance towards drought avoidance may increase ecosystem drought sensitivity, depending on the timing and nature of future droughts. The collective response and effect of both functional diversity and trait means may either stabilize or enhance ecosystem responses to climate extremes.

5.7 Tables

Table 5.1. Characteristics of six grassland sites included in the 'Extreme Drought in Grasslands Experiment' (EDGE). 5-year averages of Shannon's diversity index and species richness are shown for ambient plots at each site. Mean annual precipitation (MAP) and temperature (MAT) were taken from Griffin-Nolan et al. (2018). Sites include a desert grassland [Sevilleta National Wildlife Refuge, dominated by black grama, Bouteloua eriopoda (C4) - SBK] and a southern Shortgrass Steppe [Sevilleta National Wildlife Refuge, dominated by blue grama (Bouteloua gracilis (C4)) - SBL], both in New Mexico; a northern Shortgrass Steppe [Central Plains Experimental Range, dominated by B. gracilis - SGS] in Colorado; a northern mixed-grass prairie [High Plains Grassland Research Center, co-dominated by Pascopyron smithii (C3) and B. gracilis - HPG] in Wyoming; as well as a southern mixed-grass prairie [Hays Agricultural Research Center, co-dominated by P. smithii, Bouteloua curtipendula (C4), and Sporobolus asper (C4)—HYS], and a tallgrass prairie [Konza Prairie Biological Station, dominated by Andropogon gerardii (C4) and Sorghastrum nutans (C4)—KNZ], both in Kansas

Site	Grassland type	MAP (mm)	MAT (°C)	Shannon Diversity	Species Richness
Sevilleta Black Grama (SBK)	Desert	244	13.4	2.04	10
Sevilleta Blue Grama (SBL)	Shortgrass	257	13.4	3.39	12
Shortgrass Steppe (SGS)	Shortgrass	366	9.5	5.79	17
High Plains Grassland (HPG)	Mixed-Grass	415	7.9	8.25	23
Hays Agricultural Research Center (HYS)	Mixed-Grass	581	12.3	7.52	23
Konza Prairie (KNZ)	Tallgrass	864	13.0	6.14	16

Table 5.2. ANOVA table for mixed effects models for the standardized effect size (SES) of multivariate functional diversity, community-weighted trait means, and SES of phylogenetic diversity. F-values are shown for fixed effects and all interactions. Statistical significance is represented by asterisks: *p<0.05, **p<0.01, ***p<0.001. *Abbreviations:* FDis = functional dispersion; FRic = functional richness; FEve = functional evenness; PD = phylogenetic diversity; SLA = specific leaf area; LNC = leaf nitrogen content; π_{TLP} = leaf turgor loss point.

Effect	SES of functional and phylogenetic diversity				Community-weighted trait means		
	FDis	**FRic**	**FEve**	**PD**	**SLA**	**LNC**	**π_{TLP}**
Trt	3.68	0.0001	3.64	0.075	27.32***	6.99**	0.002
Site	15.31***	0.19	12.91***	51.22***	339.74***	615.62***	286.13***
Year	11.02***	3.26*	1.44	11.18***	33.44***	58.06***	122.19***
Trt*Site	2.43*	2.11	0.51	1.72	3.48**	0.26	6.30***
Trt*Year	11.98***	0.47	1.52	3.51**	15.02***	28.29***	2.34
Site*Year	30.34***	2.53***	3.07***	8.66***	26.72***	32.70***	62.54***
Trt*Site*Year	7.21***	0.89	2.17**	1.76*	9.13***	7.12***	3.52***
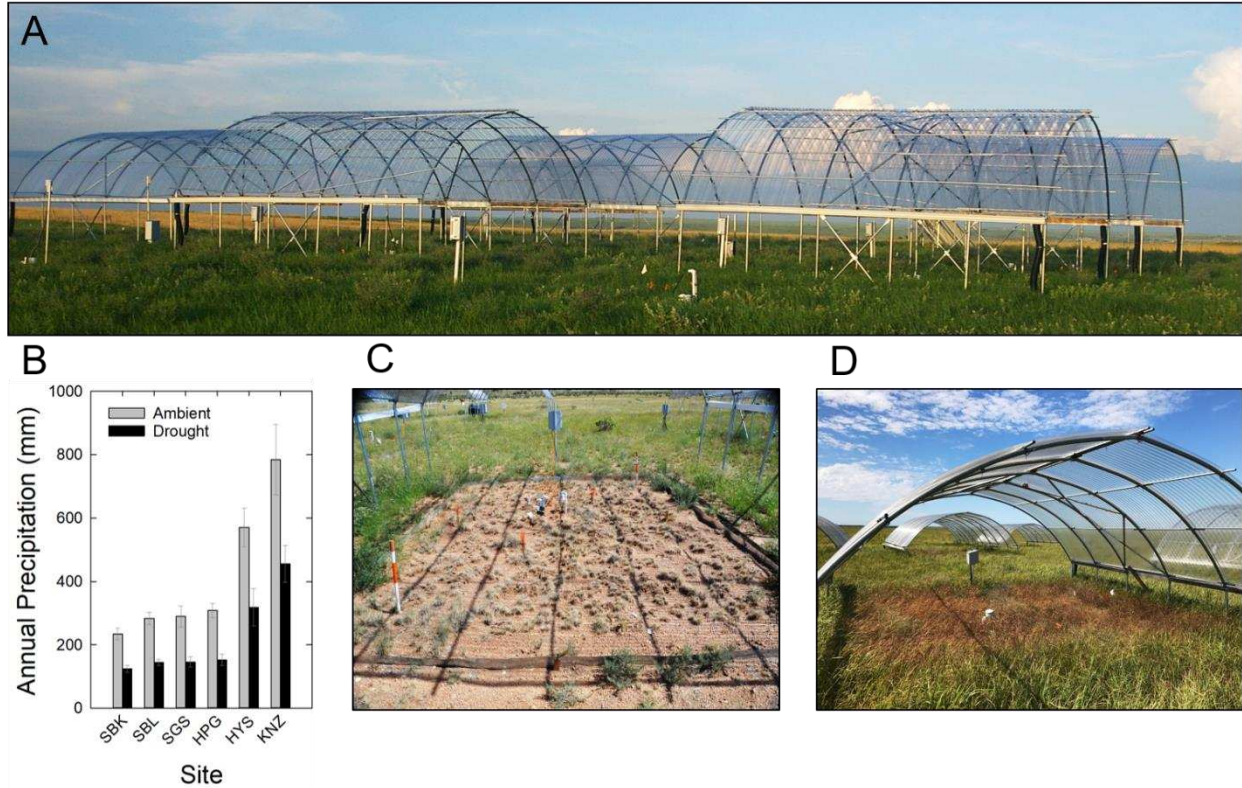
Figure 5.1. (**A**) Large rainfall exclusion shelters were established in six North American grassland sites as part of the Extreme Drought in Grasslands Experiment (EDGE; http://edge.biology.colostate.edu/). (**B**) These shelters passively remove 66% of incoming precipitation during the growing season leading to a ~40% reduction in annual precipitation for four years (error bars represent SE of mean precipitation during the four years). Drought treatments had negative effects on aboveground net primary production in all sites ranging from the Sevilleta desert grassland (SBK) in New Mexico (**C**, photo credit: Scott Collins) to the Konza tallgrass prairie (KNZ) in eastern Kansas (**D**, photo credit: Alan Knapp).
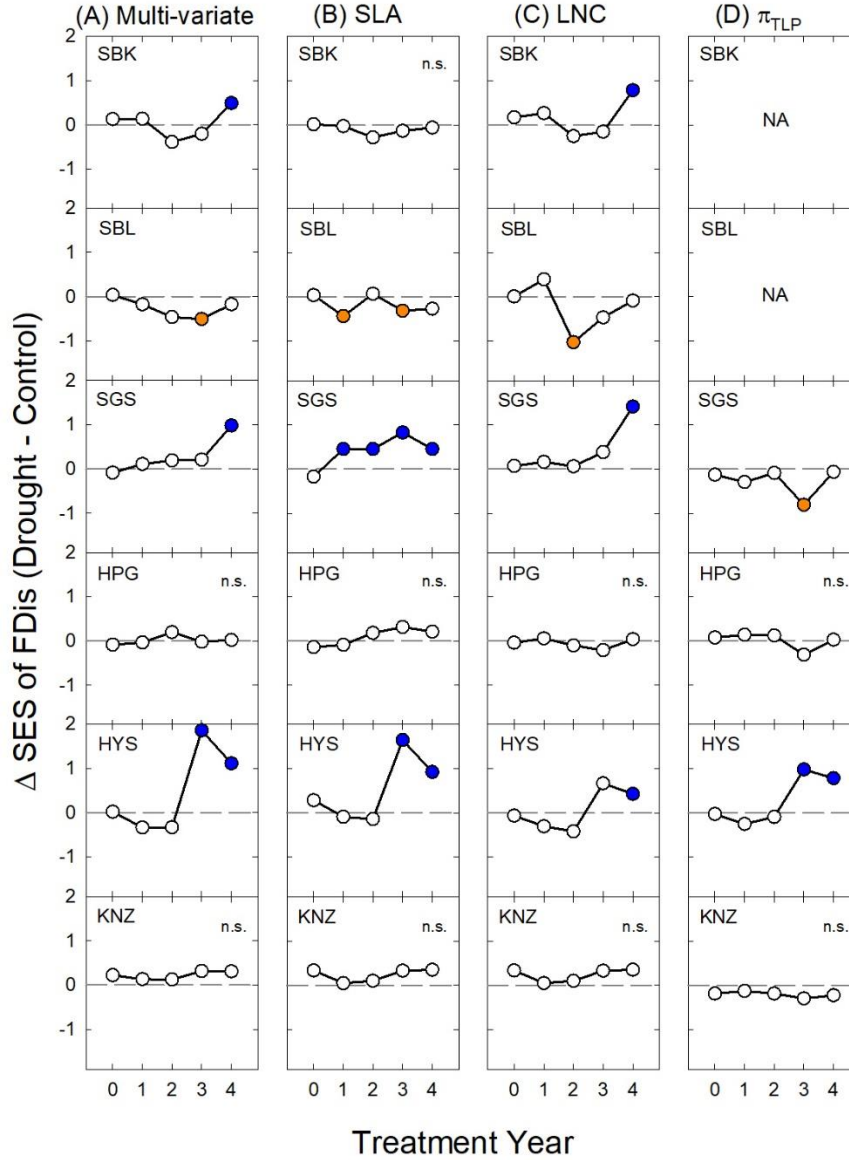
Figure 5.2. The effect of four years of drought on the standardized effect size (SES) of functional dispersion (FDis) estimated in multivariate trait space (**A**) as well as for each trait individually (**B-D**). Drought effects are shown as the difference in SES of FDis between drought and control plots for each year, including the pre-treatment year. Years with statistically significant treatment effects (p < 0.05) are represented by filled in symbols with the color representing a positive (●) or negative (●) effect of drought. Open circles represent a lack of significant difference between control and drought plots, with 'n.s.' denoting a lack of significance across all years. Note that multivariate FDis of SBK and SBL are calculated using only two traits (SLA and LNC) while all three traits are included in the calculation of multivariate FDis for every other site. *Site abbreviations*: SBK = Sevilleta black grama; SBL = Sevilleta blue grama; SGS = Shortgrass steppe; HPG = High plains grassland; HYS = Hays agricultural research station; KNZ = Konza tallgrass prairie.

100
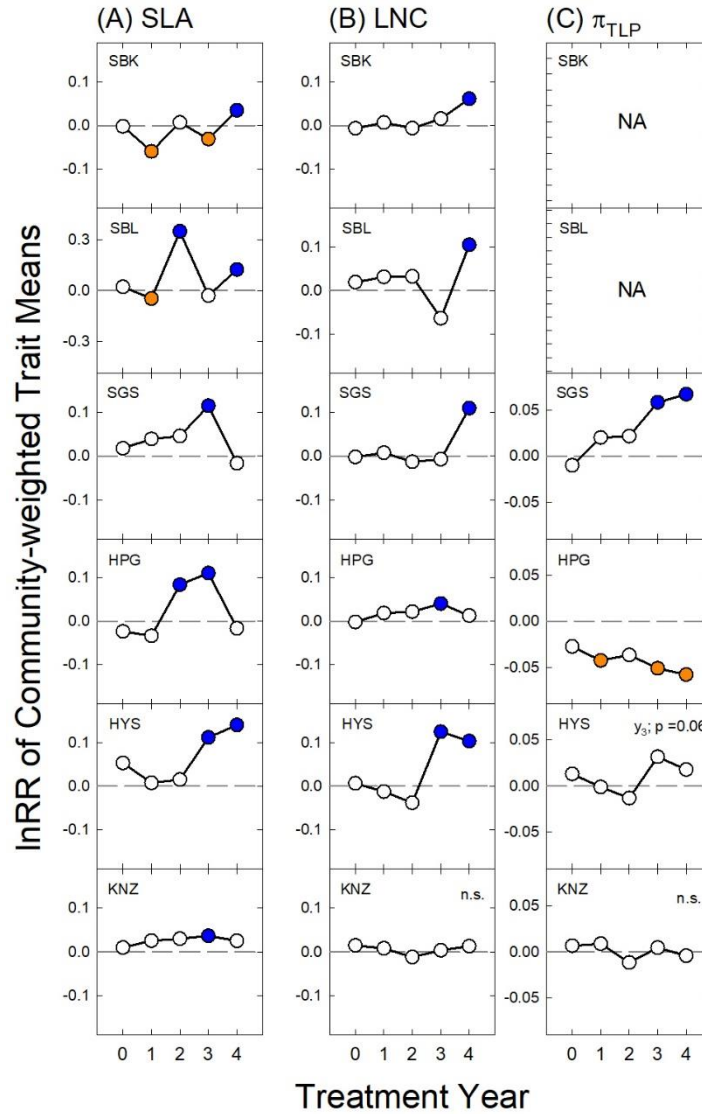
Figure 5.3. Log response ratios (lnRR) for community-weighted trait means (CWM) in response to the drought treatment (lnRR = ln(drought/control). Focal traits include **(A)** specific leaf area (SLA), **(B)** leaf nitrogen content (LNC), and **(C)** leaf turgor loss point (π_{TLP}). Years with statistically significant treatment effects ($p < 0.05$) are represented by filled in symbols with the color representing a positive (●) or negative (●) effect of drought. Open circles represent a lack of significant difference between control and drought plots, with 'n.s.' denoting a lack of significance across all years. Symbol color also reflects conservative (●) vs. acquisitive (●) resource-use strategies at the community-scale as high values of SLA, LNC, and π_{TLP} all reflect acquisitive strategies. Note that HYS experienced a moderately significant increase in π_{TLP} ($p = 0.06$) in year 3 of drought. Axis scaling is not consistent across all panels. Negative lnRR is shown for π_{TLP} such that positive values indicate less negative leaf water potential. *Site abbreviations*: SBK = Sevilleta black grama; SBL = Sevilleta blue grama; SGS = Shortgrass steppe; HPG = High plains grassland; HYS = Hays agricultural research station; KNZ = Konza tallgrass prairie.

101
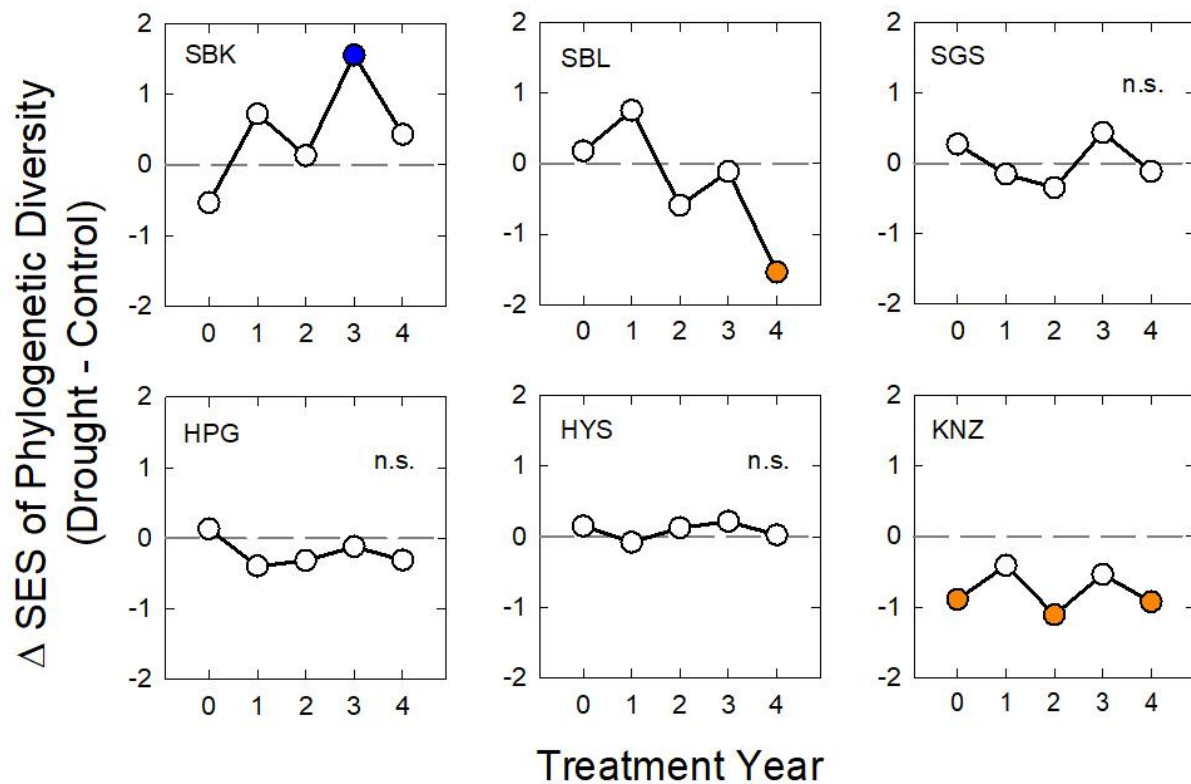
Figure 5.4. Drought effects on standardized effect size (SES) of phylogenetic diversity (PD). The effect of drought (i.e., drought – control) was calculated for the pre-treatment year and each year of the drought treatment. Years with statistically significant treatment effects ($p < 0.05$) are represented by filled in symbols with the color representing a positive (●) or negative (●) effect of drought. Open circles represent a lack of significant difference between control and drought plots, with 'n.s.' denoting a lack of significance across all years. *Site abbreviations*: SBK = Sevilleta black grama; SBL = Sevilleta blue grama; SGS = Shortgrass steppe; HPG = High plains grassland; HYS = Hays agricultural research station; KNZ = Konza tallgrass prairie.
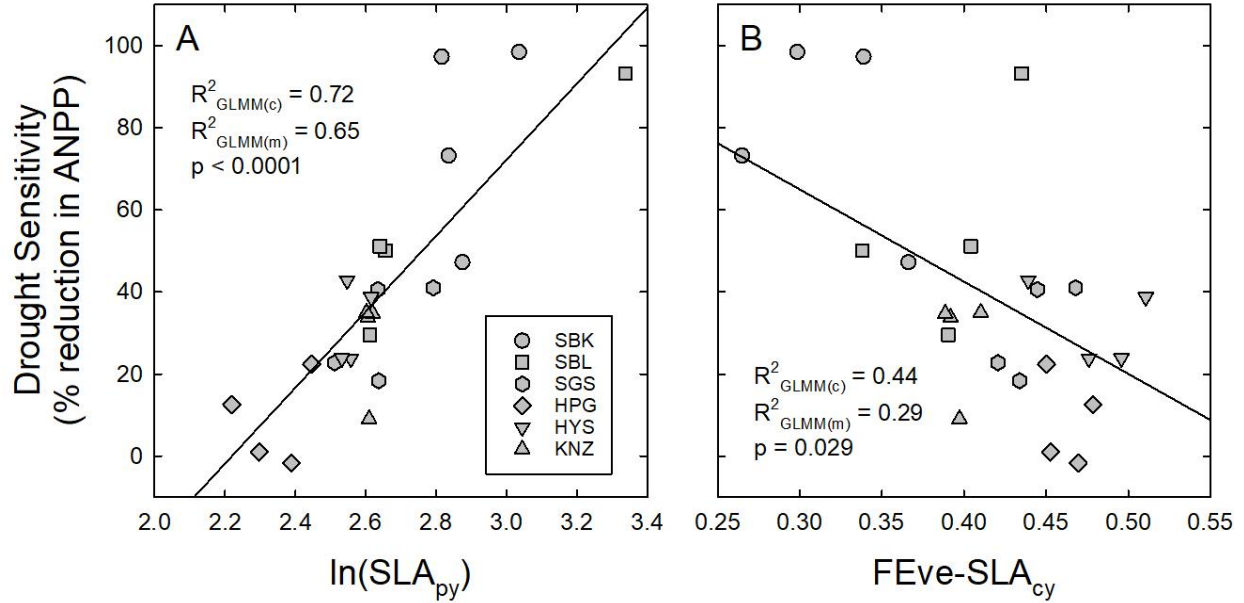
Figure 5.5. Drought sensitivity is (**A**) positively correlated with community-weighted (log-transformed) specific leaf area of the previous year (SLA$_{py}$) and (**B**) negatively correlated with current year functional evenness of specific leaf area (FEve-SLA$_{cy}$). Drought sensitivity was calculated as the absolute value of percent change in aboveground net primary production (ANPP) in drought plots relative to control plots in a given year. The plotted regression lines are from the output of two general linear mixed effect models (GLMM) including site as a random effect and the fixed effect of either SLA$_{py}$ (**A**; *Sensitivity* = 92.55*SLA$_{py}$ - 205.44) or FEve-SLA$_{cy}$ (**B**; *Sensitivity* = -224.8* FEve-SLA$_{cy}$ + 132.42). Both the marginal (m) and conditional (c) R^2 values for the GLMM are shown. *Site abbreviations*: SBK = Sevilleta black grama; SBL = Sevilleta blue grama; SGS = Shortgrass steppe; HPG = High plains grassland; HYS = Hays agricultural research station; KNZ = Konza tallgrass prairie.

CHAPTER 6: CONCLUSIONS

Climate change is expected to cause droughts of unprecedented magnitude and duration, with long-lasting implications for Earth's vegetation (Breshears et al., 2005; Trenberth, 2011). All ecosystems are negatively impacted by drought to some degree, but water-limited ecosystems are among those most sensitive (Huxman et al., 2004). Grasslands are particularly vulnerable to drought, given that aboveground net primary production (ANPP) in these ecosystems is primarily governed by precipitation (PPT) (Knapp et al. 2017). Thus, accurate forecasting of which grasslands are most sensitive to drought is imperative to conserving the many economically and aesthetically valuable services these ecosystems provide (Pendall et al. 2018). Long-term records of ANPP and PPT suggest that xeric grasslands are more sensitive to drought than mesic grasslands (Huxman et al., 2004, Del Grosso et al., 2008, Sala et al., 2012). Extreme drought, however, is rare by definition (Smith, 2011) with limited observations in the long-term record. Thus, forecasting ecosystem sensitivity to extreme drought requires novel experimental frameworks which test physiological mechanisms of drought sensitivity.

In the previous chapters, I have utilized both observational (Chapter 2) and experimental data (Chapter 5) to describe the sensitivity of ANPP to drought across six grasslands. Following a systematic literature review, I identified key research objectives for improving plant-trait-based frameworks for understanding ecosystem and community responses to water availability (Chapter 3). Informed by these guidelines, I adapted methodologies from woody plant physiology literature to validate a high-throughput method for assessing herbaceous plant drought tolerance at the community scale (Chapter 4). Lastly, I assessed the impacts of long-term drought on community functional composition and the corresponding effect that has on ecosystem function of North

American grasslands. Here, I summarize these results, highlight their ecological implications, and discuss avenues of future research.

Ecological resilience, or the capacity of an ecosystem to recover from a stressful event (Tilman and Downing, 1994), is as important as ecological resistance (i.e. inverse of sensitivity) for projecting long-term consequences of climate extremes (Hoover et al. 2014). Theory suggests that legacy effects of drought should be negative (i.e. lower ANPP than expected following the return of average PPT; Sala et al., 2012). In chapter 2, however, I report positive legacy effects of the 2012 drought in half of the grassland sites I surveyed, with only one site exhibiting a negative legacy effect. From a management perspective, the high ecological resilience observed here shows promise for both grazing potential and continued carbon storage following short-term drought, especially as positive legacies were also observed on a regional scale using remote sensing data (Hermance et al. 2015). As predicted by Smith (2011), ecosystem sensitivity to the 2012 drought was highly correlated with the magnitude of ANPP legacy effects in 2013. If this relationship holds true following long-term drought, which are expected to yield negative legacy effects (Yahdjian and Sala 2006; Reichmann et al. 2013), then climate change type droughts are likely to have long-lasting negative implications for ecosystem function. The ecological mechanisms of the legacy effects observed in 2013 are unclear, although optimal precipitation patterns (i.e. rainfall event size and timing) and soil nutrient status likely played a role (Whitford et al. 1995; Reynolds et al. 1999; Muldavin et al. 2008; Hofer et al. 2017). Chronic drought can lead to community compositional changes due to species re-ordering and migration (Smith et al., 2009). Such compositional shifts alter the functional attributes of plant communities (i.e., plant traits), which may provide insight into ecosystem response to and recovery from drought.

Plant traits have been recognized as valuable for providing insight into ecosystem responses to environmental variability, both in terms of function and stability (McGill et al. 2006; Suding et al. 2008). As ANPP is largely determined by the traits of the most abundant species (*sensu* the 'mass-ratio hypothesis'; Grime 1998), weighting traits by relative abundance may reveal mechanisms of differential ecosystem sensitivity to drought. However, only 4% of the 568 manuscripts reviewed in chapter 3 weighted traits by species relative abundance. Moreover, not a single study measured community-weighted hydraulic traits, which are most likely to provide a physiological understanding of plant response to drought (Reich, 2014; Rosado et al. 2014; Brodribb, 2017). While hydraulic traits were well-surveyed in the literature as whole (>200 manuscripts), the field is highly dominated by population-scale surveys of woody species. Thus, herbaceous plant trait surveys could be improved by a selection of traits that reflect physiological functions directly related to water availability with traits weighted by species relative abundance. The high-throughput method for assessing leaf turgor loss point (π_{TLP}) from osmometry measurements, highlighted in chapter 4, shows promise for future community-scale surveys of hydraulic traits. The model for predicting π_{TLP} from osmotic potential at full turgor (π_o) ($\pi_{TLP}=0.80\pi_o–0.845$) was nearly identical to a previously described model for woody species (Bartlett et al., 2012a). Additionally, π_o was well correlated with other metrics linked to drought tolerance (e.g., leaf vulnerability to cavitation), as well as the climatic extremes of a species distribution. Given the efficiency of this method and its utility across plant functional types, it is only a matter of time before collaborative trait databases (such as TRY; www.try-db.org) accumulate enough data for global analyses of community-scale drought tolerance.

The 'response-and-effect' trait framework outlines how plant traits can be used to describe both a species' influence on ecosystem function as well as its response to environmental variability

(Suding et al. 2008). The conceptual framework highlighted in chapter 3 outlines how this framework can be incorporated into the hierarchical response framework proposed by Smith et al. (2009) to predict ecosystem responses to chronic water limitation. Critical to this theoretical fusion, however, is the identification of appropriate response and effect traits within the context of extreme drought. The positive correlation between π_o and MAP shows promise for this trait, especially as most commonly measured plant traits are not well correlated with precipitation (Wright et al., 2004); however, this correlation does not describe how species will shift in response to altered water availability. Thus, future research should assess the temporal and spatial variability of π_o and link this mechanistic trait with changes in species relative abundance. The degree to which a species shifts in response to chronic resource change (predicted via response traits) can be linked with effect traits to predict corresponding linear or non-linear changes in ecosystem function. As highlighted by Suding et al. (2008), a species response to environmental change and its corresponding effect on ecosystem function are not necessarily described by the same trait. For example, spatial/temporal variation in specific leaf area (SLA) is often not correlated with water-availability (Griffin-Nolan et al., 2018a; Wright et al. 2004), however, community-weighted SLA explained >70% of the variability in ANPP responses to the EDGE treatments (see chapter 5). Future research should further investigate the relationships between response and effect traits, as they may help determine the long-term consequences of shifts in functional composition following drought.

The EDGE experiment was established to assess the differential sensitivity of ANPP to drought across six temperate grasslands. As expected, xeric sites experienced the greatest relative reductions in ANPP, while both wet and cool sites were less sensitive. Contrary to expectations, long-term drought led to decreased community drought tolerance (as evidenced by increased

community-weighted SLA, leaf nitrogen content, and π_{TLP}) and increased functional diversity. Additionally, ANPP sensitivity to drought was positively correlated with SLA and negatively correlated with functional diversity. The role these two mechanisms will play in determining ecosystem recovery from and response to potential recurrent drought will be fascinating to assess. As alluded to in chapter 2, legacy effects of multi-year droughts are expected to be negative due to plant mortality. Given the widespread plant mortality observed following four years of drought, especially at the driest sites and particularly for dominant C_4 grasses (Whitney et al., 2019), it is expected that legacy effects of the EDGE treatments will be negative. Complete recovery of ecosystem function following the removal of the EDGE shelters will largely depend on the resilience of dominant C_4 species, as they are the primary contributors to ANPP (Grime 1998; Smith and Knapp 2003). Rapid recovery of these species will likely be driven by the extent to which large rain events (i.e. deluges) re-instate soil moisture during periods of optimal growth (Heisler-White et al., 2008; Muldavin et al., 2008). The removal of the competitive influence of these dominant species, along with the nature of the EDGE drought treatments (i.e. removal of summer rainfall), allowed for the invasion and success of subordinate species (e.g., C_3 grasses, forbs, and ephemeral species) and attendant changes in functional composition. The shift to a C_3-dominted may increase the relative importance of winter precipitation and snowmelt in governing ANPP during recovery years.

Sustained alterations to community composition following climate extremes are likely to affect ecosystem responses to recurrent drought (Smith et al. 2009); however, most studies to date investigate plant community responses to a single cumulative drought event (De Boeck et al., 2011; Jentsch et al., 2011; Hoover et al., 2014; Felton et al., 2019). While there is some evidence that plant physiological acclimation can improve resistance to recurrent drought (Walter et al.,

2011), such "drought memory" is not exhibited by North American prairie grasses (Lemoine et al., 2018) and is unlikely to affect ecosystem responses to recurrent drought. Legacy effects of the experimental drought imposed here on ecosystem responses to recurrent drought will in part depend on the persistence of the observed changes in functional composition (Smith et al., 2009). Given the shift from C_4 to C_3 dominance observed across many of the EDGE sites, spring or winter droughts would be particularly detrimental to ANPP and carbon storage. Previous studies have assessed the importance of drought timing and seasonality (De Boeck et al. 2011); however, no study to my knowledge has investigated the ecosystem responses to recurrent droughts of varying seasonality.

Ecological research never ends, with experimental limitations and mishaps providing an opportunity to inform future studies. For instance, the role of intraspecific trait variability in determining community responses to drought was not assessed in this dissertation. The changes in functional composition described in chapter 5 were due to species re-ordering, yet species were likely exhibiting physiological plasticity throughout the experiment (Smith et al. 2009; Bartlett et al. 2014; Wellstein et al. 2017). While such measurements add further complexity, intraspecific trait plasticity is a key mechanism of ecosystem drought resistance and resilience (Jung et al. 2014). Additionally, intra-annual precipitation variability was not considered even though rainfall patterns are a major driver of grassland ANPP (Heisler-White et al., 2009). Climate model projections suggest precipitation will be distributed in fewer but larger rainfall events in the future (Easterling et al., 2000; IPCC, 2013). In grasslands, these large events are expected to stimulate production in semi-arid grasslands and potentially reduce ANPP in mesic grasslands (Heisler-White et al., 2009). The impact of such deluge events occurring during an extreme multi-year drought, and the consequences for ANPP and functional composition, have yet to be studied.

Future research in plant physiology should address the mechanisms of herbaceous plant mortality, especially considering the extent of C_4 grass mortality observed here (>95% at SBK). The role of hydraulic failure, carbon starvation, and herbivory in determining woody species mortality have been well studied (reviewed by McDowell et al. 2008). Research on the mechanisms of drought-induced mortality of herbaceous species, however, is in its infancy (Craine et al., 2013; Ocheltree et al., 2016). The quantification of herbaceous plant isohydricity, via simultaneous measurements of stomatal and hydraulic sensitivity to dehydration, represents a promising avenue for discovering such mechanisms (Skelton et al., 2015). At the community scale, stomatal sensitivity can be estimated simply from the correlation between pre-dawn and midday measurements of leaf water potential (Martínez-Vilalta et al., 2014). Applying this theory to remotely-sensed leaf water content has led to ecosystem scale metrics of isohydricity, which are well correlated with biomass sensitivity to vapor pressure deficit (Konings et al., 2017). Such classifications of iso/anisohydry are sensitive to spatial/temporal environmental heterogeneity (Feng et al. 2019) and warrant cautious interpretation. Nonetheless, they represent an exciting step towards a more mechanistic understanding of ecosystem sensitivity to drought.

Finally, it is important to note that extreme droughts of the next century will occur against a backdrop of numerous other global change drivers (e.g., increased temperature, N-deposition, elevated CO_2 concentrations, land-use change). Given the speed of global change, there is a need for coordinated multi-factorial experiments that manipulate multiple environmental variables and utilize an integrated experimental-modeling framework. Data from experiments and observations can constrain predictive models of the terrestrial ecosystem carbon cycle (Luo et al. 2015) with model output informing future experiments. A predictive understanding of ecosystem sensitivity to climate change is not possible without such collaborative efforts (Luo et al. 2011).

REFERENCES

Ackerly, D. (2004). Functional strategies of chaparral shrubs in relation to seasonal water deficit and disturbance. *Ecological Monographs*, 74(1), 25–44.

Adams, H. D., Zeppel, M. J., Anderegg, W. R., Hartmann, H., Landhäusser, S. M., Tissue, D. T. et al. (2017). A multi-species synthesis of physiological mechanisms in drought-induced tree mortality. *Nature ecology & evolution*, 1(9), 1285.

Ahlström, A., Raupach, M. R., Schurgers, G., Smith, B., Arneth, A., Jung, M., et al. (2015). The dominant role of semi-arid ecosystems in the trend and variability of the land CO2 sink. *Science*, 348(6237), 895-899.

Allen, C. D., Macalady, A. K., Chenchouni, H., Bachelet, D., McDowell, N., Vennetier, M. et al. (2010). A global overview of drought and heat-induced tree mortality reveals emerging climate change risks for forests. *Forest ecology and management*, 259(4), 660-684.

Ames, G. M., Anderson, S. M., & Wright, J. P. (2016). Multiple environmental drivers structure plant traits at the community-level in a pyrogenic ecosystem. Functional Ecology, 30(5), 789-798.

Anderegg, W. R., Berry, J. A., Smith, D. D., Sperry, J. S., Anderegg, L. D., & Field, C. B. (2012). The roles of hydraulic and carbon stress in a widespread climate-induced forest die-off. *Proceedings of the National Academy of Sciences*, 109(1), 233-237.

Anderegg, W. R., Schwalm, C., Biondi, F., Camarero, J. J., Koch, G., Litvak, M., et al. (2015). Pervasive drought legacies in forest ecosystems and their implications for carbon cycle models. Science, 349(6247), 528-532.

Anderegg, W. R., Klein, T., Bartlett, M., Sack, L., Pellegrini, A. F., Choat, B., & Jansen, S. (2016). Meta-analysis reveals that hydraulic traits explain cross-species patterns of drought-induced tree mortality across the globe. *Proceedings of the National Academy of Sciences*, 113(18), 5024-5029.

Anderegg, W. R. L., Konings, A. G., Trugman, A. T., Yu, K., Bowling, D. R., Gabbitas, R. et al. (2018). Hydraulic diversity of forests regulates ecosystem resilience during drought. *Nature*, 561(7724), 538–541

Avolio, M., Forrestel, E., Chang, C., La Pierre, K., Burghardt, K., & Smith, M. (2019). Demystifying Dominant Species. *New Phytologist*. doi:10.1111/nph.15789.

Baker M. (2016). Is there a reproducibility crisis? A Nature survey lifts the lid on how researchers view the 'crisis' rocking science and what they think will help. *Nature*, 533(7604), 452-455.

Bardgett, R. D., Mommer, L., & De Vries, F. T. (2014). Going underground: root traits as drivers of ecosystem processes. *Trends in Ecology & Evolution*, 29(12), 692-699.

Bartlett, M. K., Scoffoni, C., Ardy, R., Zhang, Y., Sun, S., Cao, K., & Sack, L. (2012a). Rapid determination of comparative drought tolerance traits: using an osmometer to predict turgor loss point. *Methods in Ecology and Evolution*, 3(5), 880-888.

Bartlett, M. K., Scoffoni, C., & Sack, L. (2012b). The determinants of leaf turgor loss point and prediction of drought tolerance of species and biomes: a global meta-analysis. *Ecology Letters*, 15(5), 393-405.

Bartlett, M. K., Zhang, Y., Kreidler, N., Sun, S., Ardy, R., Cao, K., & Sack, L. (2014). Global analysis of plasticity in turgor loss point, a key drought tolerance trait. *Ecology letters*, 17(12), 1580-1590.

Bartlett, M. K., Zhang, Y., Yang, J., Kreidler, N., Sun, S. W., Lin, L., et al. (2016). Drought tolerance as a driver of tropical forest assembly: resolving spatial signatures for multiple processes. *Ecology*, 97(2), 503-514.

Bates, D., Mächler, M., Bolker, B., & Walker, S. (2014). Fitting Linear Mixed-Effects Models using lme4. arXiv preprint arXiv:1406.5823.

Beck J., Böller M., Erhardt A., Schwanghart W. (2014). Spatial bias in the GBIF database and its effect on modeling species' geographic distributions. *Ecological Informatics*, 19, 10-15.

Blackman, C. J., Brodribb, T. J., & Jordan, G. J. (2010). Leaf hydraulic vulnerability is related to conduit dimensions and drought resistance across a diverse range of woody angiosperms. *New Phytologist*, 188(4), 1113-1123.

Blackman, C. J., Brodribb, T. J., & Jordan, G. J. (2012). Leaf hydraulic vulnerability influences species' bioclimatic limits in a diverse group of woody angiosperms. *Oecologia*, 168(1), 1-10.

Blackman, C. J., Gleason, S. M., Chang, Y., Cook, A. M., Laws, C., & Westoby, M. (2014). Leaf hydraulic vulnerability to drought is linked to site water-availability across a broad range of species and climates. *Annals of Botany*, 114(3), 435-440.

Borgy, B., Violle, C., Choler, P., Denelle, P., Munoz, F., Kattge, J., et al. (2017). Plant community structure and nitrogen inputs modulate the climate signal on leaf traits. *Global Ecology and Biogeography*, 26(10), 1138-1152.

Botta-Dukát, Z. (2005). Rao's quadratic entropy as a measure of functional diversity based on multiple traits. *Journal of Vegetation Science*, 16(5), 533–540.

Breshears, D. D., Cobb, N. S., Rich, P. M., Price, K. P., Allen, C. D., Balice, R. G., et al. (2005). Regional vegetation die-off in response to global-change-type drought. *PNAS*, 102(42), 15144–15148.

Brodribb, T. J., & Holbrook, N. M. (2003). Stomatal closure during leaf dehydration, correlation with other leaf physiological traits. *Plant Physiology*, 132(4), 2166-2173.

Brodribb T.J., Feild T.S., and Sack L. (2010). Viewing leaf structure and evolution from a hydraulic perspective. *Functional Plant Biology*, 37(6), 488-498.

Brodribb, T. J. (2017). Progressing from 'functional' to mechanistic traits. *New Phytologist*, 215(1), 9-11.

Bruelheide, H., Dengler, J., Purschke, O., Lenoir, J., Jiménez-Alfaro, B., Hennekens, S. M. et al (2018). Global trait–environment relationships of plant communities. *Nature Ecology & Evolution*, 2(12), 1906–1917.

Burke, I. C., Kittel, T. G. F., Lauenroth, W. K., Snook, P., Yonker, C. M., & Parton, W. J. (1991). Regional analysis of the central Great Plains. *BioScience*, 41(10), 685-692.

Burke, I. C., Yonker, C. M., Parton, W. J., Cole, C. V., Schimel, D. S., & Flach, K. (1989). Texture, climate, and cultivation effects on soil organic matter content in US grassland soils. *Soil science society of America journal*, 53(3), 800-805.

Butterfield, B. J., Bradford, J. B., Munson, S. M., & Gremer, J. R. (2017). Aridity increases below-ground niche breadth in grass communities. *Plant Ecology*, 218(4), 385-394.

Cadotte, M. W., & Tucker, C. M. (2017). Should Environmental Filtering be Abandoned? *Trends in Ecology and Evolution*, 32(6), 429–437.

Cantarel, A. A. M., Bloor, J. M. G., & Soussana, J. F. (2013). Four years of simulated climate change reduces above-ground productivity and alters functional diversity in a grassland ecosystem. *Journal of Vegetation Science*, 24(1), 113–126.

Carmona, C. P., Mason, N. W., Azcárate, F. M., & Peco, B. (2015). Inter-annual fluctuations in rainfall shift the functional structure of Mediterranean grasslands across gradients of productivity and disturbance. *Journal of vegetation science*, 26(3), 538-551.

Carmona, C. P., de Bello, F., Mason, N. W. H., & Lepš, J. (2016). Traits Without Borders: Integrating Functional Diversity Across Scales. *Trends in Ecology & Evolution*, 31(5), 382–394.

Churkina, G., & Running, S. W. (1998). Contrasting climatic controls on the estimated productivity of global terrestrial biomes. *Ecosystems*, 1(2), 206-215.

Ciais, P., Sabine, C., Bala, G., Bopp, L., Brovkin, V., Canadell, J., et al. (2013). Carbon and Other Biogeochemical Cycling. In *Climate Change 2013*.

Clark, J. S., Grimm, E. C., Donovan, J. J., Fritz, S. C., Engstrom, D. R., & Almendinger, J. E. (2002). Drought cycles and landscape responses to past aridity on prairies of the northern Great Plains, USA. *Ecology*, 83(3), 595-601.

Collins, S. L., Koerner, S. E., Plaut, J. A., Okie, J. G., Brese, D., Calabrese, L. B., et al. (2012). Stability of tallgrass prairie during a 19-year increase in growing season precipitation. *Functional Ecology*, 26(6), 1450-1459.

Cook, B. I., Ault, T. R., & Smerdon, J. E. (2015). Unprecedented 21st century drought risk in the American Southwest and Central Plains. *Science Advances*, 1(1), e1400082.

Copeland, S. M., Harrison, S. P., Latimer, A. M., Damschen, E. I., Eskelinen, A. M., Fernandez-Going, B., et al. (2016). Ecological effects of extreme drought on Californian herbaceous plant communities. *Ecological Monographs*, 86(3), 295–311.

Cornwell, W. K., & Ackerly, D. D. (2009). Community assembly and shifts in plant trait distributions across an environmental gradient in coastal California. *Ecological Monographs,* 79(1), 109-126.

Cox, P. M., Betts, R. A., Jones, C. D., Spall, S. A., & Totterdell, I. J. (2000). erratum: Acceleration of global warming due to carbon-cycle feedbacks in a coupled climate model. *Nature*, 408(6813), 750.

Craine, J. M., Ocheltree, T. W., Nippert, J. B., Towne, E. G., Skibbe, A. M., Kembel, S. W., & Fargione, J. E. (2013). Global diversity of drought tolerance and grassland climate-change resilience. Nature Climate Change, 3(1), 63.

Dai, A. (2011). Drought under global warming: a review. *Wiley Interdisciplinary Reviews: Climate Change*, 2(1), 45-65.

Dai, A. (2013). Increasing drought under global warming in observations and models. *Nature Climate Change*, 3(1), 52.

Dalgleish, H. J., & Hartnett, D. C. (2006). Below-ground bud banks increase along a precipitation gradient of the North American Great Plains: a test of the meristem limitation hypothesis. *New Phytologist*, 171(1), 81-89.

De Boeck, H. J., Dreesen, F. E., Janssens, I. A., & Nijs, I. (2011). Whole-system responses of experimental plant communities to climate extremes imposed in different seasons. *New Phytologist*, 189(3), 806-817.

De La Riva, E. G., Lloret, F., Pérez-Ramos, I. M., Marañón, T., Saura-Mas, S., Díaz-Delgado, R., & Villar, R. (2017). The importance of functional diversity in the stability of Mediterranean

shrubland communities after the impact of extreme climatic events. *Journal of Plant Ecology*, 10(2), 281–293.

Del Grosso, S., Parton, W., Stohlgren, T., Zheng, D., Bachelet, D., Prince, S., et al. (2008). Global potential net primary production predicted from vegetation class, precipitation, and temperature. *Ecology*, 89(8), 2117-2126.

Díaz, S., & Cabido, M. (1997). Plant functional types and ecosystem function in relation to global change. *Journal of Vegetation Science*, 8(4), 463-474.

Diaz, S., Cabido, M., & Casanoves, F. (1998). Plant functional traits and environmental filters at a regional scale. *Journal of Vegetation Science*, 9(1), 113-122.

Díaz, S., Cabido, M., Zak, M., Martínez Carretero, E., Araníbar, J., Diaz, S., et al. (1999). Plant functional traits, ecosystem structure and land-use history along a climatic gradient in central-western Argentina. *Journal of Vegetation Science*, 10(5), 651–660.

Dıaz, S., & Cabido, M. (2001). Vive la difference: plant functional diversity matters to ecosystem processes. *Trends in ecology & evolution*, 16(11), 646-655.

Díaz, S., Kattge, J., Cornelissen, J. H. C., Wright, I. J., Lavorel, S., Dray, S., et al. (2016). The global spectrum of plant form and function. *Nature*, 529(7585), 167–171.

Diffenbaugh, N. S., Giorgi, F., & Pal, J. S. (2008). Climate change hotspots in the United States. *Geophysical Research Letters*, 35(16).

Easterling, D. R., Meehl, G. A., Parmesan, C., Changnon, S. A., Karl, T. R., & Mearns, L. O. (2000). Climate extremes: observations, modeling, and impacts. *Science*, 289(5487), 2068-2074.

Edwards, E. J., & Still, C. J. (2008). Climate, phylogeny and the ecological distribution of C4 grasses. *Ecology letters*, 11(3), 266-276.

Enquist, B. J., Economo, E. P., Huxman, T. E., Allen, A. P., Ignace, D. D., & Gillooly, J. F. (2003). Scaling metabolism from organisms to ecosystems. *Nature*, 423(6940), 639.

Esperón-Rodríguez, M., Curran, T. J., Camac, J. S., Hofmann, R. W., Correa-Metrio, A., & Barradas, V. L. (2018). Correlation of drought traits and the predictability of osmotic potential at full leaf turgor in vegetation from New Zealand. *Austral ecology*, 43(4), 397-408.

Evans, J., & Poorter, H. (2001). Photosynthetic acclimation of plants to growth irradiance: the relative importance of specific leaf area and nitrogen partitioning in maximizing carbon gain. *Plant, Cell & Environment*, 24(8), 755-767.

Evert R. F. and Eichhorn S. E. (2013). Raven Biology of Plants. Freeman and Co, 598-599

Fahey, T. J., & Knapp, A. K. (Eds.). (2007). Principles and standards for measuring primary production. Oxford University Press.

Faith, D. P. (1992). Conservation evaluation and phylogenetic diversity. *Biological conservation*, 61(1), 1-10.

Fay, P. A., Carlisle, J. D., Knapp, A. K., Blair, J. M., & Collins, S. L. (2003). Productivity responses to altered rainfall patterns in a C4-dominated grassland. *Oecologia*, 137(2), 245-251.

Felton, A. J., & Smith, M. D. (2017). Integrating plant ecological responses to climate extremes from individual to ecosystem levels. *Phil. Trans. R. Soc. B*, 372(1723), 20160142.

Felton, A. J., Knapp, A. K., & Smith, M. D. (2019). Carbon exchange responses of a mesic grassland to an extreme gradient of precipitation. *Oecologia*, 189(3), 565-576.

Feng, X., Ackerly, D. D., Dawson, T. E., Manzoni, S., McLaughlin, B., Skelton, R. P., et al. (2019). Beyond isohydricity: The role of environmental variability in determining plant drought responses. *Plant, cell & environment*, 42(4), 1104-1111.

Fernandes, V. M., Machado de Lima, N. M., Roush, D., Rudgers, J., Collins, S. L., & Garcia-Pichel, F. (2018). Exposure to predicted precipitation patterns decreases population size and alters community structure of cyanobacteria in biological soil crusts from the Chihuahuan Desert. *Environmental microbiology*, 20(1), 259-269.

Field, C. B., Behrenfeld, M. J., Randerson, J. T., & Falkowski, P. (1998). Primary production of the biosphere: integrating terrestrial and oceanic components. *Science*, 281(5374), 237-240.

Forrestel, E. J., Donoghue, M. J., Edwards, E. J., Jetz, W., du Toit, J. C., & Smith, M. D. (2017). Different clades and traits yield similar grassland functional responses. *PNAS*, 114(4), 705-710.

Frenette-Dussault, C., Shipley, B., Léger, J. F., Meziane, D., & Hingrat, Y. (2012). Functional structure of an arid steppe plant community reveals similarities with Grime's C-S-R theory. *Journal of Vegetation Science*, 23(2), 208–222.

Freschet, G. T., Cornelissen, J. H., Van Logtestijn, R. S., & Aerts, R. (2010). Evidence of the 'plant economics spectrum' in a subarctic flora. *Journal of Ecology*, 98(2), 362-373.

Fu, X., Meinzer, F. C., Woodruff, D. R., Liu, Y. Y., Smith, D. D., McCulloh, K. A., & Howard, A. R. (2019). Coordination and trade-offs between leaf and stem hydraulic traits and stomatal regulation along a spectrum of isohydry to anisohydry. *Plant, cell & environment,* https://doi.org/10.1111/pce.13543

Garnier, E., Cortez, J., Billès, G., Navas, M. L., Roumet, C., Debussche, M., et al. (2004). Plant functional markers capture ecosystem properties during secondary succession. *Ecology*, 85(9), 2630–2637.

Gherardi, L. A., & Sala, O. E. (2015). Enhanced interannual precipitation variability increases plant functional diversity that in turn ameliorates negative impact on productivity. *Ecology Letters*, 18(12), 1293–1300.

Griffin, D., & Anchukaitis, K. J. (2014). How unusual is the 2012–2014 California drought?. *Geophysical Research Letters*, 41(24), 9017-9023.

Griffin-Nolan, R. J., Bushey, J. A., Carroll, C. J., Challis, A., Chieppa, J., Garbowski, M., et al. (2018a). Trait selection and community weighting are key to understanding ecosystem responses to changing precipitation regimes. *Functional Ecology*, 32(7), 1746-1756.

Griffin-Nolan, R. J., Carroll, C. J. W., Denton, E. M., Johnston, M. K., Collins, S. L., Smith, M. D., & Knapp, A. K. (2018b). Legacy effects of a regional drought on aboveground net primary production in six central US grasslands. *Plant Ecology*, 219(5), 505–515.

Griffin-Nolan, R. J., Ocheltree, T. W., Mueller, K. E., Blumenthal, D. M., Kray, J. A., & Knapp, A. K. (2019). Extending the osmometer method for assessing drought tolerance in herbaceous species. *Oecologia*, 189(2), 353-363.

Grime, J. P. (1998). Benefits of plant diversity to ecosystems: immediate, filter and founder effects. *Journal of Ecology*, 86(6), 902-910.

Grime, J. P. (2006). Trait convergence and trait divergence in herbaceous plant communities: Mechanisms and consequences. *Journal of Vegetation Science*, 17(2), 255–260.

Guittar, J., Goldberg, D., Klanderud, K., Telford, R. J., & Vandvik, V. (2016). Can trait patterns along gradients predict plant community responses to climate change? *Ecology*, 97(10), 2791-2801.

Hallett, L. M., Stein, C., & Suding, K. N. (2017). Functional diversity increases ecological stability in a grazed grassland. *Oecologia*, 183(3), 831–840.

Hermance, J. F., Augustine, D. J., & Derner, J. D. (2015). Quantifying characteristic growth dynamics in a semi-arid grassland ecosystem by predicting short-term NDVI phenology from daily rainfall: a simple four parameter coupled-reservoir model. *International Journal of Remote Sensing*, 36(22), 5637-5663.

Hernández-Calderón, E., Méndez-Alonzo, R., Martínez-Cruz, J., González-Rodríguez, A., & Oyama, K. (2014). Altitudinal changes in tree leaf and stem functional diversity in a semi-tropical mountain. *Journal of vegetation science*, 25(4), 955-966.

Hofer, D., Suter, M., Buchmann, N., & Lüscher, A. (2017). Nitrogen status of functionally different forage species explains resistance to severe drought and post-drought overcompensation. *Agriculture, ecosystems & environment*, 236, 312-322.

Hoover, D. L., Knapp, A. K., & Smith, M. D. (2014). Resistance and resilience of a grassland ecosystem to climate extremes. *Ecology*, 95(9), 2646-2656.

Hsu, J. S., Powell, J., & Adler, P. B. (2012). Sensitivity of mean annual primary production to precipitation. *Global Change Biology*, 18(7), 2246–2255.

Huntingford, C., Fisher, R. A., Mercado, L., Booth, B. B., Sitch, S., Harris, P. P., et al. (2008). Towards quantifying uncertainty in predictions of Amazon 'dieback'. *Philosophical Transactions of the Royal Society B: Biological Sciences*, 363(1498), 1857-1864.

Huxman, T. E., Smith, M. D., Fay, P. A., Knapp, A. K., Shaw, M. R., Loik, M. E., et al. (2004). Convergence across biomes to a common rain-use efficiency. *Nature*, 429(6992), 651.

IPCC (2013) Climate Change 2013. The physical science basis. Working group I contribution to the fifth assessment report of the intergovernmental panel on climate change. Stocker TF, Qin D, Plattner GK, Tignor MMB, Allen SK, Boschung J, Nauels A, Xia Y, Bex V Midgley PM, eds. Cambridge University Press, Cambridge

Isbell, F., Craven, D., Connolly, J., Loreau, M., Schmid, B., Beierkuhnlein, C., et al. (2015). Biodiversity increases the resistance of ecosystem productivity to climate extremes. *Nature*, 526(7574), 574–577.

Jentsch, A., Kreyling, J., Elmer, M., Gellesch, E., Glaser, B., Grant, K., et al. (2011). Climate extremes initiate ecosystem-regulating functions while maintaining productivity. *Journal of Ecology*, 99(3), 689-702.

Jung, V., Albert, C. H., Violle, C., Kunstler, G., Loucougaray, G., & Spiegelberger, T. (2014). Intraspecific trait variability mediates the response of subalpine grassland communities to extreme drought events. *Journal of Ecology*, 102(1), 45-53.

Karl, T. R., Melillo, J. M., Peterson, T. C., & Hassol, S. J. (Eds.). (2009). Global climate change impacts in the United States. Cambridge University Press.

Kattge, J., Diaz, S., Lavorel, S., Prentice, I. C., Leadley, P., Bönisch, G., et al. (2011). TRY–a global database of plant traits. *Global Change Biology*, 17(9), 2905-2935.

Kembel W., S., Cowan D., P., Helmus R., M., Cornwell K., W., Morlon, H., Ackerly D., D., et al. (2010). Picante: R tools for integrating phylogenies and ecology. *Bioinformatics*, 26(11), 1463–1464.

Kieft, T. L., White, C. S., Loftin, S. R., Aguilar, R., Craig, J. A., & Skaar, D. A. (1998). Temporal dynamics in soil carbon and nitrogen resources at a grassland–shrubland ecotone. *Ecology*, 79(2), 671-683.

Kikuta, S. B. and Richter, H. (1992). Leaf discs or press saps? A comparison of techniques for the determination of osmotic potentials in freeze-thawed leaf material. *Journal of Experimental Botany,* 43(8), 1039-44.

Kimball, S., Funk, J. L., Spasojevic, M. J., Suding, K. N., Parker, S., & Goulden, M. L. (2016). Can functional traits predict plant community response to global change? *Ecosphere*, 7(12). doi:10.1002/ecs2.1602

Klumpp, K., and Soussana J. F. (2009). Using functional traits to predict grassland ecosystem change: a mathematical test of the response-and-effect trait approach. *Global Change Biology*, 15(12), 2921-2934.

Knapp, A. K., Briggs, J. M., Hartnett, D. C., & Collins, S. L. (1998). Grassland Dynamics: Long-Term Ecological Research in Tallgrass Prairie. Long-term Ecological Research Network Series (Vol. 1). New York: Oxford University Press.

Knapp, A. K., & Smith, M. D. (2001). Variation among biomes in temporal dynamics of aboveground primary production. *Science*, 291(5503), 481–484.

Knapp, A. K., Carroll, C. J., Denton, E. M., La Pierre, K. J., Collins, S. L., & Smith, M. D. (2015). Differential sensitivity to regional-scale drought in six central US grasslands. *Oecologia*, 177(4), 949-957.

Knapp, A. K., Ciais, P., & Smith, M. D. (2017). Reconciling inconsistencies in precipitation-productivity relationships: implications for climate change. *New Phytologist*, 214(1), 41-47.

Knapp, A. K., Avolio, M. L., Beier, C., Carroll, C. J., Collins, S. L., Dukes, J. S., et al. (2017). Pushing precipitation to the extremes in distributed experiments: recommendations for simulating wet and dry years. *Global change biology*, 23(5), 1774-1782.

Knapp, A. K., Carroll, C. J., Griffin-Nolan, R. J., Slette, I. J., Chaves, F. A., Baur, L. E., ... & Mao, W. (2018). A reality check for climate change experiments: Do they reflect the real world?. *Ecology*, 99(10), 2145-2151.

Koerner, S. E., & Collins, S. L. (2014). Interactive effects of grazing, drought, and fire on grassland plant communities in North America and South Africa. *Ecology*, 95(1), 98–109.

Koide, R. T., Robichaux, R. H., Morse, S. R., & Smith, C. M. (1989). Plant water status, hydraulic resistance and capacitance. In Plant physiological ecology (pp. 161-183). Springer, Dordrecht.

Konings, A. G., Williams, A. P., & Gentine, P. (2017). Sensitivity of grassland productivity to aridity controlled by stomatal and xylem regulation. *Nature Geoscience*, 10(4), 284.

Kooyers, N. J. (2015). The evolution of drought escape and avoidance in natural herbaceous populations. *Plant Science*, 234, 155-162.

Kraft, N. J. B., Adler, P. B., Godoy, O., James, E. C., Fuller, S., & Levine, J. M. (2015). Community assembly, coexistence and the environmental filtering metaphor. *Functional Ecology*, 29(5), 592–599.

Kramer, P. J., & Boyer, J. S. (1995). Water relations of plants and soils. Academic press.

Kunkel, K. E., Stevens, L. E., Stevens, S.E. et al. (2013). Regional Climate Trends and Scenarios for the U.S. National Climate Assessment. Part 4. Climate of the U.S. Great Plains, *NOAA Technical Report NESDIS*, 142(4), 82.

Kursar, T. A., Engelbrecht, B. M., Burke, A., Tyree, M. T., EI Omari, B., & Giraldo, J. P. (2009). Tolerance to low leaf water status of tropical tree seedlings is related to drought performance and distribution. *Functional Ecology*, 23(1), 93-102.

Laliberte, E., & Legendre, P. (2010). A distance-based framework for measuring functional diversity from multiple traits. *Ecology*, 91(1), 299–305.

Laliberté, E., Legendre, P., Shipley, B., & Laliberté, M. E. (2014). Package 'FD'. Measuring functional diversity from multiple traits, and other tools for functional ecology.

Langley, J. A., Chapman, S. K., La Pierre, K. J., Avolio, M., Bowman, W. D., Johnson, D. S., et al. (2018). Ambient changes exceed treatment effects on plant species abundance in global change experiments. *Global Change Biology*, 24(12), 5668–5679.

Lauenroth, W. K., & Sala, O. E. (1992). Long-term forage production of North American shortgrass steppe. *Ecological applications*, 2(4), 397-403.

Lavorel, S., & Garnier, E. (2002). Predicting changes in community composition and ecosystem functioning from plant traits: revisiting the Holy Grail. *Functional Ecology*, 16, 545–556.

Lebrija-Trejos, E., Lobato, M. C. C., & Sternberg, M. (2011). Reproductive traits and seed dynamics at two environmentally contrasting annual plant communities: from fieldwork to theoretical expectations. *Israel journal of ecology & evolution*, 57(1-2), 73-90.

Lefcheck, J. S. (2016). piecewiseSEM : Piecewise structural equation modelling in r for ecology, evolution, and systematics. *Methods in Ecology and Evolution*, 7(5), 573–579.

Lemoine, N. P., Griffin-Nolan, R. J., Lock, A. D., & Knapp, A. K. (2018). Drought timing, not previous drought exposure, determines sensitivity of two shortgrass species to water stress. *Oecologia*, 188(4), 965-975.

Levin, S. A. (1992). The problem of pattern and scale in ecology: the Robert H. MacArthur award lecture. *Ecology*, 73(6), 1943-1967.

Levitt J. 1980. Responses of plants to environmental stresses. Volume II. Water, radiation, salt, and other stresses. New York: Academic Press.

Li, L., McCormack, M. L., Ma, C., Kong, D., Zhang, Q., Chen, X. et al. (2015). Leaf economics and hydraulic traits are decoupled in five species-rich tropical-subtropical forests. *Ecology Letters*, 18(9), 899-906.

Liu MZ and Osborne CP. (2008). Leaf cold acclimation and freezing injury in C3 and C4 grasses of the Mongolian Plateau. *Journal of experimental Botany*, 59(15), 4161-4170.

Liu, C., He, N., Zhang, J., Li, Y., Wang, Q., Sack, L., & Yu, G. (2018). Variation of stomatal traits from cold temperate to tropical forests and association with water use efficiency. *Functional ecology*, 32(1), 20-28.

Liu, H., & Osborne, C. P. (2015). Water relations traits of C4 grasses depend on phylogenetic lineage, photosynthetic pathway, and habitat water availability. *Journal of Experimental Botany*, 66(3), 761–773.

Lo Gullo, M. A., Nardini, A., Salleo, S., & Tyree, M. T. (1998). Changes in root hydraulic conductance (KR) of *Olea oleaster* seedlings following drought stress and irrigation. *New Phytologist*, 140(1), 25-31.

Luo, Y., Keenan, T. F., & Smith, M. (2015). Predictability of the terrestrial carbon cycle. *Global change biology*, 21(5), 1737-1751.

Luo, Y.Q., Melillo, J., Niu, S., Beier, C., Clark, J.S., Classen, A.T., Davidson, E., Dukes, J.S., Evans, R.D., Field, C.B., Czimczik, C.I., Keller, M., Kimball, B.A., Kueppers, L.M., Norby, R.J., Pelini, S.L., Pendall, E., Rastetter, E., Six, J., Smith, M., Tjoelker, M.G., Torn, M.S. (2011). Coordinated approaches to quantify long-term ecosystem dynamics in response to global change. *Global Change Biol*, 17: 843-854.

Maréchaux, I., Bartlett, M. K., Gaucher, P., Sack, L., & Chave, J. (2016). Causes of variation in leaf-level drought tolerance within an Amazonian forest. *Journal of Plant Hydraulics*, 3, e004.

Maréchaux, I., Bartlett, M. K., Sack, L., Baraloto, C., Engel, J., Joetzjer, E., & Chave, J. (2015). Drought tolerance as predicted by leaf water potential at turgor loss point varies strongly across species within an Amazonian forest. *Functional Ecology*, 29(10), 1268-1277.

Mart, K. B., Veneklaas, E. J., & Bramley, H. (2016). Osmotic potential at full turgor: an easily measurable trait to help breeders select for drought tolerance in wheat. *Plant Breeding*, 135(3), 279-285.

Martínez-Vilalta, J., Poyatos, R., Aguadé, D., Retana, J., & Mencuccini, M. (2014). A new look at water transport regulation in plants. *New Phytologist*, 204(1), 105-115.

Mason, N. W. H., MacGillivray, K., Steel, J. B., & Wilson, J. B. (2003). An index of functional diversity. Journal of Vegetation Science, 14(4), 571–578.

Mason, N. W. H., De Bello, F., Mouillot, D., Pavoine, S., & Dray, S. (2013). A guide for using functional diversity indices to reveal changes in assembly processes along ecological gradients. *Journal of Vegetation Science*, 24(5), 794–806.

McDowell, N., Pockman, W. T., Allen, C. D., Breshears, D. D., Cobb, N., Kolb, T., et al. (2008). Mechanisms of plant survival and mortality during drought: why do some plants survive while others succumb to drought?. *New Phytologist*, 178(4), 719-739.

Meinzer F.C., McCulloh K.A., Lachenbruch B., Woodruff D.R., Johnson D.M. (2010). The blind men and the elephant: the impact of context and scale in evaluating conflicts between plant hydraulic safety and efficiency. *Oecologia*, 164: 287–296.

Meinzer, F. C., Woodruff, D. R., Marias, D. E., Mcculloh, K. A., & Sevanto, S. (2014). Dynamics of leaf water relations components in co-occurring iso- and anisohydric conifer species. *Plant Cell and Environment*, 37(11), 2577–2586.

Meinzer, F. C., Woodruff, D. R., Marias, D. E., Smith, D. D., McCulloh, K. A., Howard, A. R., & Magedman, A. L. (2016). Mapping 'hydroscapes' along the iso-to anisohydric continuum of stomatal regulation of plant water status. *Ecology Letters*, 19(11), 1343-1352.

Milla, R., Reich, P. B., Niinemets, Ü., & Castro-Díez, P. (2008). Environmental and developmental controls on specific leaf area are little modified by leaf allometry. *Functional Ecology*, 22(4), 565-576.

Mitchell, P. J., O'grady, A. P., Pinkard, E. A., Brodribb, T. J., Arndt, S. K., Blackman, C. J., et al. (2016). An ecoclimatic framework for evaluating the resilience of vegetation to water deficit. *Global Change Biology*, 22(5), 1677-1689.

Moles, A. T., Perkins, S. E., Laffan, S. W., Flores-Moreno, H., Awasthy, M., Tindall, M. L., et al. (2014). Which is a better predictor of plant traits: temperature or precipitation? *Journal of Vegetation Science*, 25(5), 1167-1180.

Muldavin, E. H., Moore, D. I., Collins, S. L., Wetherill, K. R., & Lightfoot, D. C. (2008). Aboveground net primary production dynamics in a northern Chihuahuan Desert ecosystem. *Oecologia*, 155(1), 123-132.

Muscarella, R., Uriarte, M., Erickson, D. L., Swenson, N. G., Kress, W. J., & Zimmerman, J. K. (2016). Variation of tropical forest assembly processes across regional environmental gradients. *Perspectives in Plant Ecology, Evolution and Systematics*, 23, 52-62.

Naeem, S., & Wright, J. P. (2003). Disentangling biodiversity effects on ecosystem functioning: deriving solutions to a seemingly insurmountable problem. *Ecology Letters*, 6(6), 567–579.

Nakagawa, S., & Schielzeth, H. (2013). A general and simple method for obtaining R2 from generalized linear mixed-effects models. *Methods in Ecology and Evolution*, 4(2), 133–142.

Nardini, A., Pedà, G., & Rocca, N. L. (2012). Trade-offs between leaf hydraulic capacity and drought vulnerability: morpho-anatomical bases, carbon costs and ecological consequences. *New Phytologist*, 196(3), 788-798.

Newbold, T., Butchart, S. H. M., Şekercioğlu, Ç. H., Purves, D. W., & Scharlemann, J. P. W. (2012). Mapping Functional Traits: Comparing Abundance and Presence-Absence Estimates at Large Spatial Scales. *PLoS ONE*, 7(8), e44019.

Niinemets, Ü., & Sack, L. (2006). Structural determinants of leaf light-harvesting capacity and photosynthetic potentials. In *Progress in Botany* (pp. 385-419). Springer Berlin Heidelberg.

Nippert, J. B., & Knapp, A. K. (2007). Soil water partitioning contributes to species coexistence in tallgrass prairie. *Oikos*, 116(6), 1017–1029.

Nobel, P. S. (1999). *Physicochemical & environmental plant physiology*. Academic press.

Noy-Meir, I. (1973). Desert Ecosystems: Environment and Producers. *Annual Review of Ecology and Systematics*, 4(1), 25–51.

O'Brien, K. L., & Leichenko, R. M. (2000). Double exposure: assessing the impacts of climate change within the context of economic globalization. *Global environmental change*, 10(3), 221-232.

Ocheltree, T. W., Nippert, J. B., & Prasad, P. V. (2016). A safety vs efficiency trade-off identified in the hydraulic pathway of grass leaves is decoupled from photosynthesis, stomatal conductance and precipitation. *New Phytologist*, 210(1), 97-107.

Ochoa-Hueso, R., Collins, S. L., Delgado-Baquerizo, M., Hamonts, K., Pockman, W. T., Sinsabaugh, R. L., et al. (2018). Drought consistently alters the composition of soil fungal and bacterial communities in grasslands from two continents. *Global change biology*, 24(7), 2818-2827.

Ode, D. J., Tieszen, L. L., & Lerman, J. C. (1980). The Seasonal Contribution of C3 and C4 Plant Species to Primary Production in a Mixed Prairie. *Ecology*, 61(6), 1304-1311.

Oesterheld, M., Loreti, J., Semmartin, M., & Sala, O. E. (2001). Inter-annual variation in primary production of a semi-arid grassland related to previous-year production. *Journal of Vegetation Science*, 12(1), 137–142.

Ogle, K., Barber, J. J., Barron-Gafford, G. A., Bentley, L. P., Young, J. M., Huxman, T. E., et al. (2015). Quantifying ecological memory in plant and ecosystem processes. *Ecology letters*, 18(3), 221-235.

Ospina, S., Rusch, G. M., Easdale, T. A., Finegan, B., Casanoves, F., & Ibrahim, M. (2017). Community aggregated traits disclose functional responses to seasonal resource fluctuations and spatial heterogeneity. *Journal of Vegetation Science*, 28(2), 291-302.

Ozinga, W. A., Bekker, R. M., Schaminee, J. H., & Van Groenendael, J. M. (2004). Dispersal potential in plant communities depends on environmental conditions. *Journal of Ecology*, 92(5), 767-777.

Paine, C. T., Deasey, A., & Duthie, A. B. (2018). Towards the general mechanistic prediction of community dynamics. *Functional ecology*, 32(7), 1681-1692.

Paine, R. T. (1966). Food web complexity and species diversity. *The American Naturalist*, 100(910), 65-75.

Pakeman, R. J. (2014). Functional trait metrics are sensitive to the completeness of the species' trait data? *Methods in Ecology and Evolution*, 5(1), 9–15.

Paruelo, J. M., Lauenroth, W. K., Burke, I. C., & Sala, O. E. (1999). Grassland precipitation-use efficiency varies across a resource gradient. *Ecosystems*, 2(1), 64-68.

Pendall, E., D. Bachelet, R. T. Conant, B. El Masri, L. B. Flanagan, A. K. Knapp, J. Liu, S. Liu, and S. M. Schaeffer. (2018). Chapter 10: Grasslands. In Second State of the Carbon Cycle Report (SOCCR2): A Sustained Assessment Report [Cavallaro, N., G. Shrestha, R. Birdsey, M. A. Mayes, R. G. Najjar, S. C. Reed, P. Romero-Lankao, and Z. Zhu (eds.)]. U.S. Global Change Research Program, Washington, DC, USA, pp. 399-427,.

Perez-Harguindeguy, N., Diaz, S., Garnier, E., Lavorel, S., Poorter, H., Jaureguiberry, P., & Urcelay, C. (2013). New handbook for standardised measurement of plant functional traits worldwide. *Australian Journal of botany*, 61(3), 167-234.

Pérez-Ramos, I. M., Roumet, C., Cruz, P., Blanchard, A., Autran, P., & Garnier, E. (2012). Evidence for a 'plant community economics spectrum'driven by nutrient and water limitations in a Mediterranean rangeland of southern France. *Journal of Ecology*, 100(6), 1315-1327.

Pérez-Ramos, I. M., Díaz-Delgado, R., de la Riva, E. G., Villar, R., Lloret, F., & Marañón, T. (2017). Climate variability and community stability in Mediterranean shrublands: the role of functional diversity and soil environment. *Journal of Ecology*, 105(5), 1335–1346.

Petchey, O. L., & Gaston, K. J. (2002). Functional diversity (FD), species richness and community composition. *Ecology Letters*, 5(3), 402–411.

Petrie, M. D., Collins, S. L., & Litvak, M. E. (2015). The ecological role of small rainfall events in a desert grassland. *Ecohydrology*, 8(8), 1614-1622.

Peuke, A. D., Rokitta, M., Zimmermann, U., Schreiber, L., & Haase, A. (2001). Simultaneous measurement of water flow velocity and solute transport in xylem and phloem of adult plants of Ricinus communis over a daily time course by nuclear magnetic resonance spectrometry. *Plant, Cell & Environment*, 24(5), 491-503.

Plaut, J. A., Wadsworth, W. D., Pangle, R., Yepez, E. A., McDowell, N. G., & Pockman, W. T. (2013). Reduced transpiration response to precipitation pulses precedes mortality in a pinon–juniper woodland subject to prolonged drought. *New Phytologist*, 200(2), 375-387.

Pockman, W. T., Sperry, J. S., & O'leary, J. W. (1995). Sustained and significant negative water pressure in xylem. *Nature*, 378(6558), 715-716.

Ponce-Campos, G. E., Moran, M. S., Huete, A., Zhang, Y., Bresloff, C., Huxman, T. E., et al. (2013). Ecosystem resilience despite large-scale altered hydroclimatic conditions. *Nature*, 494(7437), 349.

Poorter, H., & Garnier, E. (1999). Ecological significance of inherent variation in relative growth rate and its components. *Handbook of functional plant ecology*, 20, 81-120.

Prieto, I., Roumet, C., Cardinael, R., Dupraz, C., Jourdan, C., Kim, J. H. et al. (2015). Root functional parameters along a land-use gradient: evidence of a community-level economics spectrum. *Journal of Ecology*, 103(2), 361-373.

Qi, W., Zhou, X., Ma, M., Knops, J. M. H., Li, W., & Du, G. (2015). Elevation, moisture and shade drive the functional and phylogenetic meadow communities' assembly in the northeastern Tibetan Plateau. *Community Ecology*, 16(1), 66–75.

Reich, P. B., Walters, M. B., & Ellsworth, D. S. (1997). From tropics to tundra: global convergence in plant functioning. *PNAS*, 94(25), 13730-13734.

Reich, P. B., Ellsworth, D. S., & Walters, M. B. (1998). Leaf structure (specific leaf area) modulates photosynthesis–nitrogen relations: evidence from within and across species and functional groups. *Functional Ecology*, 12(6), 948-958.

Reich, P., & Oleksyn, J. (2004). Global patterns of plant leaf N and P in relation to temperature and latitude. *PNAS*, 101(30), 11001–11006.

Reich, P. B., Wright, I. J., & Lusk, C. H. (2007). Predicting leaf physiology from simple plant and climate attributes: a global GLOPNET analysis. *Ecological Applications*, 17(7), 1982-1988.

Reich, P. (2012). Key canopy traits drive forest productivity. *Proceedings of the Royal Society B: Biological Sciences*, 279(1736), 2128–2134.

Reich, P. B. (2014). The world-wide 'fast–slow' plant economics spectrum: a traits manifesto. *Journal of Ecology*, 102(2), 275-301.

Reichmann, L. G., Sala, O. E., & Peters, D. P. (2013). Precipitation legacies in desert grassland primary production occur through previous-year tiller density. *Ecology*, 94(2), 435-443.

Reynolds, J. F., Virginia, R. A., Kemp, P. R., De Soyza, A. G., & Tremmel, D. C. (1999). Impact of drought on desert shrubs: effects of seasonality and degree of resource island development. *Ecological Monographs*, 69(1), 69-106.

Richardson, S. J., Peltzer, D. A., Allen, R. B., & McGlone, M. S. (2005). Resorption proficiency along a chronosequence: responses among communities and within species. *Ecology, 86(1)*, 20-25.

Ricklefs, R. E., & Latham, R. E. (1992). Intercontinental correlation of geographical ranges suggests stasis in ecological traits of relict genera of temperate perennial herbs. *The American Naturalist*, 139(6), 1305-1321.

Riva, E. G., Pérez-Ramos, I. M., Tosto, A., Navarro-Fernández, C. M., Olmo, M., Marañón, T., & Villar, R. (2016). Disentangling the relative importance of species occurrence, abundance and intraspecific variability in community assembly: a trait-based approach at the whole-plant level in Mediterranean forests. *Oikos*, 125(3), 354-363.

Rosado, B. H. P., Dias, A. T. C., & de Mattos, E. A. (2013). Going back to basics: Importance of ecophysiology when choosing functional traits for studying communities and ecosystems. *Natureza a Conservacao*, 11(1), 15–22.

Rosenberg NJ. (1987). Climate of the Great Plains region of the United States. Great Plains Quarterly, 22-32.

Rota, C., Manzano, P., Carmona, C. P., Malo, J. E., & Peco, B. (2017). Plant community assembly in Mediterranean grasslands: understanding the interplay between grazing and spatio-temporal water-availability. *Journal of Vegetation Science*, 28(1), 149-159.

Sack, L., Melcher, P. J., Zwieniecki, M. A., & Holbrook, N. M. (2002). The hydraulic conductance of the angiosperm leaf lamina: a comparison of three measurement methods. *Journal of Experimental Botany*, 53(378), 2177-2184.

Sack, L., Cowan, P. D., Jaikumar, N., & Holbrook, N. M. (2003). The 'hydrology'of leaves: co-ordination of structure and function in temperate woody species. *Plant, Cell & Environment*, 26(8), 1343-1356.

Sack, L., & Holbrook, N. M. (2006). Leaf hydraulics. *Annu. Rev. Plant Biol.*, 57, 361-381.

Sage, R. F., & Monson, R. K. (1998). C4 plant biology. Elsevier.

Sala, O. E., Parton, W. J., Joyce, L. A., & Lauenroth, W. K. (1988). Primary production of the central grassland region of the United States. *Ecology*, 69(1), 40-45.

Sala, O. E., Gherardi, L. A., Reichmann, L., Jobbagy, E., & Peters, D. (2012). Legacies of precipitation fluctuations on primary production: theory and data synthesis. *Philosophical Transactions of the Royal Society B: Biological Sciences*, 367(1606), 3135-3144.

Schlesinger, W. H., & Bernhardt, E. S. (2013). Biogeochemistry: an analysis of global change. Academic press.

Scoffoni, C., Rawls, M., McKown, A., Cochard, H., & Sack, L. (2011). Decline of leaf hydraulic conductance with dehydration: relationship to leaf size and venation architecture. *Plant Physiology*, 156(2), 832-843.

Seastedt, T. R., & Knapp, A. K. (1993). Consequences of nonequilibrium resource availability across multiple time scales: the transient maxima hypothesis. *The American Naturalist*, 141(4), 621-633.

Sfair, J. C., Rosado, B. H., & Tabarelli, M. (2016). The effects of environmental constraints on plant community organization depend on which traits are measured. *Journal of Vegetation Science*, 27(6), 1264-1274.

Shi, Z., Thomey, M. L., Mowll, W., Litvak, M., Brunsell, N. A., Collins, S. L., et al. (2014). Differential effects of extreme drought on production and respiration: synthesis and modeling analysis. *Biogeosciences*, 11(3), 621-633.

Shipley, B., De Bello, F., Cornelissen, J. H. C., Laliberté, E., Laughlin, D. C., & Reich, P. B. (2016). Reinforcing loose foundation stones in trait-based plant ecology. *Oecologia*, 180(4), 923-931.

Siefert, A., Violle, C., Chalmandrier, L., Albert, C. H., Taudiere, A., Fajardo, A., et al. (2015). A global meta-analysis of the relative extent of intraspecific trait variation in plant communities. *Ecology Letters*, 18(12), 1406-1419.

Silver, W. L., Ryals, R., & Eviner, V. (2010). Soil carbon pools in California's annual grassland ecosystems. *Rangeland Ecology & Management*, 63(1), 128-136.

Silvertown, J., Dodd, M. E., Gowing, D. J., & Mountford, J. O. (1999). Hydrologically defined niches reveal a basis for species richness in plant communities. *Nature*, 400(6739), 61.

Šímová, I., Violle, C., Svenning, J. C., Kattge, J., Engemann, K., Sandel, B., et al. (2018). Spatial patterns and climate relationships of major plant traits in the New World differ between woody and herbaceous species. *Journal of Biogeography*, 45(4), 895–916.

Skelton, R. P., West, A. G., & Dawson, T. E. (2015). Predicting plant vulnerability to drought in biodiverse regions using functional traits. *PNAS*, 112(18), 5744-5749.

Slik, J. W. F. (2004). El Nino droughts and their effects on tree species composition and diversity in tropical rain forests. *Oecologia*, 141(1), 114-120.

Smith, M. D., & Knapp, A. K. (2003). Dominant species maintain ecosystem function with non-random species loss. *Ecology Letters*, 6(6), 509-517.

Smith, M. D., Knapp, A. K., & Collins, S. L. (2009). A framework for assessing ecosystem dynamics in response to chronic resource alterations induced by global change. *Ecology*, 90(12), 3279–3289.

Smith, M. D. (2011). An ecological perspective on extreme climatic events: a synthetic definition and framework to guide future research. *Journal of Ecology*, 99(3), 656-663.

Soudzilovskaia, N. A., Elumeeva, T. G., Onipchenko, V. G., Shidakov, I. I., Salpagarova, F. S., Khubiev, A. B., et al. (2013). Functional traits predict relationship between plant abundance dynamic and long-term climate warming. *PNAS*, 110(45), 18180–18184.

Spasojevic, M. J., & Suding, K. N. (2012). Inferring community assembly mechanisms from functional diversity patterns: The importance of multiple assembly processes. *Journal of Ecology*, 100(3), 652–661.

Stamakis, A. (2014). RAxML version 8: a tool for phylogenetic analysis and post-analysis of large phylogenies. *Bioinformatics*, 30, 1312–1313.

Stevens, C. J., Lind, E. M., Hautier, Y., Harpole, W. S., Borer, E. T., Hobbie, S., et al. (2015). Anthropogenic nitrogen deposition predicts local grassland primary production worldwide. *Ecology,* 96(6), 1459-1465.

Suding, K. N., Lavorel, S., Chapin, F. S., Cornelissen, J. H., Diaz, S., Garnier, E. et al. (2008). Scaling environmental change through the community-level: a trait-based response-and-effect framework for plants. *Global Change Biology*, 14(5), 1125-1140.

Swenson, N. G. (2014). Functional and phylogenetic ecology in R. New York: Springer.

ter Steege, H., Pitman, N.C.A., Phillips, O.L., Chave, J., Sabatier, D. et al. (2006). Continental-scale patterns of canopy tree composition and function across Amazonia. *Nature*, 443, 444–447.

Thuiller, W., Lavorel, S., Midgley, G. U. Y., Lavergne, S., & Rebelo, T. (2004). Relating plant traits and species distributions along bioclimatic gradients for 88 Leucadendron taxa. *Ecology*, 85(6), 1688-1699.

Tilman, D., & Downing, J. A. (1994). Biodiversity and stability in grasslands. *Nature*, 367(6461), 363–365.

Tilman, D., Wedin, D., & Knops, J. (1996). Productivity and sustainability influenced by biodiversity in grassland ecosystems. *Nature*, 379(6567), 718–720.

Tilman, D., Knops, J., Wedin, D., Reich, P., Ritchie, M., & Siemann, E. (1997). The Influence of Functional Diversity and Composition on Ecosystem Processes. *Science*, 277(5330), 1300–1302.

Trenberth, K. E. (2011). Changes in precipitation with climate change. *Climate Research*, 47(1-2), 123-138.

Trenberth, K. E., Dai, A., Van Der Schrier, G., Jones, P. D., Barichivich, J., Briffa, K. R., & Sheffield, J. (2014). Global warming and changes in drought. *Nature Climate Change*, 4(1), 17.

Turner, N. C. (1988). Measurement of plant water status by the pressure chamber technique. *Irrigation science*, 9(4), 289-308.

Valencia, E., Maestre, F. T., Bagousse-Pinguet, L., Quero, J. L., Tamme, R., Börger, L., et al. (2015). Functional diversity enhances the resistance of ecosystem multifunctionality to aridity in Mediterranean drylands. *New Phytologist*, 206(2), 660-671.

van der Sande, M. T., Arets, E. J., Peña-Claros, M., Avila, A. L., Roopsind, A., Mazzei, L., et al. (2016). Old-growth Neotropical forests are shifting in species and trait composition. *Ecological Monographs*, 86(2), 228-243

van der Sande, M. T., Arets, E. J., Peña-Claros, M., Hoosbeek, M. R., Cáceres-Siani, Y., van der Hout, P., & Poorter, L. (2018). Soil fertility and species traits, but not diversity, drive productivity and biomass stocks in a Guyanese tropical rainforest. *Functional ecology*, 32(2), 461-474.

Veron, S. V., Paruelo, J. M., Sala, O. E. & Lauenroth, W. K. (2002). Environmental controls of primary production in agricultural systems of the Argentine Pampas. *Ecosystems* 5, 625–635

Vile, D., Shipley, B., & Garnier, E. (2006). Ecosystem productivity can be predicted from potential relative growth rate and species abundance. *Ecology Letters*, 9(9), 1061–1067.

Villéger, S., Mason, N. W., & Mouillot, D. (2008). New multidimensional functional diversity indices for a multifaceted framework in functional ecology. *Ecology*, 89(8), 2290-2301.

Violle, C., Navas, M. L., Vile, D., Kazakou, E., Fortunel, C., Hummel, I., & Garnier, E. (2007). Let the concept of trait be functional!. *Oikos*, 116(5), 882-892.

Vitousek, P. M., Mooney, H. A., Lubchenco, J., & Melillo, J. M. (1997). Human domination of Earth's ecosystems. *Science*, 277(5325), 494-499.

Wagg, C., O'Brien, M. J., Vogel, A., Scherer-Lorenzen, M., Eisenhauer, N., Schmid, B., & Weigelt, A. (2017). Plant diversity maintains long-term ecosystem productivity under frequent drought by increasing short-term variation. *Ecology*, 98(11), 2952-2961.

Walter, J., Nagy, L., Hein, R., Rascher, U., Beierkuhnlein, C., Willner, E., & Jentsch, A. (2011). Do plants remember drought? Hints towards a drought-memory in grasses. *Environmental and Experimental Botany*, 71(1), 34-40.

Weaver, J. E. (1958). Classification of root systems of forbs of grassland and a consideration of their significance. *Ecology*, 39(3), 393–401.

Webb, W., Szarek, S., Lauenroth, W., Kinerson, R., & Smith, M. (1978). Primary productivity and water use in native forest, grassland, and desert ecosystems. *Ecology*, 59(6), 1239-1247.

Webb, W. L., Lauenroth, W. K., Szarek, S. R., & Kinerson, R. S. (1983). Primary production and abiotic controls in forests, grasslands, and desert ecosystems in the United States. *Ecology*, 64(1), 134-151.

Weiher, E., Werf, A., Thompson, K., Roderick, M., Garnier, E., & Eriksson, O. (1999). Challenging Theophrastus: a common core list of plant traits for functional ecology. *Journal of vegetation science*, 10(5), 609-620.

Wellstein, C., Poschlod, P., Gohlke, A., Chelli, S., Campetella, G., Rosbakh, S., et al. (2017). Effects of extreme drought on specific leaf area of grassland species: A meta-analysis of experimental studies in temperate and sub-Mediterranean systems. *Global Change Biology*, 23(6), 2473–2481.

Whitford, W. G., Martinez-Turanzas, G., & Martinez-Meza, E. (1995). Persistence of desertified ecosystems: explanations and implications. *Environmental Monitoring and Assessment*, 37(1-3), 319-332.

Whitney, K. D., Mudge, J., Natvig, D. O., Sundararajan, A., Pockman, W. T., Bell, J., et al. (2019). Experimental drought reduces genetic diversity in the grassland foundation species Bouteloua eriopoda. *Oecologia*, https://doi.org/10.1007/s00442-019-04371-7.

Wieczynski, D. J., Boyle, B., Buzzard, V., Duran, S. M., Henderson, A. N., Hulshof, C. M., et al. (2019). Climate shapes and shifts functional biodiversity in forests worldwide. *PNAS*, 116(2), 587-592.

Woodhouse, C. A., & Overpeck, J. T. (1998). 2000 years of drought variability in the central United States. *Bulletin of the American Meteorological Society*, 79(12), 2693-2714.

Wright, I. J., Reich, P. B., & Westoby, M. (2001). Strategy shifts in leaf physiology, structure and nutrient content between species of high-and low-rainfall and high-and low-nutrient habitats. *Functional Ecology*, 15(4), 423-434.

Wright, I. J., Reich, P. B., Westoby, M., Ackerly, D. D., Baruch, Z., Bongers, F., et al. (2004). The worldwide leaf economics spectrum. *Nature*, 428(6985), 821–827.

Wright, I. J., Reich, P. B., Cornelissen, J. H. C., Falster, D. S., Hikosaka, K., Lamont, B. B., et al. (2005). Assessing the generality of leaf trait of global relationships. *New Phytologist*, 166(2), 485–496.

Yahdjian, L., & Sala, O. E. (2002). A rainout shelter design for intercepting different amounts of rainfall. *Oecologia*, 133(2), 95–101.

Yahdjian, L., Sala, O. E., & Austin, A. T. (2006). Differential controls of water input on litter decomposition and nitrogen dynamics in the Patagonian steppe. *Ecosystems*, 9(1), 128-141.

Yahdjian, L., & Sala, O. E. (2006). Vegetation structure constrains primary production response to water availability in the Patagonian steppe. *Ecology*, 87(4), 952-962.

Yu, K., & D'Odorico, P. (2015). Hydraulic lift as a determinant of tree–grass coexistence on savannas. *New Phytologist*, 207(4), 1038-1051.

Zhu, S. D., Chen, Y. J., Ye, Q., He, P. C., Liu, H., Li, R. H., et al. (2018). Leaf turgor loss point is correlated with drought tolerance and leaf carbon economics traits. *Tree Physiology*, 38(5), 658–663.

Zimmermann M. (1983). Xylem structure and the ascent of sap. Berlin, Germany: Springer.

APPENDIX 1

A1.1 Supplementary Tables

Table A1.1. Results from general linear models

Model		Coefficient	Std. Error	t	p-value	r²
Legacy vs. Sensitivity (Directional)	y0	-2.2131	0.9713	-2.2786	0.0849	0.68
	a	5.2327	1.7805	-2.939	**0.0424**	
Legacy vs. Sensitivity (Magnitude)	y0	-1.886	0.4962	-3.8007	**0.0191**	0.88
	a	4.9285	0.9096	5.4182	**0.0056**	
Legacy (mag) vs. (2013 PPT - 2012 PPT / MAP)	y0	0.7983	1.2925	0.6176	0.5702	<0.01
	a	-0.1997	3.363	-0.0594	0.9555	
Legacy (mag) vs. SPEI	y0	2.5886	1.5567	1.6629	0.1717	0.27
	a	1.0234	0.8393	1.2194	0.2897	
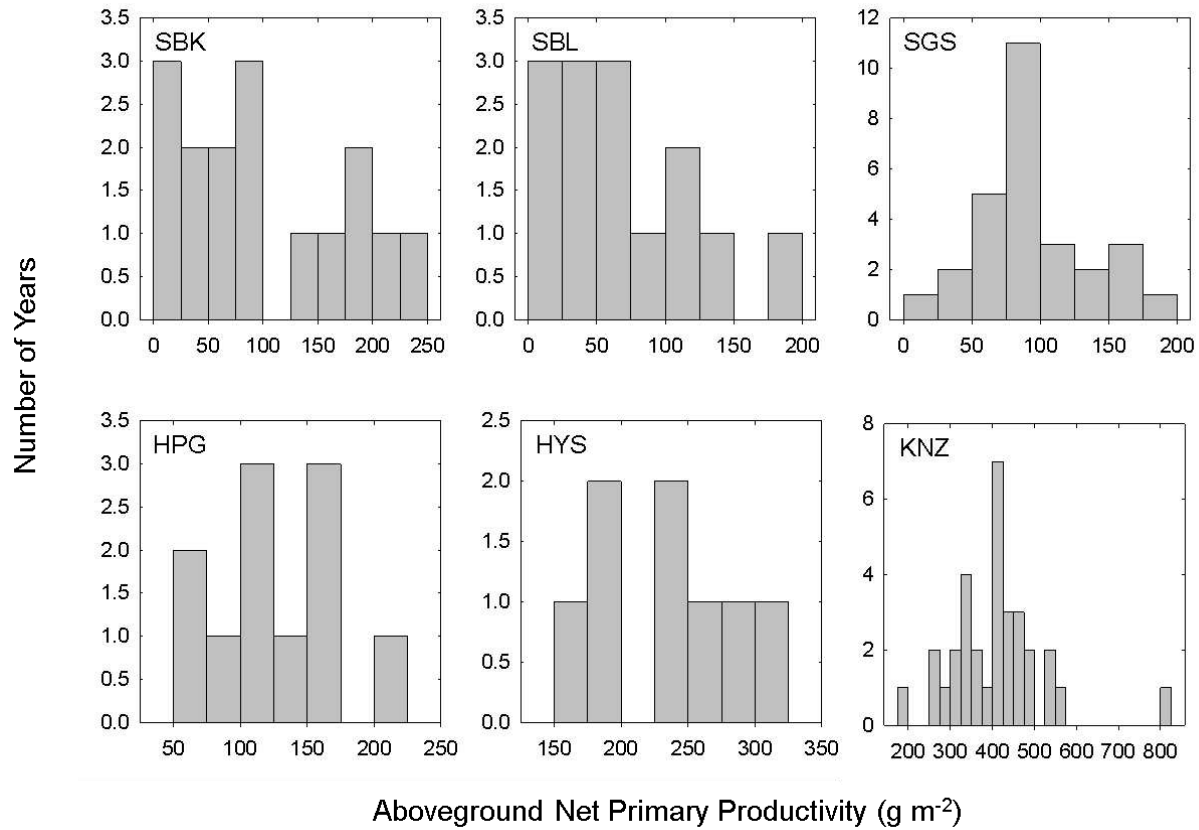
Figure A1.1. Distribution of annual ANPP values from the long-term dataset for each site. Long-term mean ANPP is generally used for cross-site comparisons of grassland responses to precipitation (Sala et al. 1988). SBK = Sevilleta Black grama, SBL = Sevilleta Blue grama, SGS = Shortgrass Steppe, HPG = High Plains Grasslands, HYS= Hays Agricultural Research Center, KNZ = Konza Prairie.
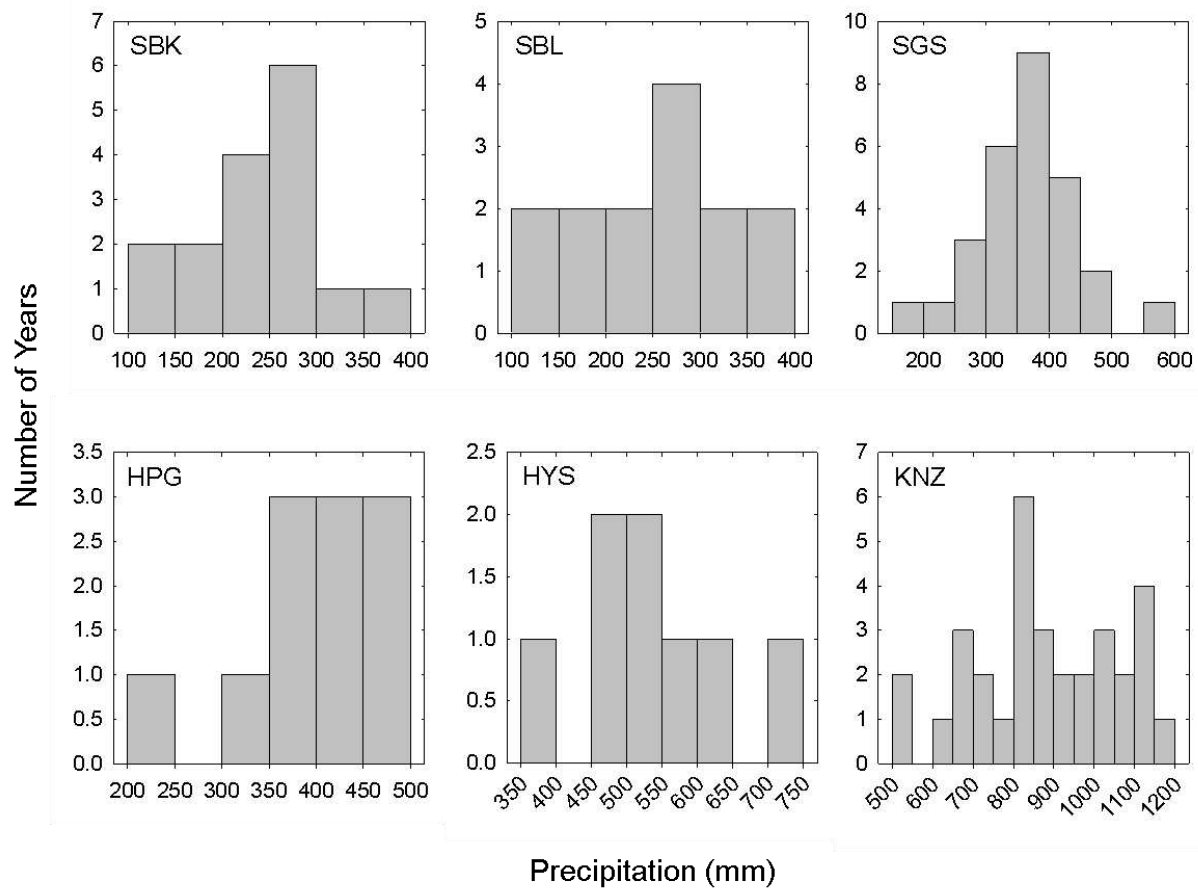
Figure A1.2. Distribution of annual precipitation values from the long-term dataset of each site. SBK = Sevilleta Black grama, SBL = Sevilleta Blue grama, SGS = Shortgrass Steppe, HPG = High Plains Grasslands, HYS= Hays agricultural research center, KNZ = Konza Prairie.

Figure A1.3. ANPP anomalies for all six sites across the entire long-term record. ANPP anomalies in 2012 (drought) and 2013 (legacy effect) are shown in red and blue, respectively. SBK = Sevilleta Black grama, SBL = Sevilleta Blue grama, SGS = Shortgrass Steppe, HPG = High Plains Grasslands, HYS= Hays agricultural research center, KNZ = Konza Prairie.
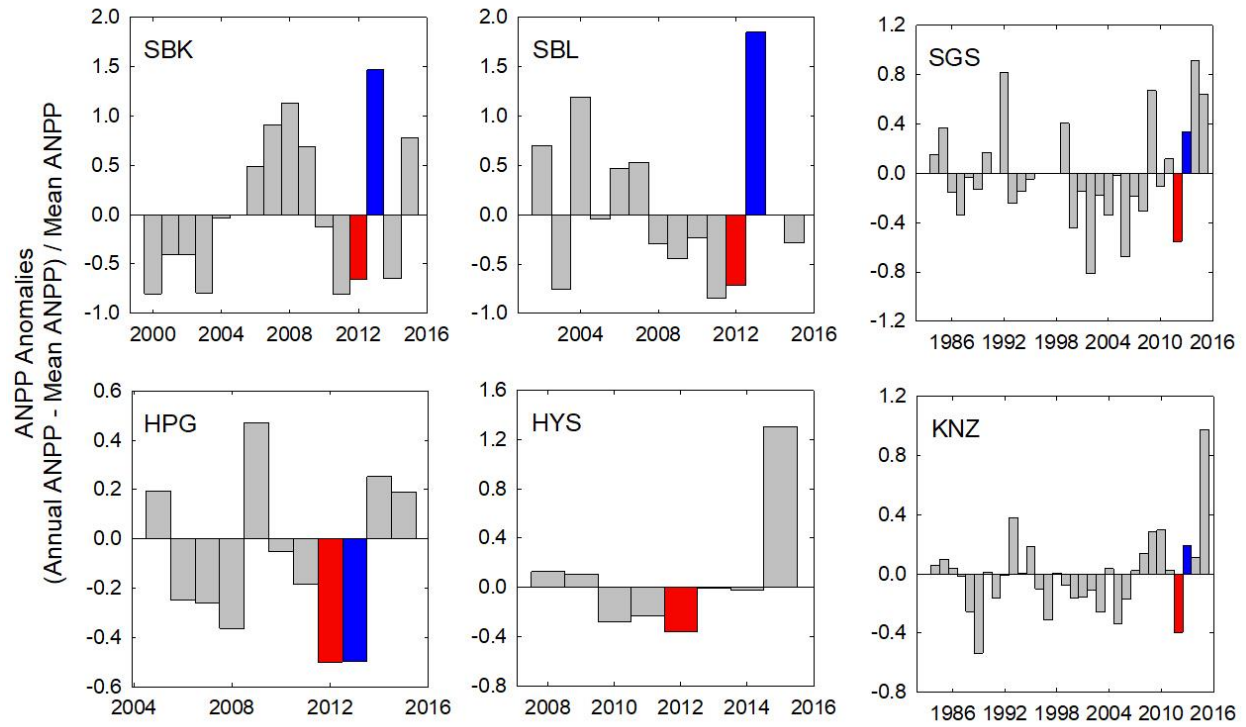
APPENDIX 2

A2.1 Supplementary Methods

A list of manuscripts was compiled from a broad literature search (Web of Science, Thomson Reuters, Manhattan, NY, USA) using the following key words: ("soil moisture" OR "soil water" OR precipitation OR rainfall OR "water-availability" OR drought OR aridity) AND ("leaf trait*" OR "root trait*" OR "below-ground trait*" OR "stem trait*" OR "plant trait*" OR "reproductive trait*" OR "regenerat* trait*" OR "growth trait*" OR "morpho* trait*" OR "photosynth* trait*" OR "hydraulic* trait*" OR "physio* trait*" OR "community weighted trait*" OR "community weighted mean" OR "biochem* trait*" OR "chem* trait*" OR "phenolog* trait*" OR "anatom* trait*" OR "economic trait*").

We chose to limit our analysis to traits measured in non-cultivated terrestrial vascular plants. Thus, our initial results from this search were refined by excluding papers with the following key words: (agricultur* OR agro* OR agri* OR wheat OR rice OR corn OR crop*). The search was further refined by excluding papers within the following "Web of Science" research areas: biotechnology applied microbiology, entomology, paleontology, agriculture, engineering, geochemistry, geophysics, science technology other topics, veterinary sciences, toxicology, research experimental medicine, food science technology, zoology, pharmacology pharmacy, physical geography, oceanography, materials science, geography, geology, fisheries, life sciences, biomedicine other topics, marine freshwater biology.

A2.2 Supplementary Results

A2.2.1 Trait category-organ dichotomy

As Woody (W) species dominate the literature (~30% more manuscripts than for herbaceous (H) species), data are presented as proportions of either W or H manuscripts, including manuscripts that assessed both. Some manuscripts fit into multiple categories (e.g. traits measured

along both spatial and temporal precipitation gradients); thus, the proportions presented do not sum to 100.

Clear differences were observed at the organ-scale of trait measurements (Fig. A2.2). Stem traits were more represented in W species (W: 44%; H: 20%), while reproductive organs were more commonly studied among H species (W: 13%; H: 36%). For both H and W species, traits were most commonly measured on leaves (> 80%) with a clear lack of belowground traits measured for both growth forms (W: 19%; H: 21%). Whole-plant traits, such as organ biomass ratios, were more commonly measured in herbaceous species (W: 49%; H: 61%).

There were also differences within trait categories (Fig. A2.2), with hydraulic traits being understudied in H species (W: 47%; H: 26%) and the opposite trend observed for photosynthetic traits (W: 13%; H: 36%). Morphological traits were ubiquitous in this subset of traits literature (W: 83%; H: 88%). Slight differences were observed in the relative frequency of anatomical (W: 30%; H: 19%), phenological (W: 13%; H: 20%), and biochemical traits (W: 39%; H: 32%).

Following a comparison of H and W manuscripts, the datasets were combined to survey trends across growth forms (Fig. 3.2). The most commonly measured traits were morphological (480 manuscripts) followed by photosynthetic and hydraulic traits (258 and 232 manuscripts, respectively; Fig. 3.2A). Indeed, morphology was the most commonly measured trait category across all plant organs (Fig. 3.2B). Certain trends were expected when the data were combined to observe the frequency of traits measured within each plant organ, such as the predominance of photosynthetic traits within leaves and phenological traits within reproductive organs (Fig. 3.2B). Hydraulic traits were well surveyed in 'leaf-trait' and 'stem-trait' manuscripts (42% and 37%, respectively) with limited research on belowground or whole-plant hydraulics (<10% of 'belowground-trait' or 'whole-plant-trait' manuscripts). Indeed, very few 'belowground-trait' or

'whole-plant-trait' manuscripts addressed traits beyond morphology, which was assessed in >90% of these manuscripts (Fig. 3.2B).

A2.2.2 Water-availability gradients

There were few differences between W and H manuscripts in the types of water-availability gradients observed and/or types of experimental manipulations imposed (Fig. A2.2); however, certain trends can be generalized across growth forms. For example, plant traits were most commonly measured across spatial precipitation gradients (W: 37%; H: 30%) or soil moisture gradients manipulated in a greenhouse setting (W: 30%; H: 41%). There were few studies that reported traits along temporal precipitation gradients (Inter-annual – W: 16%; H: 9% and seasonal – W: 4%; H: 3%), local edaphic microclimatic gradients (W: 7%; H: 8%), or experimental field manipulations of water-availability (W: 13%; H: 15%).

A2.2.3 Ecological-scale

Trends in the ecological scale of measurement were also comparable across growth forms (Fig. A2.2). The most common method observed was an assessment of traits for multiple species with no comparison across populations of those species (W and H ~35%). Single species studies were the second most common type of study, with an equivalent frequency of studies assessing traits across populations or within one population (W and H ~22% for both methods). Very few studies measured traits of multiple species across multiple populations (W: 12%; H: 15%) and even fewer measured traits at the community-level, with trait values weighted by species abundance (W: 3%; H: 7%).

A2.3 Supplementary Tables

Table A2.1. Manuscripts that measure community-weighed traits. Also shown are the trait-weighting methods, ecosystems, type of water-availability gradient, as well as a list of traits and their relationship, or lack thereof, with increased water-availability (positive [+], negative [-], or nonlinear/optimal relationship [+/-]). Studies were most often conducted within grasslands (n=11), along precipitation gradients (n=14), and in relation to leaf traits. Few manuscripts present CWTs related to plant hydraulics or belowground responses to water. See References section for full citation. Traits: SLA = specific leaf area, Height = maximum plant height, LDMC = leaf dry matter content, LNC = leaf nitrogen content, LA = leaf area, Sm = seed mass, gs = stomatal conductance, Wd = wood density, SRL = specific root length, LMA = leaf mass per area, Leaf chl = leaf chlorophyll content, RMF = root mass fraction, RDMC = root dry matter content, SRA = specific root length, LCC = leaf carbon content, SPI = stomatal pore index, WUEi = intrinsic water use efficiency.

Citation	Ecosystem	Trait weighting methods	Water-availability gradient	Traits (Significant response)	Traits (n.s response)
Spasojevic et al. 2012	Alpine tundra	By % cover; all species along transects	Microclimate (edaphic)	LA(+), Height(+), leaf chl(+)	SLA, max gs
Cornwell and Ackerly 2009	Chapparel, broadleaf evergreen forest, shrubland, oak savanna	By % cover; all species in plot	Precipitation (spatial/seasonal)	LA(+), SLA(+), LNC-mass(+), LNC-area(-), Wd(-), xylem vessel area(+), lumen fraction(+)	Xylem vessel density
Carmona et al. 2015	Grassland	By % cover; all species in plot	Precipitation (interannual)	Height(+), SLA(+), Seed mass(-)	none
Cantarel et al. 2013	Grassland	By % contribution to NPP; all species with >5% cover	field manipulation	LDMC(+), LNC(-)	SLA
Pérez-Ramos et al 2012	Grassland	By % cover; species representing >80% cover	Microclimate (edaphic)	Height(+), SLA(+), LDMC(-), Delta C13(-), Rooting depth(+)	Leaf thickness, LNC, RMF, RDMC, SRA,

					Root tissue density
Qi et al. 2015	Grassland	By % cover; species representing 95% cover	Precipitation (spatial)	Height(-), Seed mass(-)	SLA
Rota et al. 2017	Grassland	presence/absence data, mean of trait values for 75% of present species	Precipitation (spatial/interannual)	Seed mass(-)	Height, SLA
Jung et al. 2014	Grassland	% cover of species in plots representing >80% cover	field manipulation	SLA(+), LCC(-), LDMC(-)	LNC
Guittar et al. 2016	Grassland	By % cover, species representing 84-99% cover	Precipitation (spatial)	none	LA, SLA, Height, Seed mass, fecundity, RGR, bud number
Butterfield et al. 2017	Grassland	By % cover; species with greater than 1% cover	Precipitation (spatial)	SLA(+), SRL(+), Root tissue density(-)	Seed mass
Forrestel et al. 2017	Grassland	By % cover; grass species with >2% cover	Precipitation (spatial)	Height (+), LA (+), dC13 (+), LCC (+), leaf C:N (+), stomatal length (+), SPI (+) LNC (-)	Stomatal density, SLA, LDMC
Kimball et al. 2016	Grassland/shrubland	By % cover; species representing 90% cover	Field manipulation	Root length (+), WUEi(+), Height(+), LMA(+/-), PSII efficiency(+/-), SRL(+/-), LNC(+/-), Leaf transpiration(+/-)	none

Valencia et al. 2015	Mediterranean drylands	By % cover; species representing 80% cover	Precipitation (spatial)	Branch ramification(-), Leaf length(+), LA(+), LDMC(+), SLA(-)	Height, Branching density, Leaf width, Leaf thickness
Lebrija-Trejos et al. 2011	Mediterranean drylands	weighed by presence/absence - all plants present	Precipitation (spatial)	none	Seed mass and dispersal
Riva et al. 2016	Mediterranean Forest	By % cover; species representing 90% cover	Microclimate (edaphic)	Delta C13(-), Height(+), SRL(+), SLA(+), LA(+), Leaf chl(+)	SDMC, RDMC, LDMC, LNC
Ozinga et al. 2004	Multiple plant communities (Netherlands)	By % of plots where traits were present	Precipitation (spatial)	wind dipersal(+), water dispersal(+)	Animal dispersal
Ames et al. 2016	Pine Savanna	By % cover; species representing at least 70% cover	Precipitation (spatial)	SLA(+), LDMC(-)	none
Sfair et al. 2016	Savannah	By % cover; dominant species only	Microclimate (edaphic)	none	SLA, internode mass fraction, Wd, Height
Hernández-Calderón et al. 2014	Tropical dry forest	By basal area, all tree species along a transect	Microclimate (edaphic)	Height(+)	Huber value, LMA, Bark density, LDMC, Wd, LA

|					
Ospina et al. 2017	Tropical grassland	By % cover, dominant 36 species, representing each functional type	Precipitation (seasonal)	Leaf size(+), SLA(+), LDMC(-), leaf lifespan(-), LNC(+), LPC(+), Leaf Ca(+), Leaf K(+), Leaf Mg(+), flowering time(+)	Height, Rooting depth, Flowering period length
Muscarella et al. 2016	Tropical montane forests	By % cover; all woody species in plots	Precipitation (spatial)	Wd(-), LMA(-), Height(+)	
Sande et al. 2016	Tropical rainforest	By basal area; all species with >10cm DBH	Precipitation (spatial)	SLA(-), LA(+), LNC(-), LPC(-), leaf N:P(+/-), Leaf chl(+/-), LDMC(+), leaf strength(+), LMF(+/-)	Wd, stem diameter
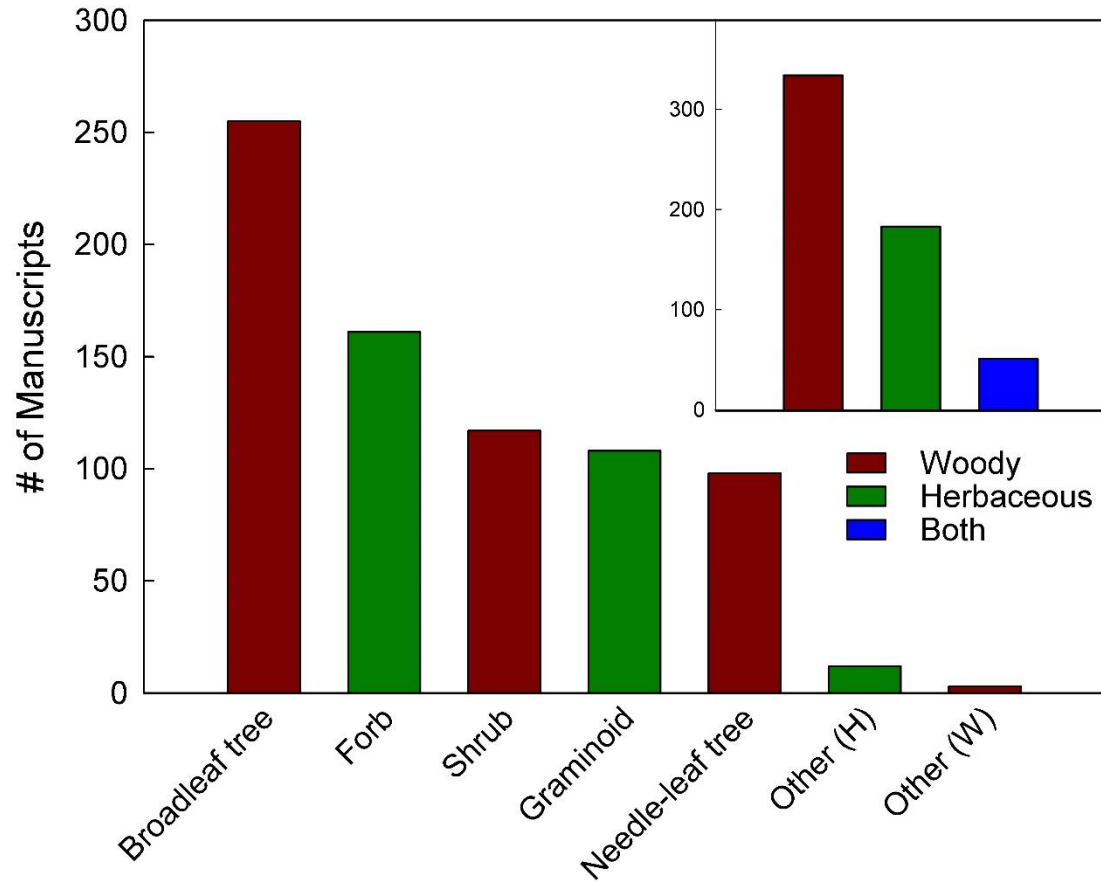
Figure A2.1. Number of manuscripts published for each plant functional type (PFT). A total of 568 manuscripts were assessed that measured plant traits within woody and herbaceous functional types. Many studies describe traits of a variety of PFTs (i.e. both shrubs and broad-leaf trees), thus the bars for each specific growth form do not add to the total number of manuscripts. *Inset:* While woody species dominate this study area, a clear dichotomy was observed, whereby manuscripts focus on either woody (n=334) or herbaceous (n=183) plants, with very few studies comparing/contrasting the two groups (n=51; "Both").
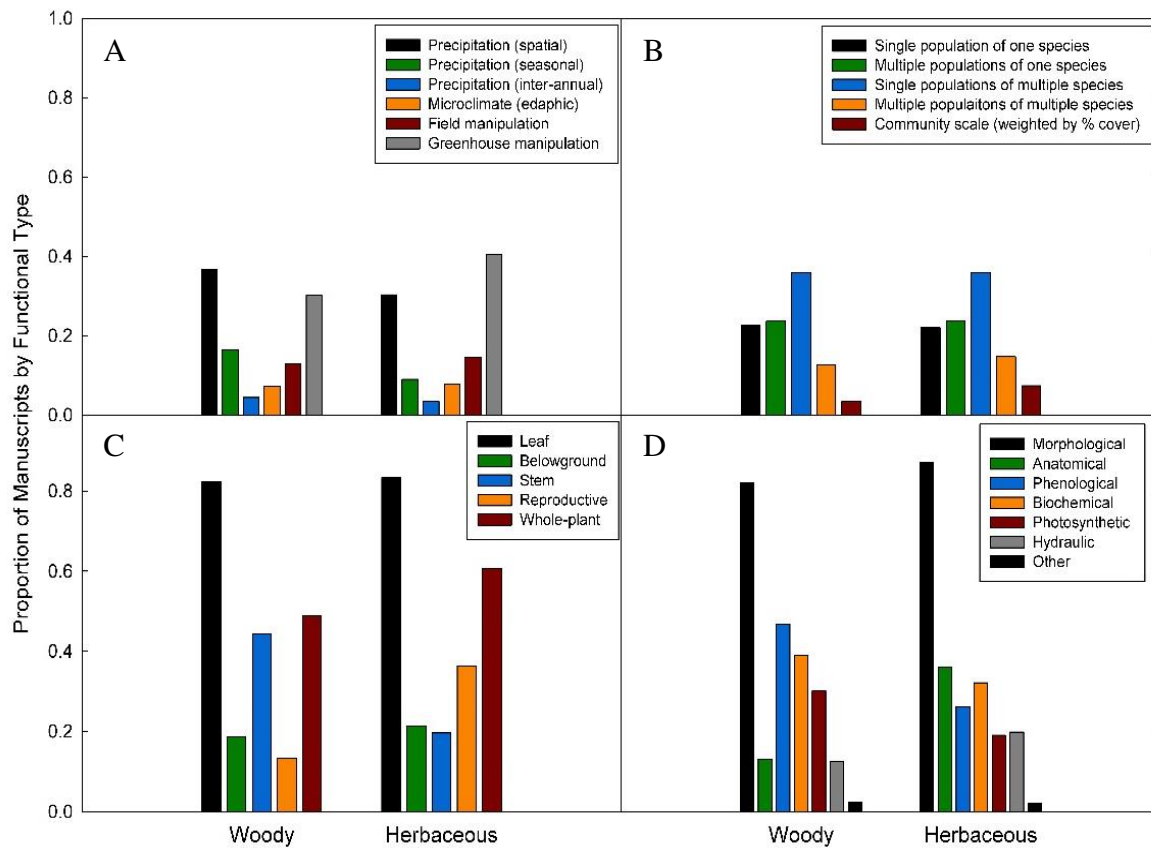
Figure A2.2. A comparison between woody and herbaceous plants of how traits are measured in the context of altered water-availability. Data are shown as the proportion of manuscripts describing traits of either woody or herbaceous species to control for the disproportionate amount of manuscripts in the woody species category. Due to the overlap in types of traits measured in each manuscript, the above proportions do not sum to 100. (A) Traits were generally measured along soil moisture gradients at a spatial scale (spatial precipitation gradient or local edaphic gradients) temporal scale (inter-annual vs. seasonal variability) or based on treatments experimentally induced in greenhouse or field settings. (B) The ecological scale at which traits are measured (i.e. single/multiple species, and single/multiple populations, or community-weighted traits) was similar across woody and herbaceous species. Differences between woody and herbaceous plant trait surveys are also shown based on relative amounts of manuscripts that assess traits of different organs (C) and trait categories (D). See Table 3.1 for trait category definitions.

APPENDIX 3

A3.1 Supplementary Tables

Table A3.1. AIC values for model selection of hydraulic vulnerability curves. The smallest AIC value is bolded and indicates which model was selected. See Table 4.1 for site and species abbreviations.

Species	Linear	Exponential	Sigmoidal	Logarithmic
HPG PASM	33.49829284	36.36309095	24.20948904	**16.79106038**
HPG BOGR	46.56643857	46.64550331	44.4524744	**41.76438899**
HYS BOCU	39.38186408	**38.49130067**	39.36072243	41.21214399
HYS SPAS	42.35625513	44.52375257	40.35492496	**39.78470237**
KNZ ANGE	27.60180308	**-19.39289517**	6.655180514	21.22504166
KNZ SONU	36.00414915	**20.5603233**	23.81823154	35.94354252

Table A3.2. Climatic variables taken from BioClim to calculate bioclimatic envelopes

Temperature variables	Precipitation variables
Mean annual temperature	Mean annual precipitation
Mean diurnal temperature range	Precipitation during wettest month
Isothermality	Precipitation during driest month
Temperature seasonality	Precipitation seasonality
Max temperature during warmest quarter	Precipitation during wettest quarter
Min temperature during coldest quarter	Precipitation during driest quarter
Annual temperature range	Precipitation during hottest quarter
Mean temperature during wettest quarter	Precipitation during coldest quarter
Mean temperature during driest quarter	
Mean temperature during warmest quarter	
Mean temperature during coldest quarter	

Table A3.3. Model statistics for method comparison. Symbols are osmotic potential at full turgor estimated from p-v curves (π_{o*pv}) and an osmometer (π_{o*pv}) as well as leaf turgor loss point (π_{tlp}).

Model	R^2	RMSE	PRESS
$\pi_{tlp} = 1.103\pi_{o*pv} - 0.294$ (fig 4.1)	0.9624	0.1033	0.2667
$\pi_{o*pv} = 0.690\pi_{o*osm} - 0.5481$ (fig. 4.2)	0.6715	0.2718	1.7814
$\pi_{o*osm} = 1.000\pi_{o*predicted} - 5.611e^{-6}$ (fig. 4.3 - herbaceous)	0.7813	0.2669	1.6590
$\pi_{o*osm} = 0.9998\pi_{o*predicted} - 8.526e^{-5}$ (graminoids)	0.6976	0.2510	0.9832
$\pi_{tlp} = 0.800\pi_{o*osm} - 0.845$ (fig. 4.4 - herbaceous)	0.7204	0.2816	1.7986
$\pi_{tlp} = 0.944\pi_{o*osm} - 0.611$ (fig. 4.5 - graminoids)	0.9581	0.0903	0.1005

Table A3.4. AICc values for predicting p-v curve estimates of osmotic potential at full turgor (π_{o*pv}) and turgor loss point (π_{tlp}) from osmometer estimates of osmotic potential at full turgor as well as leaf dry matter content (ldmc) and apoplastic fraction (a_f). Bolded models are the selected models based on lowest AICc.

| Model	AICc	R^2
Osmotic potential at full turgor		
$\pi_{o*pv} = \pi_{o*osm}$	**10.56781**	**0.6694**
$\pi_{o*pv} = \pi_{o*osm} \times ldmc$	12.24293	0.7171
$\pi_{o*pv} = \pi_{o*osm} \times a_f$	13.95537	0.6904
$\pi_{o*pv} = \pi_{o*osm} \times ldmc \times a_f$	22.74938	0.8041
$\pi_{o*pv} = ldmc$	16.9671	0.537
$\pi_{o*pv} = a_f$	28.24673	0.1617
$\pi_{o*pv} = a_f \times ldmc$	23.17696	0.4971
Turgor loss point		
$\pi_{tlp} = \pi_{o*osm}$	**13.27802**	**0.7217**
$\pi_{tlp} = \pi_{o*osm} \times ldmc$	14.54337	0.7669
$\pi_{tlp} = \pi_{o*osm} \times a_f$	16.34039	0.7438
$\pi_{tlp} = \pi_{o*osm} \times ldmc \times a_f$	28.24884	0.8091
$\pi_{tlp} = ldmc$	18.84498	0.6269
$\pi_{tlp} = a_f$	34.24343	0.161
$\pi_{tlp} = a_f \times ldmc$	25.31944	0.5891
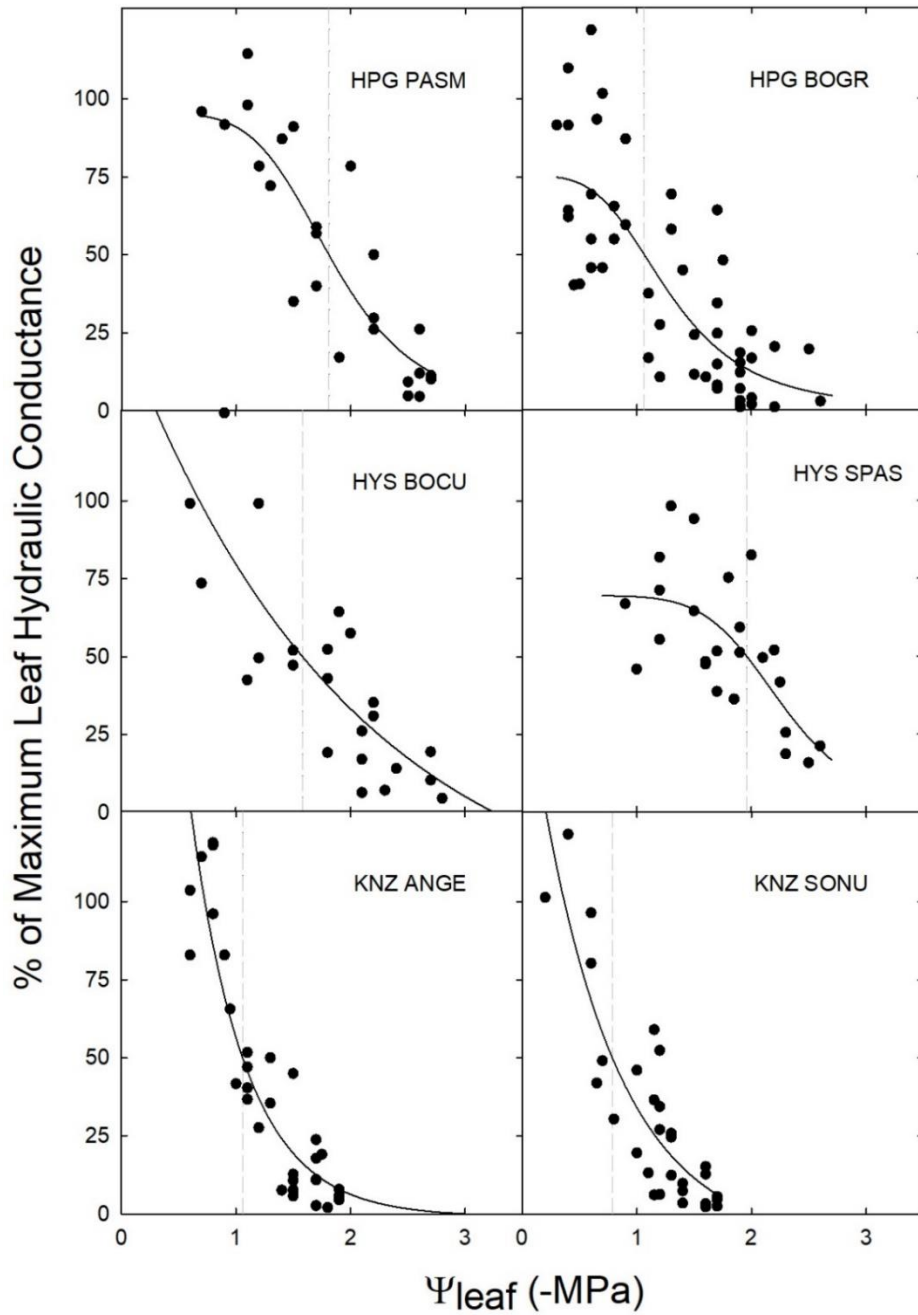
Figure A3.1. Leaf hydraulic conductivity (K_{leaf}) vulnerability curves for a subset of graminoids surveyed in this study. Dotted grey lines indicate P_{50}, the leaf water potential (Ψ_{leaf}) at which K_{leaf} decreases to 50% of K_{max}. Values for P_{50} of other species surveyed in this study were taken from Ocheltree et al. (*in revision*). See Table 4.1 in main text for site and species abbreviations.
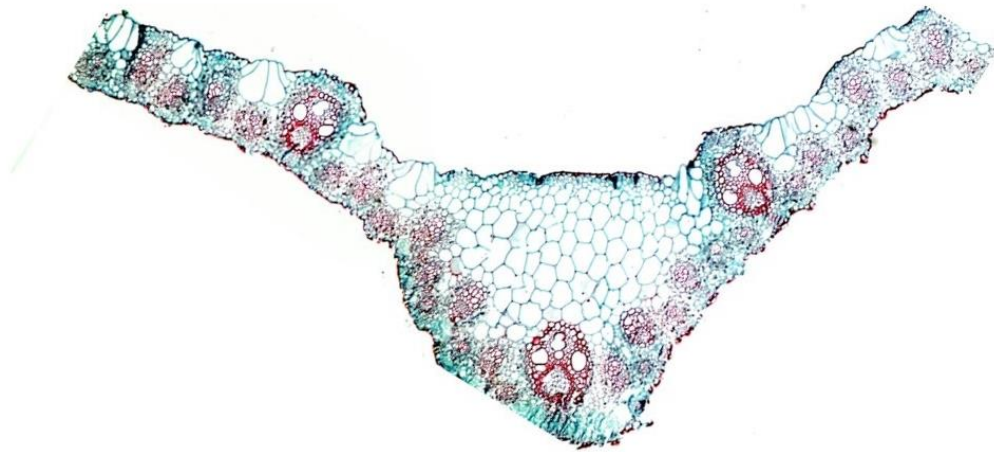
Figure A3.2. Cross section of a midrib and partial lamina from a leaf of *Sorghastrum nutans*, a perennial C4 grass from the Konza tallgrass prairie known to have a large midrib. The density of veins in the midrib is similar to that in the lamina that does not include the midrib, suggesting that it is unlikely that sampling the midrib would include a larger proportion of water from the xylem than would exclusion of the midrib. Photo credit: Troy Ocheltree

APPENDIX 4

A4.1 Sources of contributed trait data

Supplemental trait data were taken from published sources for HYS and KNZ (Craine et al. 2012; Ocheltree et al., 2016; Tucker, 2010). For the remaining sites, data was contributed from unpublished datasets. For HPG, contributed data were collected in June of 2013 (for SLA and LNC) and May of 2015 (for π_{TLP}) in an adjacent location (<100 meters from EDGE plots). For SGS, contributed data were collected in June of 2014 1(for SLA and LNC) and May of 2017 (for π_{TLP}) from areas with similar soil types and less than 2 miles from the EDGE plots. For SBK and SBL, several leaves were collected from 3-6 individuals between September and October 2017 and estimates of SLA and LNC were averaged across individuals. Leaf samples were collected from Sevilleta, Mckenzie Flats area, in the blue grama and black grama core sites. Literature sources can be found below:

Craine, J. M., Towne, E. G., Ocheltree, T. W., & Nippert, J. B. (2012). Community traitscape of foliar nitrogen isotopes reveals N availability patterns in a tallgrass prairie. Plant and Soil, 356(1–2), 395–403. https://doi.org/10.1007/s11104-012-1141-7

Ocheltree, T. W., Nippert, J. B., & Prasad, P. V. V. (2016). A safety vs efficiency trade-off identified in the hydraulic pathway of grass leaves is decoupled from photosynthesis, stomatal conductance and precipitation. New Phytologist, 210(1), 97–107. https://doi.org/10.1111/nph.13781

Tucker, S. S. (2010). Morphological and physiological traits as indicators of drought tolerance in tallgrass prairie plants. Retrieved from http://krex.k-state.edu/dspace/handle/2097/4628

A4.2 Supplementary Results

Drought led to significantly higher functional richness (FRic$_{ses}$) in the final year of drought at SBK (Fig. A4.1-A). with positive and negative effects of drought on FRic$_{ses}$ of SLA and LNC, respectively, in year 2. At SGS, increased FRic$_{ses}$ of π_{TLP} was observed in year 2. At KNZ, multi-variate FRic$_{ses}$ declined in response to drought in year two, with significant declines in FRic$_{ses}$ of LNC in the final year of drought. No changes in FRic$_{ses}$ were observed at SBL, HPG, or HYS. Drought let to a significant decline in multivariate functional evenness (FEve) in the first year of drought at SBL, however FEve eventually increasd by the final year of drought (Fig. A4.2), with a similar response observed for individual trait FEve. For SBK and KNZ, individual trait FEve responded variably to drought even though multi-variate FEve showed no significant drought response (Fig. A4.2).

Estimations of functional diversity metrics using just two traits (SLA and LNC) did not differ drastically from estimations including π_{TLP} (i.e. 3-dimensional trait space), with a few exceptions. In 2D trait space, FDis$_{ses}$ increased at HYS and SGS (Fig. A4.3) just as it did in 3D trait space (Fig. 5.2); however, significant differences between drought and control plots were apparent in years 3 and 4 of the drought (Fig. A4.3) rather than just year 4 (Fig. 5.2). Two-dimensional FRic$_{ses}$ declined significantly at KNZ in years 2-4 of the drought and increased at HYS (Fig. A4.3), which differed from FRic$_{ses}$ measured in 3-dimensional trait space (Fig. A4.1). Two-dimensional FEve did not differ between control and drought plots (Fig. A4.2), which matches the response observed in 3D trait space.

A4.3 Supplementary Tables

Table A4.1. Results from an ANOVA including the effects of site, treatment, and year on standardized effect sizes (SES) of single trait functional diversity indices: functional dispersion (FDis), functional richness (FRic), and functional evenness (FEve). Individual traits include specific leaf area (SLA), leaf nitrogen content (LNC), and leaf turgor loss point (π_{TLP}). F-values are shown for fixed effects and all interactions. Statistical significance is represented by asterisks: *p<0.05, **p<0.01, ***p<0.001.

Effect	SES FDis			SES FRic			SES FEve		
	SLA	**LNC**	π_{TLP}	**SLA**	**LNC**	π_{TLP}	**SLA**	**LNC**	π_{TLP}
Trt	7.17**	2.12	0.48	0.03	1.09	0.71	2.60	4.91*	1.07
Site	22.92***	7.72***	101.85***	0.58	0.70	0.45	9.40***	4.15**	1.60
Year	21.88***	32.83***	11.52***	16.18***	10.67***	3.00*	2.83*	1.41	3.54**
Trt*Site	3.44**	1.63	3.31*	1.41	0.70	1.13	2.49*	0.86	0.74
Trt*Year	7.77***	14.94***	2.22	0.20	0.95	0.33	4.73***	2.78*	2.93*
Site*Year	26.83***	17.68***	29.95***	13.54***	7.80***	2.94***	1.23	3.19***	2.64**
Trt*Site*Year	4.21***	4.24***	6.73***	1.43	0.91	0.94	1.13	0.85	0.70

Table A4.2. Results from correlation analysis and mixed effect models for predicting drought sensitivity (i.e., % reduction in ANPP in drought plots relative to control) from current and previous year functional composition parameters. P-values were compared to a Benjamin-Hochberg corrected significance level (α = 0.0047) for multiple comparisons (n=34 tests). Bolded predictor variables are those with p-values below this threshold. Statistically significant predictor variables were then included as fixed effects in separate mixed effects models with site included as a random effect. These models were compared to null models (using AIC) where null models contained only the random effect of site ($AIC_{model} - AIC_{null} < 0$ indicates a passed test). Marginal and conditional R^2 values for these mixed effects models are shown ($R^2_{GLMM(m)}$ and $R^2_{GLMM(c)}$, respectively). Subscript 'py' and 'cy' indicate previous and current year, respectively. See main text of chapter 5 for abbreviations of traits and diversity indices.

| Predictor (X) in model: *Sensitivity ~ y0 + a(X)*	Pearson-r	p-value	$AIC_{model} - AIC_{null}$	$R^2_{GLMM(m)}$	$R^2_{GLMM(c)}$
SLA$_{py}$	**0.84**	**< 0.0001**	**-18.02**	**0.71**	**0.73**
FEve-SLA$_{cy}$	**-0.62**	**0.0013**	**-0.42**	**0.29**	**0.44**
FEve$_{cy}$	**-0.59**	**0.0022**	**1.19**	**0.19**	**0.38**
FDis-SLA$_{cy}$	-0.54	0.0064			
FEve-SLA$_{py}$	-0.51	0.012			
SLA$_{cy}$	0.43	0.036			
FRic-LNC$_{py}$	-0.37	0.079			
FEve$_{py}$	-0.37	0.082			
FDis-TLP$_{cy}$	-0.42	0.103			
FDis$_{cy}$	-0.34	0.106			
FDis-TLP$_{py}$	-0.39	0.134			
TLP$_{py}$	-0.33	0.211			
FEve-TLP$_{cy}$	0.32	0.232			
FRic-TLP$_{py}$	-0.32	0.234			
FDis-SLA$_{py}$	-0.25	0.243			
FRic-SLA$_{py}$	0.25	0.248			
LNC$_{py}$	0.22	0.318			
FEve-LNC$_{cy}$	-0.21	0.325			
FRic-SLA$_{cy}$	-0.20	0.339			
FDis-LNC$_{cy}$	0.20	0.348			
LNC$_{cy}$	0.18	0.412			
FRic-LNC$_{cy}$	0.16	0.453			
PD$_{cy}$	0.16	0.457			
PD$_{py}$	-0.15	0.488			
FDis$_{py}$	-0.14	0.526			
FEve-LNC$_{py}$	-0.11	0.613			
FRic$_{cy}$	-0.10	0.632			
FEve-TLP$_{py}$	0.13	0.640			
TLP$_{cy}$	-0.12	0.660			
FRic-TLP$_{cy}$	-0.08	0.754			
FRic$_{py}$	-0.06	0.779			
FDis-LNC$_{py}$	0.05	0.824			
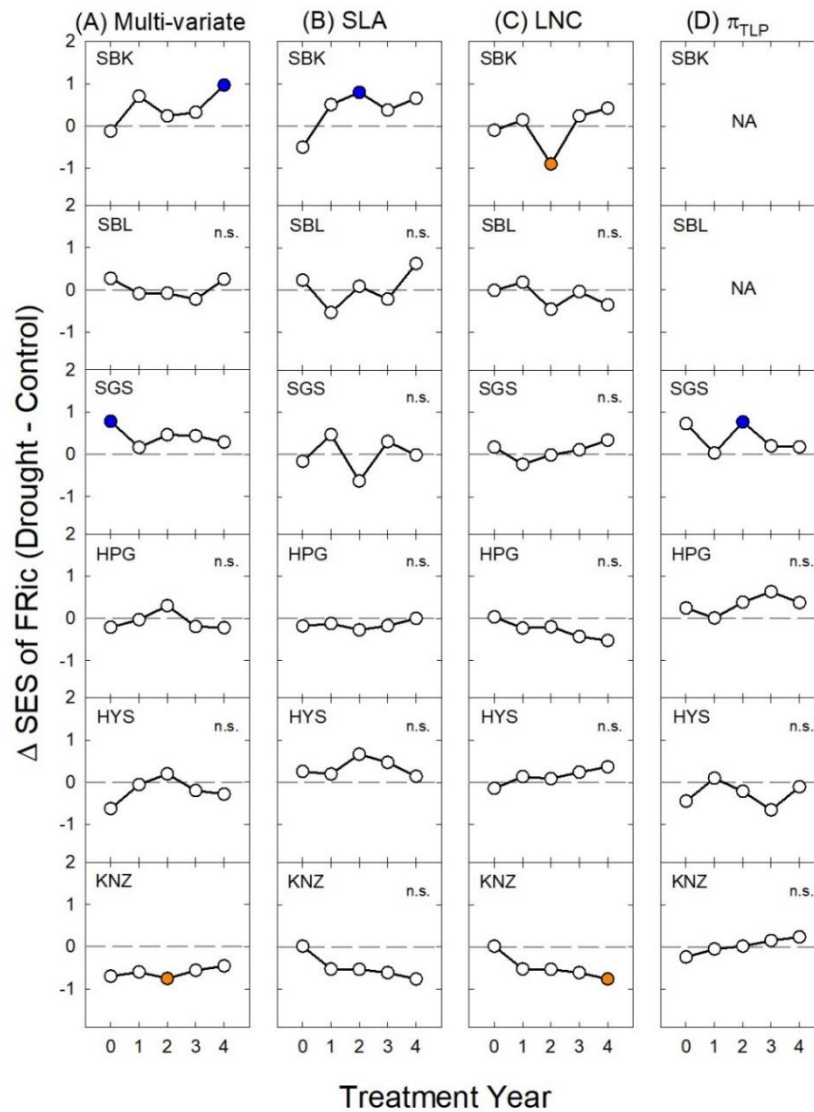
Figure A4.1. Drought treatment effect (drought – control) on standardized effect size (SES) of functional richness (FRic) estimated in multivariate trait space (**A**) as well as for each trait individually (**B-D**). The difference in SES of FDis between drought and control plots was calculated in each year, including the pre-treatment year. Years with statistically significant treatment effects ($p < 0.05$) are represented by filled in symbols with the color representing a positive (●) or negative (●) effect of drought. Open circles represent a lack of significant difference between control and drought plots, with 'n.s.' denoting a lack of significance across all years. *Site abbreviations*: SBK = Sevilleta black grama; SBL = Sevilleta blue grama; SGS = Shortgrass steppe; HPG = High plains grassland; HYS = Hays agricultural research station; KNZ = Konza tallgrass prairie.
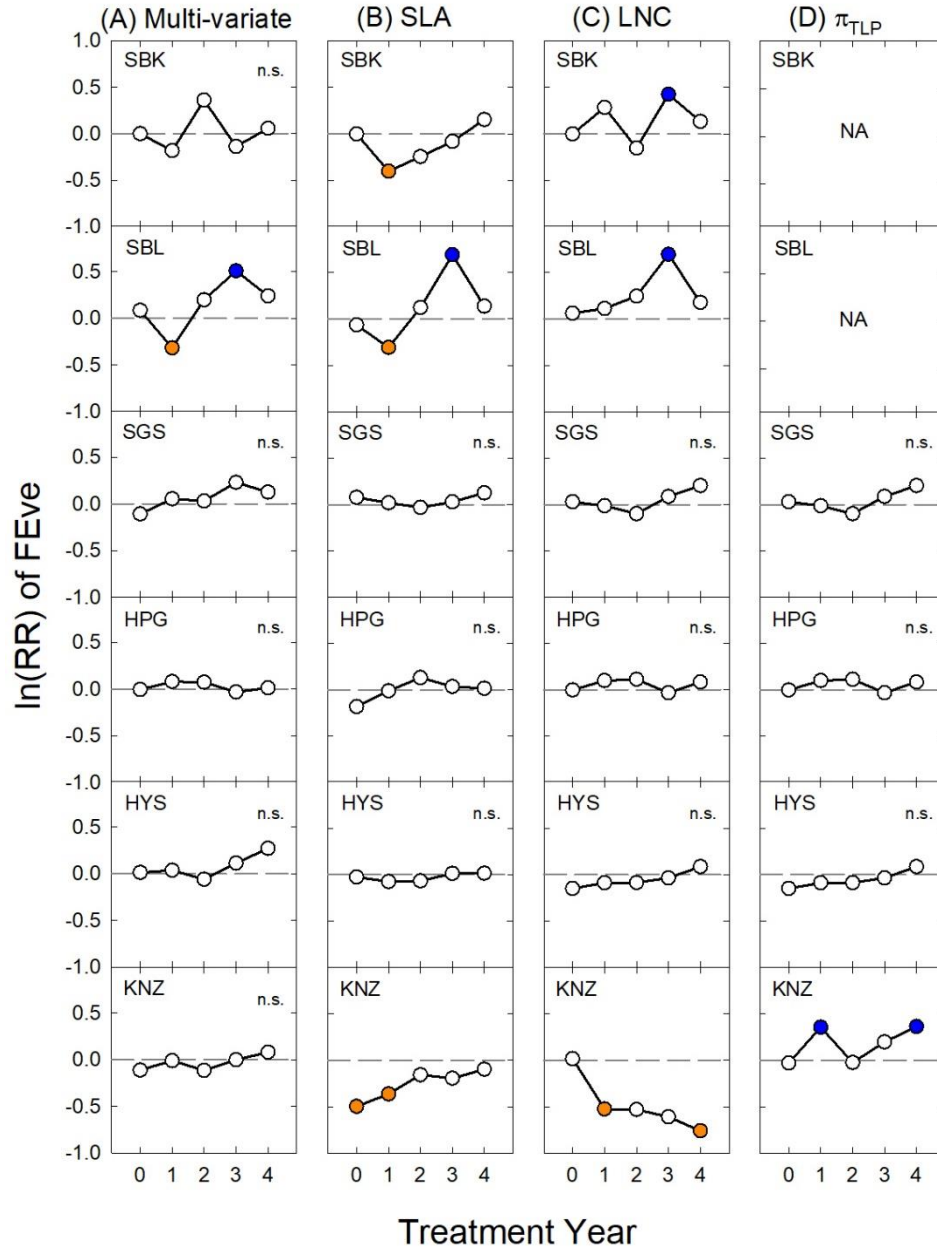
Figure A4.2. Log response ratio (lnRR) of functional evenness (FEve) estimated in multivariate trait space (**A**) as well as for each trait individually (**B-D**). The lnRR (ln(drought/control)) was calculated for each year, including the pre-treatment year. Years with statistically significant treatment effects (p < 0.05) are represented by filled in symbols with the color representing a positive (●) or negative (●) effect of drought. Open circles represent a lack of significant difference between control and drought plots, with 'n.s.' denoting a lack of significance across all years. *Site abbreviations*: SBK = Sevilleta black grama; SBL = Sevilleta blue grama; SGS = Shortgrass steppe; HPG = High plains grassland; HYS = Hays agricultural research station; KNZ = Konza tallgrass prairie.
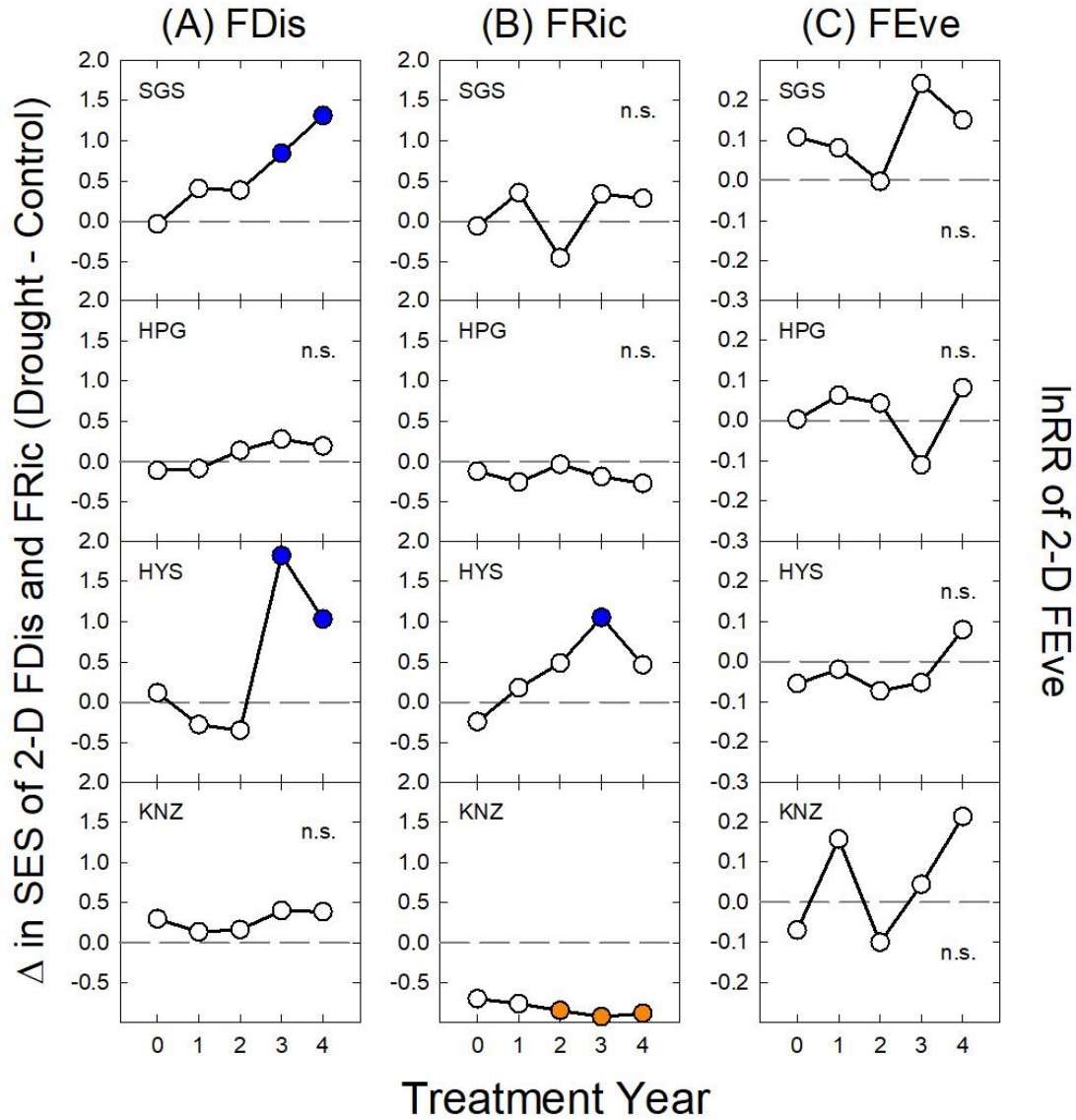
160

Figure A4.3. The response of two-dimensional multivariate functional diversity (as integrated across SLA and LNC) in response to four years of experimental drought. Functional diversity metrics include (**A**) functional dispersion (FDis), (**B**) functional richness (FRic), and (**C**) functional evenness (FEve). Both FDis and FRic are calculated as standardized effect sizes (SES) as compared to null models (see methods in main text). The response of FDis and FRic is shown simply as the difference between drought and control plots. The log response ratio is shown for FEve (ln(drought/control)). Statistically significant effects of drought on functional diversity (p <0.05) are colored in with the symbol color representing a positive (●) or negative (●) drought effect. Open circles represent a lack of significant difference between ambient and drought plots, with n.s. denoting a lack of significance across all years. Results for the New Mexico sites (SBK and SBL) are not shown as they can be found in Fig. 5.2, Fig. A4.1, and Fig. A4.2. *Site abbreviations*: SGS = Shortgrass steppe; HPG = High plains grassland; HYS = Hays agricultural research station; KNZ = Konza tallgrass prairie.

161